SCHOOL of GRADUATE STUDIES
EAST TENNESSEE STATE UNIVERSITY

East Tennessee State University
Digital Commons @ East Tennessee State University

Electronic Theses and Dissertations | Student Works

8-2019

Synthesis of Diazonium N-(Perfluoroalkyl) Benzenesulfonimide Polymers for Proton Exchange Membrane Fuel Cells (PEMFCs)

Helal Alharbi
East Tennessee State University

Follow this and additional works at: https://dc.etsu.edu/etd

 Part of the Organic Chemistry Commons

Recommended Citation
Alharbi, Helal, "Synthesis of Diazonium N-(Perfluoroalkyl) Benzenesulfonimide Polymers for Proton Exchange Membrane Fuel Cells (PEMFCs)" (2019). *Electronic Theses and Dissertations.* Paper 3601. https://dc.etsu.edu/etd/3601

This Thesis - Open Access is brought to you for free and open access by the Student Works at Digital Commons @ East Tennessee State University. It has been accepted for inclusion in Electronic Theses and Dissertations by an authorized administrator of Digital Commons @ East Tennessee State University. For more information, please contact digilib@etsu.edu.

Synthesis of Diazonium N-(Perfluoroalkyl) Benzenesulfonimide Polymers for Proton Exchange Membrane Fuel Cells (PEMFCs)

A thesis

presented to

the faculty of the Department of Chemistry

East Tennessee State University

In partial fulfilment

of the requirements for the degree

Master of Science in Chemistry

---

by

Helal Alharbi

August 2019

Dr. Hua Mei, Chair

Dr. Abbas G. Shilabin

Dr. Aleksey Vasilie

Keywords: Proton exchange membrane fuel cells (PEMFCs), Diazonium, Nafion, Perfluoro(3-xapent-4-ene) sulfonyl fluoride, Perfluoroalkyl arylsulfonimide (PFSI) polymers

ABSTRACT

Synthesis of Diazonium N-(Perfluoroalkyl) Benzenesulfonimide Polymers for Proton Exchange Membrane Fuel Cells (PEMFCs)

by

Helal Alharbi

The objective of the research is to synthesize the diazonium N-(perfluoroalkyl) benzenesulfonimide (PFSI) zwitterionic polymers as electrolytes in polymer electrolyte membrane (PEM) fuel cells. The proposed diazonium PFSI zwitterionic polymer (**I**) is expected to enhance the thermal and chemical stability, increase the proton conductivity of electrolytes, and improve the catalyst efficiency for PEM fuel cells. Synthesis of the perfluorobenzoyl peroxide initiator, homopolymerization of perfluoro (3-oxapent-4-ene) sulfonyl fluoride, coupling reaction with 4-sulfamonylacetanilide, coupling reaction with 4-nitrobenzene sulfonyl amide, n-deacetylation reaction, and diazotization reaction have been carried out successfully in the lab. The intermediate chemicals are characterized by GC-MS, IR, NMR, and GPC spectroscopies.

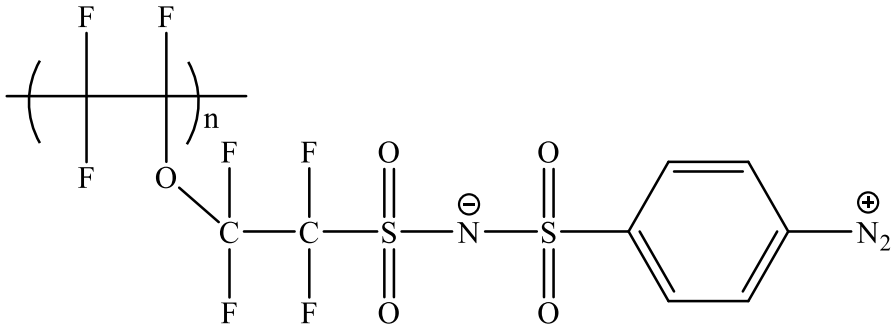

I

DEDICATION

I dedicate this research work to God Almighty, my parents, my siblings, and the department of chemistry at Qassim University.

ACKNOWLEDGEMENTS

I would like to really thank Dr. Hua Mei for her motivation, guidance and patience throughout this research work.

Thanks to Dr. Abbas G. Shilabin and Dr. Aleksey Vasiliev for serving as committee members. Thanks to Dr. Mohseni for his assistance with the instruments.

Special thanks to Dr. Mei's group for their support and assistance.

Finally, I would like to say a big thank you to the ETSU faculty, staff, and graduate students of the Chemistry Department for their assistance and support during my time at ETSU.

TABLE OF CONTENTS

Page

LIST OF FIGURES

Figure Page

LIST OF SCHEMES

Scheme Page

LIST OF ABBREVATIONS

POPF	Perfluoro (3-Oxapent-4-ene) Sulfonyl Fluoride
AFC	Alkaline Fuel Cell
DMFC	Direct Methanol Fuel Cell
PEMFC	Proton Exchange Membrane Fuel Cell
PAFC	Phosphoric Acid Fuel Cell
MCFC	Molten Carbonate Fuel Cell
SOFC	Solid Oxide Fuel Cell
EW	Equivalent weight
FTIR	Fourier Transform Infra Red
GDL	Gas Diffusion Layer
Hz	Hertz
MEA	Membrane Electrode Assembly
NMR	Nuclear Magnetic Resonance
PFSA	Perflurosulfonic acid
PFSI	Perflurosulfonylimide

ppm	Parts per million
PTFE	Polytetrafluorethylene
TMS	Tetramethylsilane
GE	General Electric Company
MHQ	N-methyl-6-hydroxyquinolinium
CL	Catalyst Layer
GFC	Gas Flow Channel
TLC	Thin Layer Chromatography
DIEA	N, N-Diisopropylethylamine
TEA	Triethylamine
TPB	Triple-Phase Boundary
GCMS	Gas Chromatography-Mass Spectrometer

CHAPTER 1

INTRODUCTION

Preface

This research provides the synthesis of a novel diazonium N-(perfluoroalkyl) benzenesulfonimide (PFSI) polymer, which is proposed to replace the traditional perfluorosulfonic acid (PFSA) polymers as the electrolytes in polymer electrolyte membrane fuel cell (PEMFC). The introduction begins with a brief narrative of fuel cells; after which, the structure of PEMFCs are explained. Next, details about the structure and classification of polymer electrolyte membrane, chemical structure and properties of PFSA polymers as membrane are discussed. And then, the proposed MEA system is elucidated. At last, the reasons of preparing the targeting polymer and its synthetic routes are illustrated.

Fuel Cells

By definition, fuel cells refer to electrochemical devices that efficiently transform the chemical energy of the reactants into heat and electricity.[1] Measurements show that the effectiveness of fuel cells ranges between 60 and 80%. Such figures are heavily dependent on the applications. Compare to the fossil fuels, there is a reduction of the main pollutants by 90% or more in internal combustion motors.[2-4] If there is a steady supply of the necessary fuel, the fuel cells do not require a recharge. Generally, a typical fuel cell is composed two electrodes that permeable to clean energy sources, and in between the electrodes lies the electrolyte. To accelerate the reaction, the catalysts like palladium and platinum are used. It is worth noting that fuel cells are used in numerous areas such as stationary combined power, transportation, as well as the supply of heat to portable machines.[3-4] Many different types of fuel cells have been developed in the past few years.

In Table 1 below, fuel cells have been classified on the basis of the electrolyte used, which is dependent on the electrochemical reaction's nature, used fuel, operating temperature, and used oxidant.

Table 1: Types of Fuel Cells[5]

Fuel Cells	**Electrolytes**	**Temperature**	**Used Fuel**	**Used Oxidant**
Proton Exchange Membrane Fuel Cell (PEMFC)	H+ conducting membrane	~80°C	Hydrogen	Air, O_2
Alkaline Fuel Cell (AFC)	KOH	~100°C	Hydrogen	O_2
Direct Methanol Fuel Cell (DMFC)	H+ conducting membrane	80-130°C	CH_3OH	Air, O_2
Phosphoric Acid Fuel Cell (PAFC)	Concentrated H_3PO_4	~200°C	Natural gas, H_2	Air, O_2
Molten Carbonate Fuel Cell (MCFC)	Molten K_2CO_3	~650°C	Natural gas, H_2	Air, O_2

Solid Oxide Fuel Cell (SOFC)	Z_rO_2	800-1000°C	Natural gas, H_2	Air, O_2

On the basis of their operating temperatures, fuel cells are classified into two major categories: high temperature such as Carbonate Fuel Cell (CFC) and Solid Oxide Fuel Cell (SOFC) and low temperature for example Proton Exchange Membrane Fuel Cell (PEMFC), Phosphoric Acid Fuel Cell (PAFC), and Alkaline Fuel Cell (AFC). Compared to the widely developed DMFCs, the hydrogen gas is used as fuel in PEM fuel cells while DMFCs are used methanol as fuel. The PEM fuel cells are generated only water as a byproduct; thus, they are more environmentally friendly in comparison to DMFCs, which emit carbon dioxide (CO_2). The PEMFCs have numerous benefits over the DMFCs such as better electrical efficiency, clean operation. While DMFCs has a high proportion of methanol-crossover, which is a significant hurdle as it reduces fuel efficiency, and hence the performance of the cells.

Proton Exchange Membrane Fuel Cells

In 1839, Sir William Robert Grove invented the PEMFC. However, it was only in the 1950s, that General Electric Company (GE) started the development of PEMFCs'.[6] Before the late 1960s, PEMFCs' did not have any practical applications until they were used as a source of power for the Gemini space mission. The PEMFC technology obtained the massive interest in the 1970s when the Nafion membrane was first used.[7] Besides portable power, stationary power, and distributed stationary power generation applications, PEMFCs are also proposed to be used in transportation as they are eco-friendly. The advantages of PEMFCs include their effective operation at high current density, relatively low operation temperature, quick startup, and a long stack life.[8]

The overall reaction taking place in PEMFCs is a reversible oxidation-reduction reaction. On the cathode, the oxygen gas, oxidant, is channeled to the gas flow channel (GFC).[9] While hydrogen fuel is channeled to the anode (GFC) through field flow plates on the other side of the cell. Hydrogen and oxygen are then transported via the gas diffusion layers (GDL) to the catalyst layers (CLs) separately. The hydrogen gas in the anode is oxidized to electrons and protons whereby the protons migrate via the proton-conducting polymer membrane to the cathode's CL. The electrons generated from the anode catalyst layers are then transported through the external circuit to the cathode current collector. The electrons combining with the protons at the cathode reduce oxygen to produce water. The membrane is electrically non-conducting, thus inhibiting the passage of electrons. Besides, water formed in this reaction is expelled out of the cathode CL via the GDL and ultimately out of the cathode GFC. The reactions taking place in a PEMFC are shown in the Scheme 1 below.

Numerous factors impact the performance of PEMFCs. Such include the high temperature that boosts its operation by enhancing the membrane's proton conductivity. However, external heat is not a requisite as exothermic reactions take place in PEMFCs; hence the utilization of a water-cooling system is required to expel excess heat.[10] In addition, PEMFCs performance deteriorates when the membrane is contaminated with CO and CO_2 and when electrodes are tainted. In this regard, a source of relatively pure hydrogen is preferable for fuel.[11,12,13]

Anode: $2H_2 \rightarrow 4H^+ + 4e^-$ ……1

Cathode: $O_2 + 4H^+ + 4e\text{-} \rightarrow 2H_2O$ …….2

Overall reaction: $2H_2 + O_2 \rightarrow 2H_2O$ ……...3

Scheme 1: The reaction taking place in a PEMFC

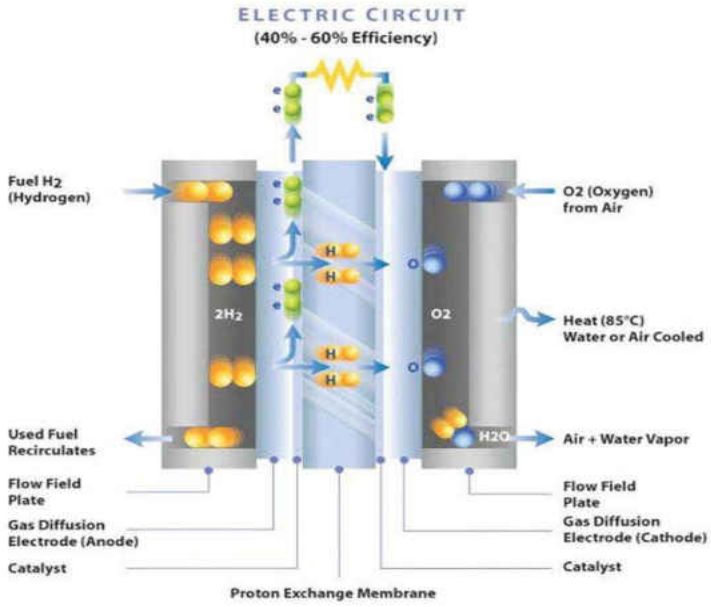

Figure 1: The PEMFC structure. Used with permission[14]

A typical PEMFC possesses three principal components, which include two bipolar-separate or flow field-plates, and the membrane electrode assembly (MEA). The MEA consists of two GDLs, two dispersed CLs, and a membrane that permits the protons to move between the electrodes for the reactions to take place. The MEA plays a primary role in controlling the cell's performance.

The cathode section of the MEA which comprise the electrolyte membrane and the carbon electrodes as shown in Figure 2. The electrochemical reaction in the cell takes place at the triple-phase boundary (TPB), where the protons, the electrons, and the reactant gases meet in the MEA.

In general, the requirements of the proton exchange membrane comprise low electric conductivity, high proton conductivity, low gas permeability, good mechanical properties, as well as chemical stability.[15,16]

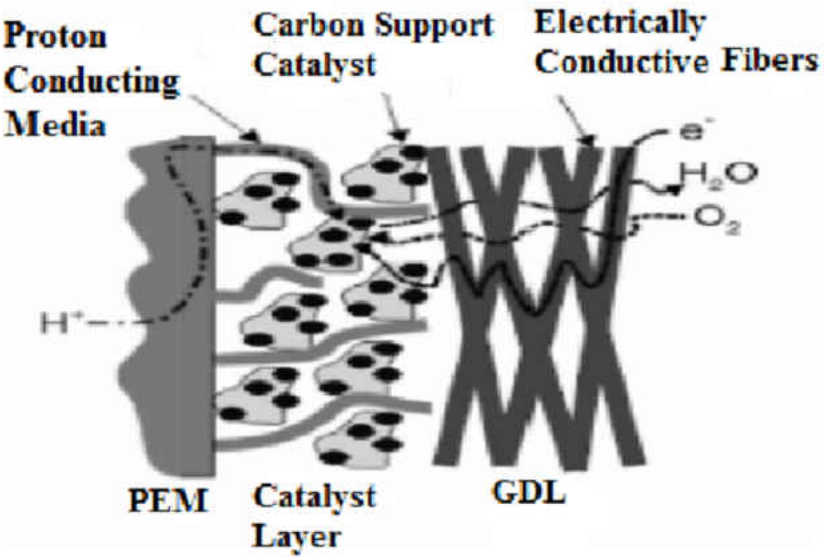

Figure 2: The extended cathode of the MEA structure.[18] Used with permission

On both sides, the CLs are directly adjacent to the membrane. Because the half-cell reactions occur in these layers, the CLs are also referred as the active layers. Since all the reactants, gases, protons and electrons have to meet the catalyst in the CLs, keeping the balance of hydrophilic and hydrophobic properties in the layer is very important. The polymer electrolyte membrane is hydrophilic for transferring the protons, while the carbon electrode is hydrophilic for allowing gases and electrons passing through. [17] Too hydrophilic with water accumulation at the cathode side can cause the swelling of the CLs, which will eventually result in the failing of the cell. On the other side, the CLs will decrease gasses transport if they are too hydrophilic. Hence, the balance between the hydrophilic fluorinated polymer and hydrophobic carbon powder is needed for the CL to provide the excellent performance of the PEMFC.

The CLs are generally fabricated by physically mixing the membrane with the catalyst and smearing the paste to the GDL. Thompson et al. asserted that, in such electrodes, up to 50%

of the catalyst particles onto carbon may be inactive.[18] Since the platinum alloys catalyst is very expensive, how to efficiently use catalyst is critical for the widely development and applications of PEMFCs. In the MEA, the catalyst utilization is determined by two main factors, proton transport resistance in CLs, and the catalyst activity.[19] Thus, the catalyst activity depends on the surface area of the catalyst particles in contact with the membrane hydrophilic moiety.[19]

The figure 3 below presents a traditional MEA structure with the catalyst randomly placed on the dense electrode.

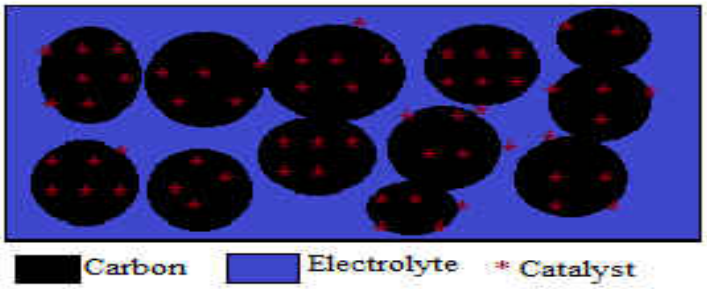

Figure 3: The structure of a traditional dense MEA in PEMFCs.[20] Used with permission

The other components of the MEA are the bipolar plates. Their operative functions involve expediting water management, separating individual cells, distributing oxidants and fuel, and transporting current away. A more detailed research on modifications and configurations of MEA components follows below.

Polymer Electrolyte Membrane

It is widely known that for PEMFCs, the most commonly used membranes materials are the perfluorosulfonic acid (PFSA) polymers such as Nafion® polymers. [21] The PFSA polymers contain two fundamental parts namely ion clusters with sulfonic acid ions and a perfluorinated alkane main chain. With the polytetrafluoroethylene (PTFE) backbone, the PFSA polymers have

excellent stability in both reductive and oxidative phases.[22] Under full hydrated conditions, PFSA polymers' proton conductivity can reach 0.10 S/cm.[4] It is essential to hydrate the membrane to enhances the proton conductivity by facilitating the protons movement.

As one of PFSA polymers, Nafion® is an extensively studied and used polymer membrane in PEMFCs because of its desirable qualities such as liquid permeability, low gas and mechanical stability, and good chemical at low temperature.[15]

As per the illustration figure 4 below, PFSA polymers are commercially accessible in the sulfonic acid form (-SO3 –H+). Nafion® polymers are formed from copolymerization of tetrafluoroethylene (TFE) and nafion monomer, perfluoro (4-methyl-3, 6-dioxaoct-7-ene)-sulfonic acid.[24]

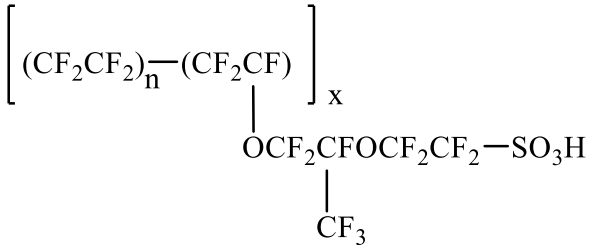

Figure 4: The chemical structure of the of Nafion® polymer [24]

In the Nafion polymer, the perfluorinated alkyl backbone, which is responsible for its excellent thermal and chemical stability, and significant mechanical strength, is fabricated from copolymerization with TFE. With the perfluoroalkyl sulfonic acid group, The Nafion polymer has the desirable proton conductivity. For instance, Nafion® 117 has pKa of −6,[25,26] which is equivalent to the super acidity of photoacid, N- methyl-6-hydroxyquinolinium (MHQ) which has pKa* ≈ -7 in excited-state.[31]

There are also some undesirable features associated with Nafion® polymers as they are working as the electrolyte. For instance, they like to form large rod-shaped micelles that decrease the contact with the microporous carbon electrodes. After certain time, the membranes are washed away, and it will result in the lower ion conductivity and finally diminished performance of PEMFC. Additionally, the sulfonic acid pendants ($-SO_3H$) in the polymers also are oxidized into anhydride ($-SO_2OSO_2-$) when the temperature is too high. Moreover, in the extremely oxidizing and acidic conditions, the integration between carbon electrodes and the electrolytes is weakened.[27] Hence, all of mentioned above diminish the PEM fuel cell's life span.

In addition, other PFSA polymers, are commercially available include, Celtec-P (BASF), Aciplex® (Asaki Kasei), POPF Gore-Select (Gore), Flemion® (AsahiGlass), and Aquivion®.

Proposed MEA System

To date, the design and fabrication of MEA attract a lot of attention in research area since these are the most important processes in fuel cell technology development. Among them, one proposed modifications is to fabricate the thin electrolyte film in the MEA. Another one involves the placing the catalyst to the membrane as near as possible. According to Yang et al.[32], after using the Pt-C-80 (Pt catalyst content 80wt. %) thin layers to replace the Pt black at the frontiers between the GDL and electrolyte, the performance of the fuel cell has big improvement. In addition, the modified 7 and 9- layer MEAs with thinner CLs have been reported to enhance the performance of PEMFCs.[19]

We also propose a new MEA system by having the electrolyte chemically grafted onto the pores of the carbon electrode as indicated in figure 5 below.[20] And then the new MEA system propose to replace the traditional ones. It is believed that the directly attachment of

electrolyte/catalyst onto electrode will enhance the catalyst utilization, the membrane proton conductivity, and stability of PEM fuel cells.

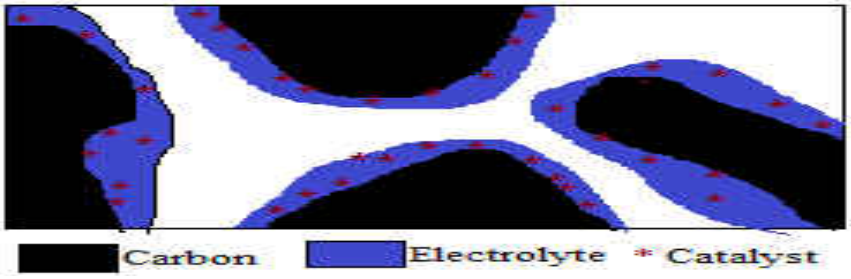

Figure 5: Proposed new MEA system. (modified from Creager [20]-used with permission)

<u>The Summary of Previous Work</u>

Analogs of diazonium PFSI monomers are prepared in our lab, and their synthesis methods are altered with the aim of providing various options for membrane structure variations, enhanced performance for PEM fuel cells, and excellent chemical and mechanical properties.

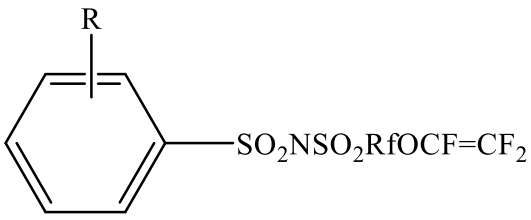

I: R= 4-$\overset{\oplus}{N}_2$, Rf= $CF_2CF_2OCF(CF_3)CF_2$

II: R= 2-$\overset{\oplus}{N}_2$ -4-CF_3 , Rf= $CF_2CF_2OCF(CF_3)CF_2$

III: R= 4-$\overset{\oplus}{N}_2$ -3-F , Rf= $CF_2CF_2OCF(CF_3)CF_2$

IV: R= 4-$\overset{\oplus}{N}_2$, Rf= CF_2CF_2

V: R= 2-$\overset{\oplus}{N}_2$ -4-CF_3 , Rf= CF_2CF_2

Figure 6. Diazonium PFSI monomers

Figure 6 describe two groups of diazonium PFSI zwitterionic monomers prepared for the further polymerization and modification of MEA in PEMFCs. The first three diazonium PFSI monomers (I-III in Figure 1) were prepared from Nafion® monomer. Monomer III is not prepared successfully due to the difficulty to purify the intermediates from the coupling reaction of brominated Nafion monomer and 3-fluoro-4-nitrobenzenesulfonylamide. The other two diazonium PFSI monomers (IV-V in Figure 1) from POPF -based monomers, CF_2=$CFOCF_2CF_2SO_2F$ (POPF), has been successfully synthesized. POPF polymers are referred with a shorter perfluoroalkyl chain, which provides a better proton conductivity compared to Nafion polymers when placed under low humidity proposed by Paddison and Elliott's calculation.[43]

Diazonium PFSI Zwitterion Polymers

In this project, a new diazonium PFSI polymers, from perfluoro (3-oxapent-4-ene) sulfonyl fluoride monomer, are proposed to be prepared as electrolytes for PEMFCs rather than the traditional used PFSA polymers. We expect the new electrolyte will dramatically increase the MEA performance under more intense conditions.

There are three major parts, the aryl diazonium moiety, the perfluoroalkyl (aryl) sulfonamide pendant, and the perfluoroalkyl backbone, in the targeting polymers. Figure 7 shows the structure of the expected new diazonium PFSI polymer.

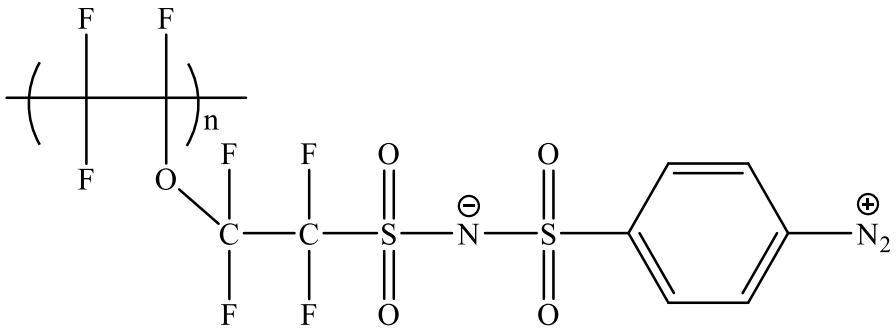

Figure 7: The structure of diazonium PFSI polymer

With the diazonium group, the PFSI polymers are anticipated to chemically attach to the carbon electrode surface as figures 8 indicated.[49] The better integration between the electrolytes and electrode will offer enhanced proton conductivity and thermal stability. The new polymer will have excellent stability in both reductive and oxidative phases due to the perfluorinated alkyl backbones in POPF polymers. Moreover, it anticipated providing significant hydrophobicity and mechanical strength.

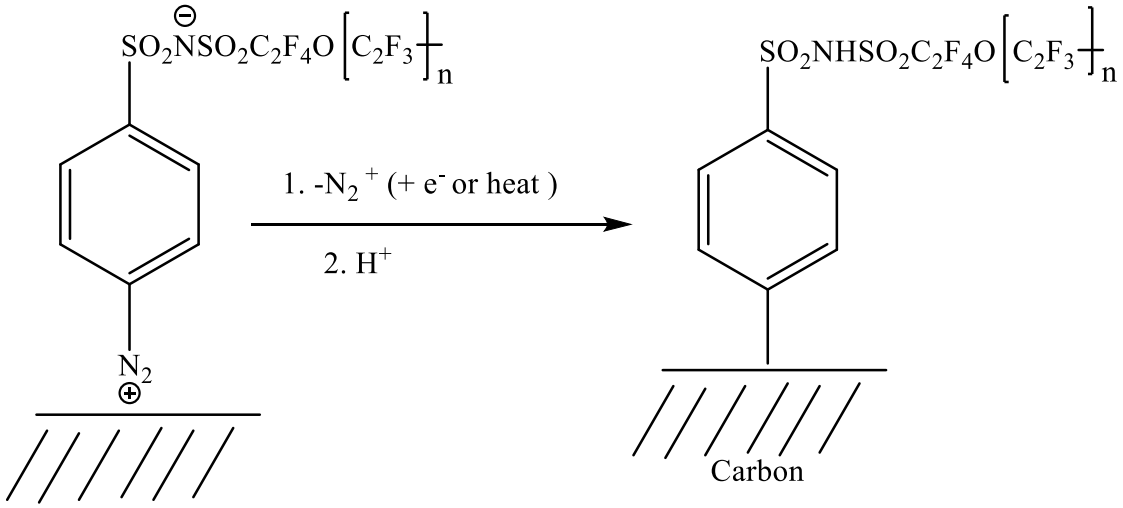

Figures 8: Grafting of functionalized diazonium zwitterion on a carbon electrode.[37, 39, 40-42]

The PFSI pendants can provide good ionic conductivity, more inert to electrochemical conditions, excellent thermal stability in acidic conditions, less susceptible to dehydration and,

oxidative degradation compared to the traditional PFSA polymers.[23] The PFSI compounds have a general chemical formula $(R_fSO_2)_2NH$. The PFSI compounds were first synthesized in the 1980s. Later, the establishment of relative gas-phase acidities (GA) for string Bronsted strong acid series were by Zhang et al. [34-36] It is notable that PFSI compounds have greater acidity compared to traditional mineral acids such as HNO_3.[37,38] As one of the bis[(perfluoroalkyl)-sulfonyl)]imide compounds, $(CF_3SO_2)_2NH$ has a pKa value = 7.8 in acetic acid compare to a pKa value = 10.2 of HNO_3 in the same condition. The super-acidity of PFSI compounds is due to two mains factors. One factor is because of perfluoroalkyl group, which is a very strong electron-withdrawing group.[26,30,35] Another factor is because the resonance stabilization over the O-S-N skeleton of the PFSI compounds' conjugate base, $(R_fSO_2)_2N^-$ as shown in Scheme 2.

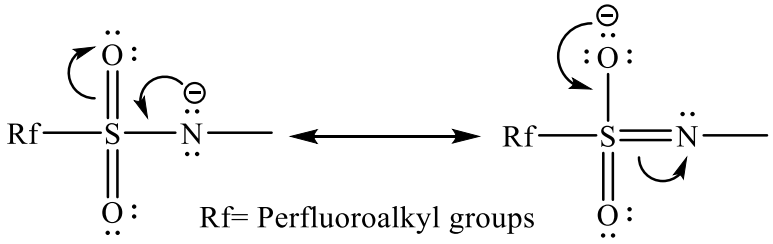

Scheme 2: Resonance structure of conjugate base of PSFI compounds.[33]

Target Polymer

The synthesis of the diazonium N-(perfluoroalkyl) benzenesulfonimide (PFSI) zwitterionic polymers (Figure 1) is prepared from perfluoro (3-oxapent-4-ene) sulfonyl fluoride (POPF) monomer. Two approaches are planned to synthesize the desired polymer. The only difference in these two routes in the preparation of PFSI is aromatic amine part. The approach II is using the reduction of nitro group, and approach I is using the deacetylation method.

4-Sulfamonylacetanilide Starting Material (Approach 1)

A six-step procedure is designed to synthesize the desired polymer: 1) synthesis of an initiator 2) an ammonolysis reaction 3) a homopolymerization 4) a coupling reaction, 5) an N-deacetylation reaction, and 6) a diazotization reaction. The overall synthesis scheme of the (Approach 1) for the target polymer is shown in Figure 9.

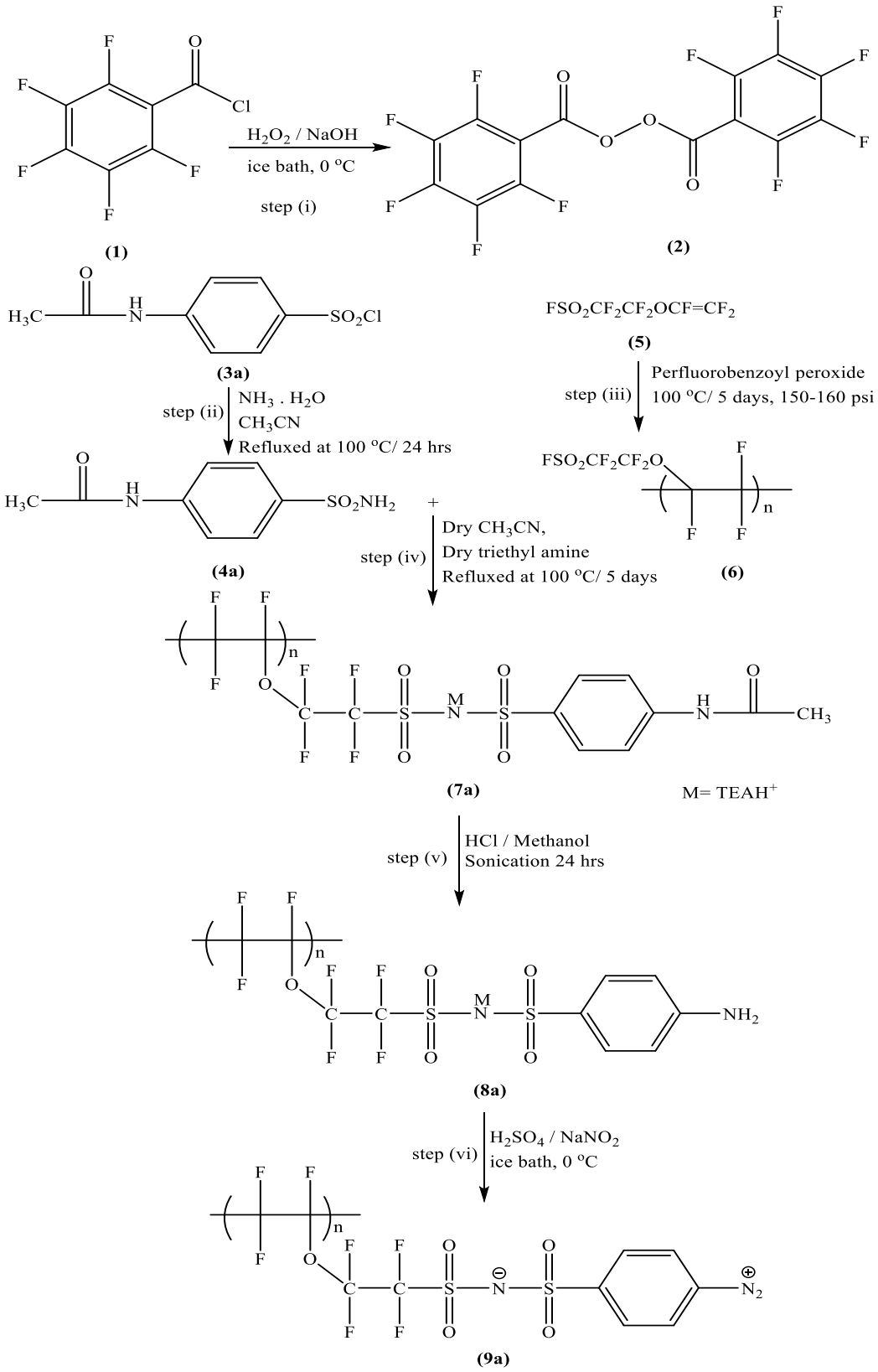

Figure 9: The overall synthesis scheme of the target polymer (Approach 1)

4-Nitrobenzenesulfonyl Amide Starting Material (Approach 2)

Another six-step procedure is designed to synthesize the desired polymer with a different starting material, 4-nitrobenzenesulfonyl amide. The second approach includes: 1) synthesis of an initiator 2) an ammonolysis reaction 3) a homopolymerization 4) a coupling reaction, 5) a reduction reaction, and 6) a diazotization reaction. The overall synthesis scheme of the (Approach 2) for the target polymer is shown in Figure 10.

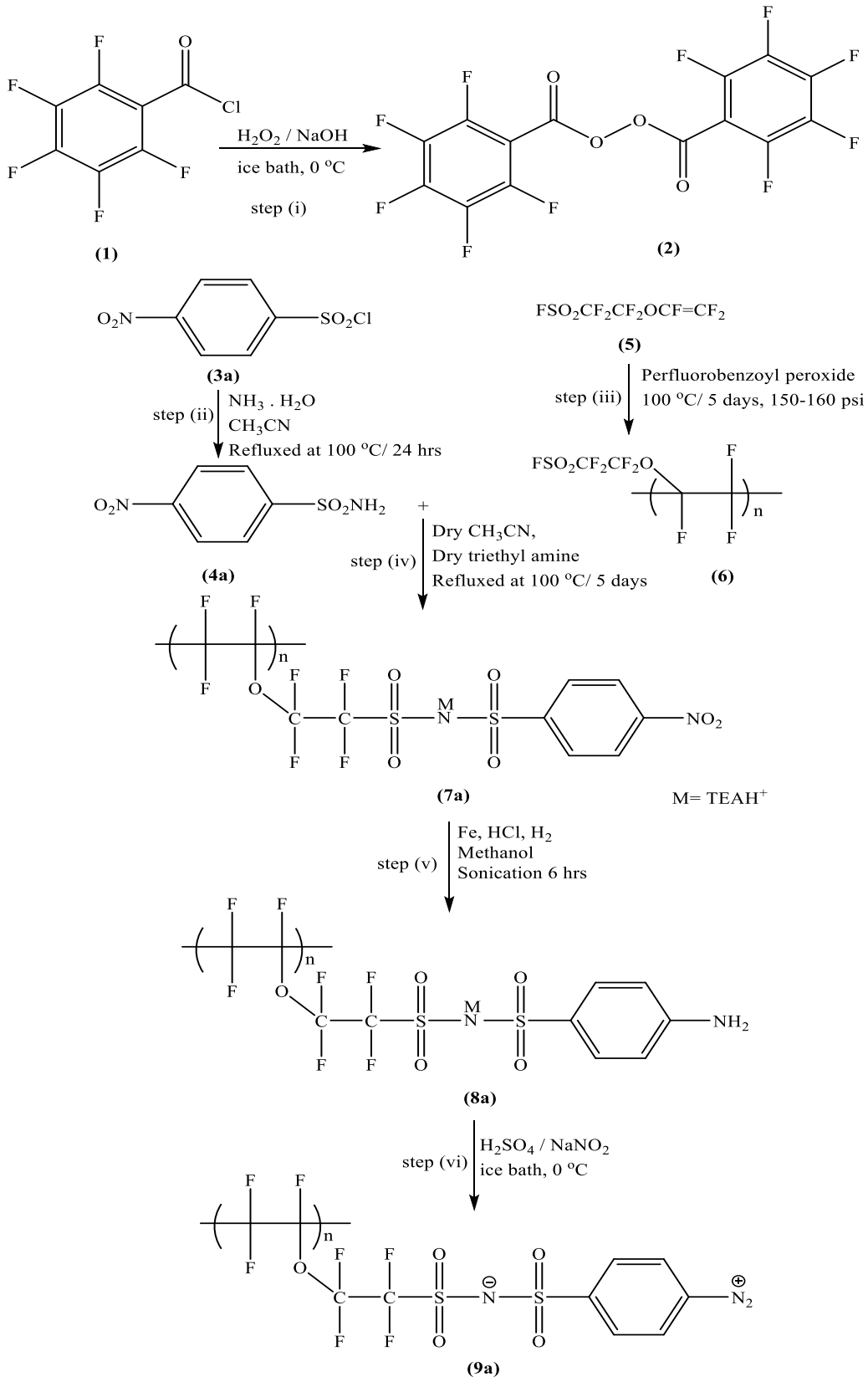

Figure 10: The overall synthesis scheme of the target polymer (Approach 2)

CHAPTER 2

RESULTS AND DISCUSSION

Prepare the Initiator

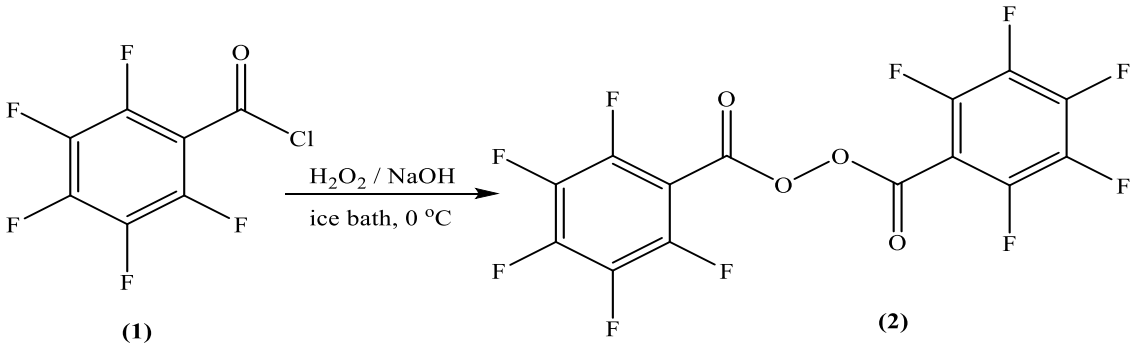

Scheme 3: The preparation of perfluorobenzoyl peroxide.[47]

Scheme 3 shows the preparation of the polymer initiator: perfluorobenzoyl peroxide. This reaction can be referred to as nucleophilic acyl substitution reaction and its overall mechanism is shown in Scheme 4. The ^{19}F-NMR spectrum indicates that the targeting purified product, perfluorobenzoyl peroxide, was obtained. According to Venzo et al., perfluorobenzoyl peroxide has three chemical shifts on the ^{19}F-NMR spectrum at -134.26, -143.73 and -158.62 ppm for ortho, para, meta positions respectively.[47] The reaction should carry out at a low temperature, 0 °C because the peroxide compounds are very reactive. Other side reactions, like the hydrolysis reaction could have occurred at room temperature. In the recrystallization process, two solvents, chloroform/methanol (1:2 by volume), was used. The solubility of the perfluorobenzoyl peroxide is good in the chloroform; therefore, it was used first.[47] The percentage yield of product was around 75-80 %, which is acceptable.

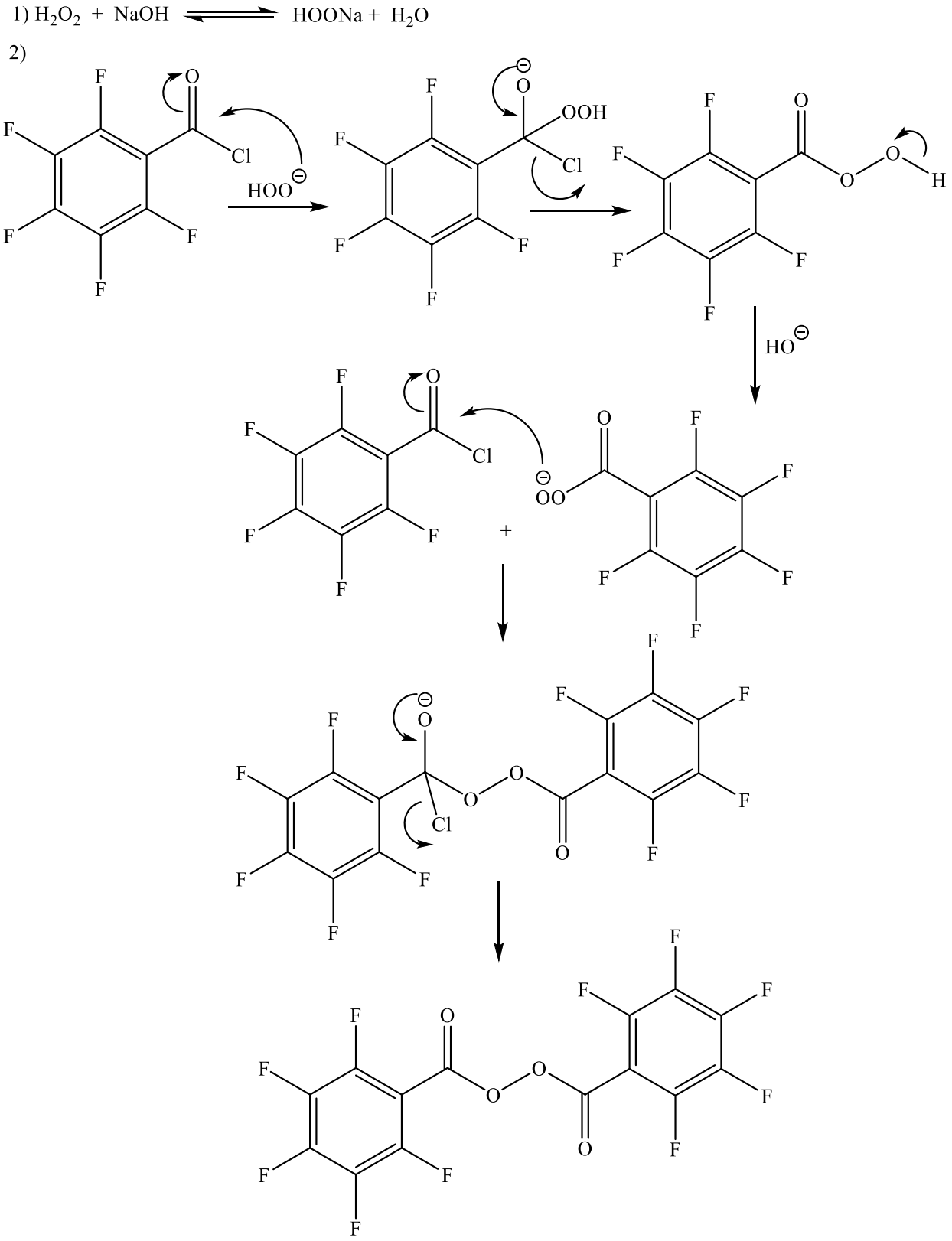

Scheme 4: The mechanism of perfluorobenzoyl peroxide preparation.[48]

Ammonolysis Reaction

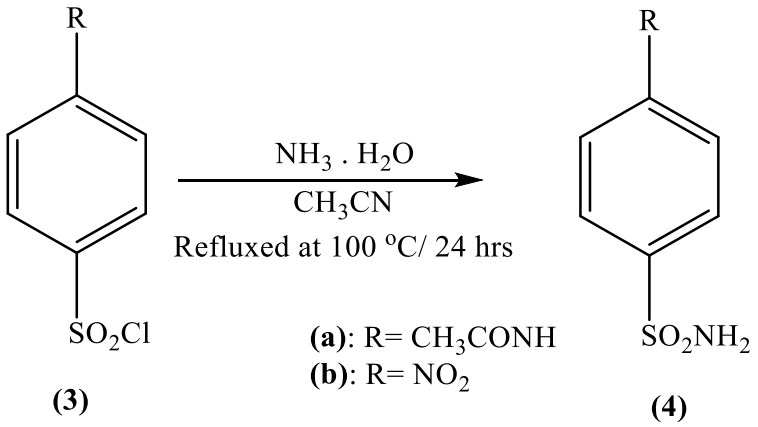

Scheme 5: The ammonolysis reactions

The synthesis of 4-substituted sulfonyl amide**(4a-b)** was conducted by refluxing 4-substituted sulfonyl chloride (**3a-3b)** in the presence of acetonitrile and excess ammonium hydroxide at 100 ^{O}C. The ratio is 1:2 for sulfonyl chloride reacting with the aqueous ammonia. The ammonolysis reaction is considered as a typical nucleophilic addition-elimination reaction as illustrated in Scheme 5, where the Cl^- ion is replaced by the NH_2- group.[58]

^{1}H-NMR spectrum indicates that both targeting products, 4-sulfamonylacetanilide **(4a)** and 4-nitrobenzenesulfonyl amide **(4b)**, were obtained successfully. The percentage yield of products is around 75%. The purification process and hydrolysis by products contribute to the percentage yield loss of products. After the ammonolysis reaction was successfully carried out by replacing NH_2- group with Cl^- ion, the chemical shift of primary aromatic amine appeared at 5.64 ppm and 5.97 ppm on the ^{1}H-NMR spectrum for 4-sulfamonylacetanilide **(4a)** and 4-nitrobenzenesulfonyl amide **(4b)**. The FT-IR Spectrum showed the absorption for the primary amine around 3300 cm^{-1} for **(4a)** and **(4b)**. Furthermore, the molecular weights, 214 g/mol and 202 g/mol, for **(4a)** and **(4b)** were shown on GC-MS chromatogram.

The excess ammonia was used to neutralize the HCl which formed as a byproduct. The ammonolysis reaction was more favorable than the hydrolysis reaction because ammonia is a stronger nucleophile compared to water.[57,58] The hydrolysis side product aryl sulfonic ammonium salt and byproduct NH_4Cl can be washed out since both have good solubility in water.

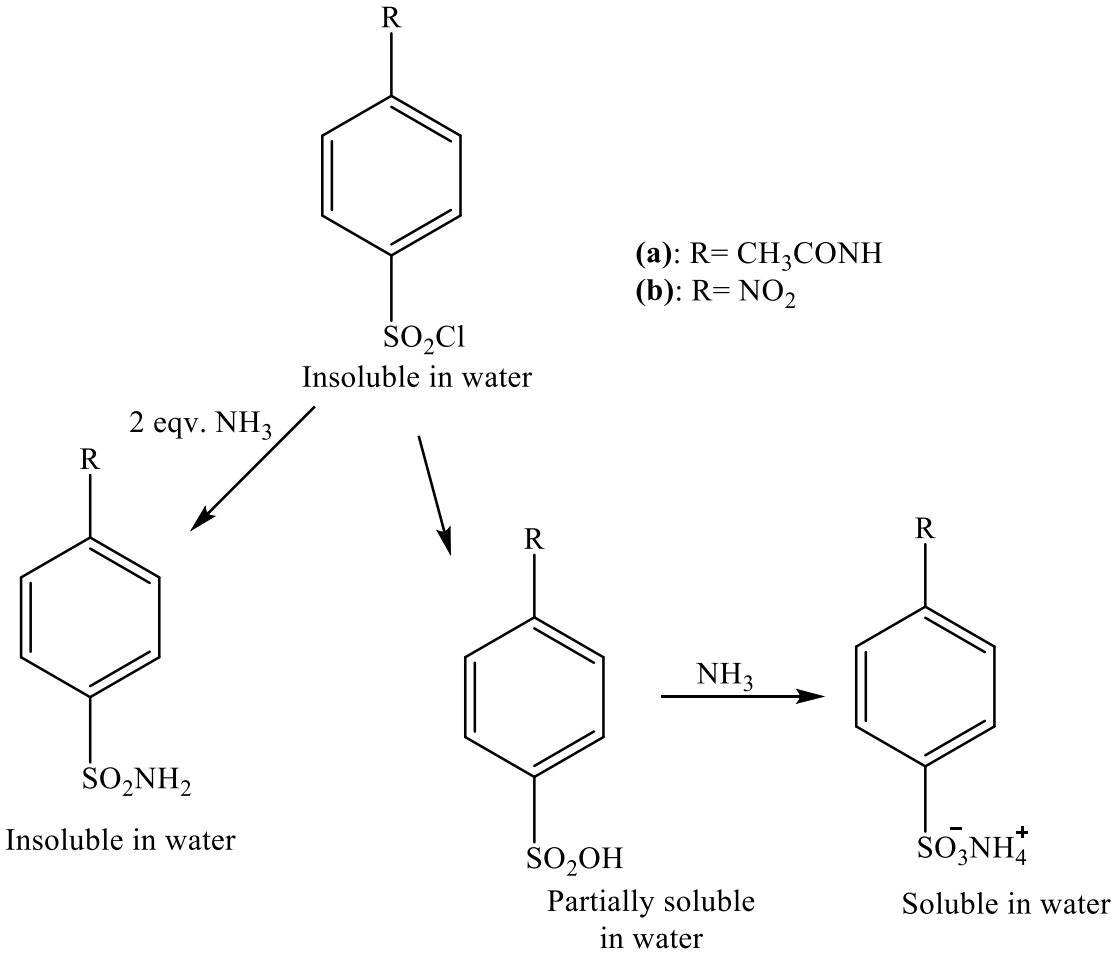

Scheme 6: The side/by products formed during the ammonolysis reaction

Polymerization Reaction

Homopolymerization of POPF monomer ($FSO_2CF_2CF_2OCF=CF_2$) is used instead of nafion monomer. Compared to Nafion® polymer, the POPF polymers have some advantages,

such as high proton conductivity, great affinity for water, low equivalent weights (EWs), as well as considerable stability at relatively high temperatures, higher than 80 ^{O}C.[28]

Due to the short side chains of perfluoroalkyl chain, the POPF polymers offer a higher proton conductivity than Nafion® polymer per the equivalent weight (EW). According to Arcella et al., a polymer with low EWs are hydrated completely at above 100 ^{O}C.[28] With low EWs between 625 and 850 g/eq, the POPF polymer show high ionic conductivity, which is above 0.13 S/cm. Hence, they are preferred alternatives of Nafion® polymers for high temperature applications of PEMFCs.[29]

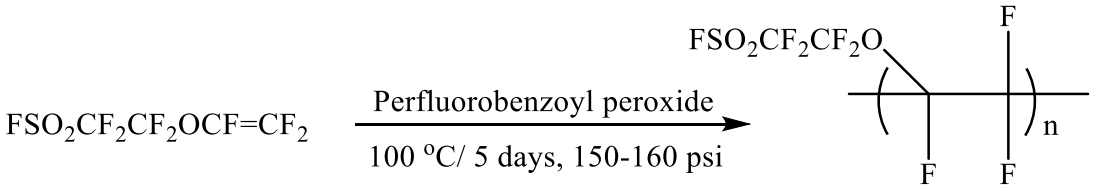

(5) **(6)**

Scheme 7: The homopolymerization of POPF monomer

Scheme 7 indicate to the free radical polymerization of ($FSO_2CF_2CF_2OCF=CF_2$) POPF monomer and its overall mechanism is indicated in Scheme 8.[50] The polymerization conversion rate of POPF monomer is higher than Nafion® monomer because the shorter perfluoroalkyl chain. The ^{19}F-NMR spectrum shows that the polymerization reaction has occurred, and the POPF polymers **(6)** was obtained with excess monomer and the perfluorobenzoyl peroxide initiator. The percentage yield of polymer is about 40 %, and it is considered acceptable compared to literature,[44] which is ~30 to 50%. The low conversion rate of free radical

polymerization mainly led to reduced yield of polymer. As an addition polymerization, longer polymerization time can increase the yield of polymer.

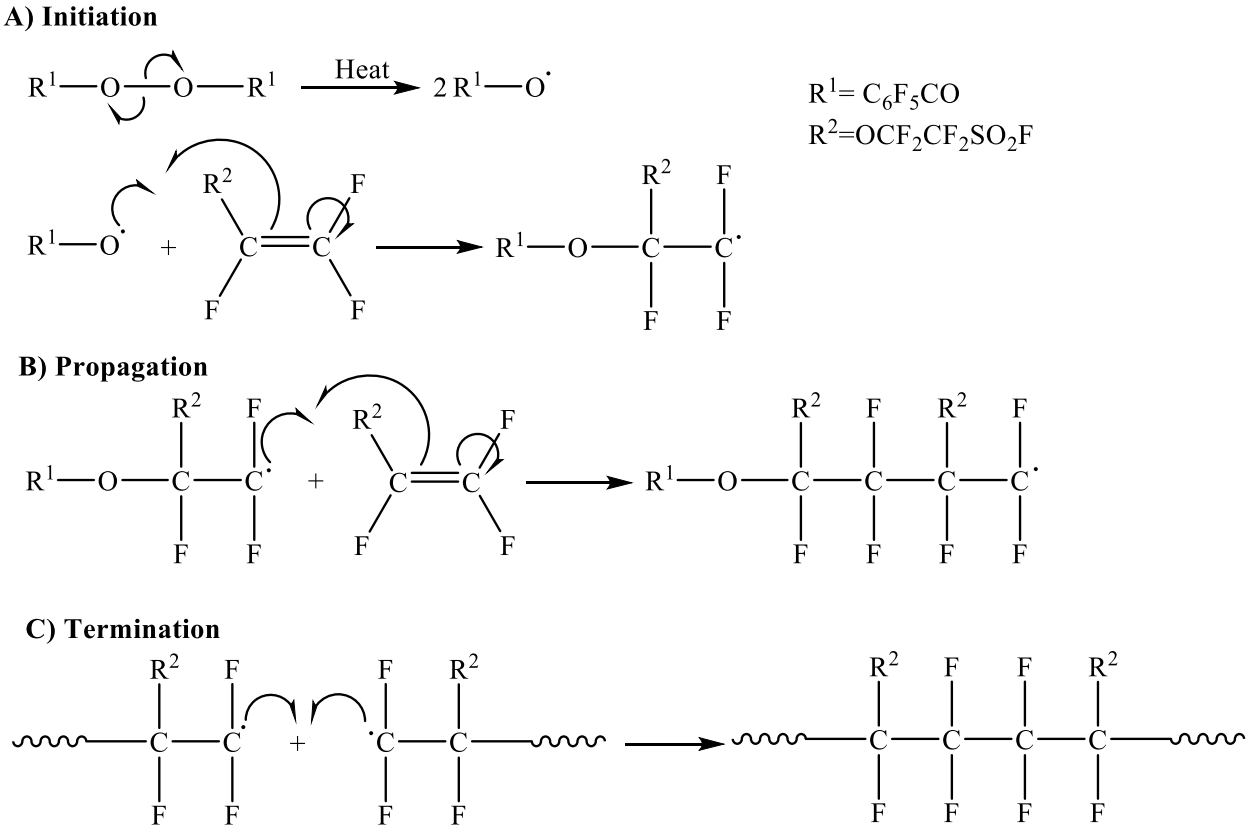

Scheme 8: The mechanism of the free radical polymerization of the POPF monomer.[50]

Linear polymers usually have higher density than branched polymers. The POPF polymer **(6)** is expected to be a linear fluoropolymer with pendant since it has density approximately 3.42 g/mL.[62,63,64] The properties of polymer generally determine by molecular weight and polydispersity index (PDI). Free radical homopolymerization of POPF monomer, ($FSO_2CF_2CF_2OCF=CF_2$), produces functionally, medium molecular weight (Mw: 45,564) polymer. The PDI for formed polymer **(6)** is 2.024. It is water insoluble polymer. The properties of polymer generally determine by molecular weight and polydispersity index (PDI). Free radical

homopolymerization of POPF monomer, ($FSO_2CF_2CF_2OCF=CF_2$), produces functionally, middle molecular weight (Mw: 45,564) polymer. The PDI for formed polymer **(6)** is 2.024. It is water insoluble polymer.

The chemical shift of the sidechain ($–SO_2F$) located at ~ 45 ppm on ^{19}FNMR spectrum. The two chemical shifts of the sidechain (CF_2) appear at -77 and -112 ppm respectively. According to the fluorine NMR spectra, multiplets at -115, -119, and -138 ppm are assigned to backbone (CF_2-CF-).[44]

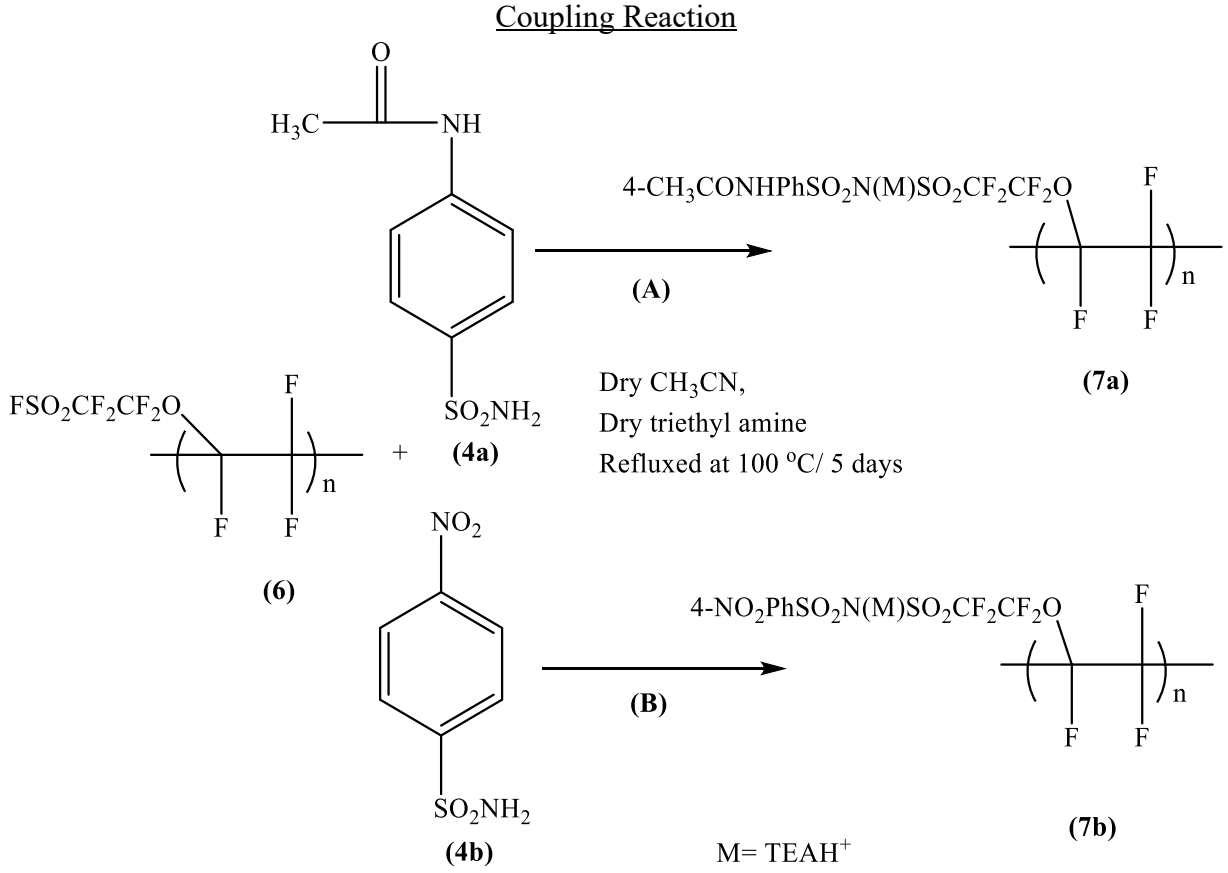

Scheme 9: The summary of the two coupling reactions

As shown in Scheme 9, both the coupling reaction start from the similar reagents and conditions. There is one difference in the structure of aromatic compounds. For coupling reaction

(A), 4-sulfamonylacetanilide, **(4a)**, has amide group at para position while in coupling reaction **(B)**, 4-nitrobenzenesulfonyl amide, **(4b)**, which has nitro group at para position of benzene ring.

The ^{19}F-NMR spectra were used to monitor the reaction process. The disappearance of fluorine peak in sulfonyl fluoride group from polymer indicate the reactions had completed. Both coupling reactions were refluxing at 100 ^{o}C for around five days under the argon gas protection. The percentage yield of coupling reaction **(A)** is higher than coupling reaction **(B)**. Compared to the nitro substituted aromatic sulfonyl amide **(4b)**, the acetamide substituted aromatic sulfonyl amide **(4a)** as the stronger nucleophile favors the nucleophilic addition-elimination reaction. This is evident from the substituent's inductive effect on the aromatic ring, the acetamide is a moderate electron donating group, and the nitro group is a strong electron withdrawing group.[57] The synthesis of the coupling products took a long reaction time to achieve the product. This can be attributed to the fact that the fluorine is not a good leaving group.[44]

The dry condition is extremely necessary for the coupling reactions.[53] The presence of any small amount of water leads to hydrolysis of the sulfonyl fluoride group (-SO_2F) in the starting polymer **(6)**. The hydrolysis side products are also hard to remove. In addition, triethylamine, the organic base catalyst, is used to improve the nucleophilicity of aromatic sulfonyl amides (**4a-b**). Furthermore, extra amount of the aromatic sulfonyl amides **(4a-b)**, was used to push the coupling reactions with polymer **(6)** rather than the hydrolysis reaction.

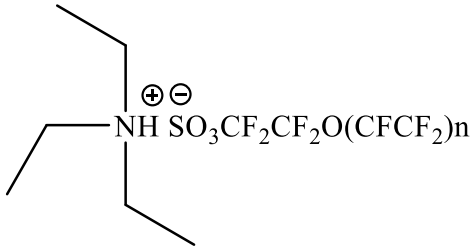

Figure 11: The possible hydrolysis byproduct from coupling reaction

In the coupling reaction **(B)**, the hydrolyzed side products are removed by the extraction with dichloromethane and water. After the basic crude product is neutralized with 1M HCl. And then the excess starting material, 4-nitrobenzene sulfonyl amide **(4b),** can be removed by vacuum sublimation. On the contrary in the coupling reaction **(A)**, the extraction process did not work since the product, **(7a)**, has low solubility in dichloromethane.

The sticky coupling product **(7a)** is because of forming the triethyl ammonium ($TEAH^+$) counterion. In order to convert $TEAH^+$ salt to amine and TEA, the coupling product is purified by acidification with concentrated HCl, and solvent extraction with dichloromethane. According to proton NMR, partially n-deacetylation reaction occurs but TEAH cation stays. The main reason is that the triethyl ammonium chloride salt is a solid, which has the similar poor solubility in water and dichloromethane as our organic product. The extraction procedure is not successful to remove the $TEAH^+$ chloride salt.

According the thin layer chromatography, two different spots were revealed with values of Rf value of 0.82 for starting material and 0.18 for the coupling product **(7a)**. Thus, the 1:1 ratio of tert-butyl methyl ether to acetone was used to separate the excess starting material **(4a)** and through column chromatography. The column chromatography succeeded in separating the coupling product **(7a)** from the starting material **(4a)**. The partial deacetylation product is

actually obtained as $TEAH^+$ form since the silicon dioxide catalyzed the coupling product and led to a partially n-deacetylation reaction.

The N, N-diisopropylethylamine (DIEA) is suggested to replace triethyl amine (TEA) as the base catalyst for the coupling reaction. The N, N-diisopropylethylamine is a slightly weaker base than trimethylamine. [61] Thus, the $DIEAH^+$ chloride salt may be easier to be removed by extraction due to its good solubility in water compared to the poor solubility of $TEAH^+$ chloride salt.

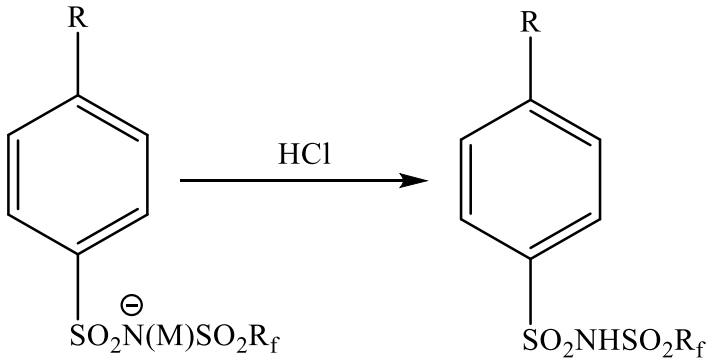

M= $TEAH^+$
R_f= $CF_2CF_2O(CFCF_2)n$

(a): R= CH_3CONH
(b): R= NO_2

Scheme 10: Acidification of the Crude Coupling Products

Reduction Reaction

To prepare the aromatic amines, the reduction of their corresponding aromatic nitro compounds is considered a common method. There are different reagents can be used to reducing the nitro group to amine,[51] for example, Fe/HCl or Fe/Acetic Acid, Zn/NaOH, Sn/HCl, Fe/ArOH, catalytic hydrogenation using Raney Ni, H_2-Pd/C and H_2-PtO_2 sodium polysulfide, NaBH4/Pt-Ni. The selection of appropriate reagents for reduction depends on reaction

conditions, type sensitive functional groups, and water-sensitivity. The reduction of the aromatic nitro compound, **(7b)**, is shown in Scheme 11.

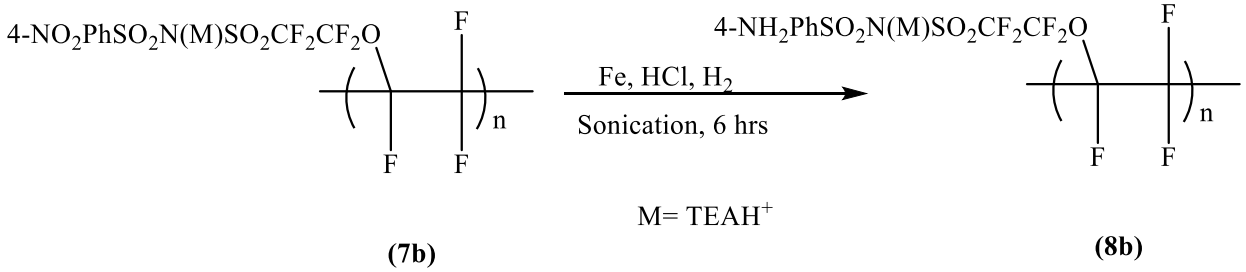

Scheme 11: Reduction of the coupling product **(7b)**

The reduction of **(8b)** was conducted by sonication **(7b)** for six hours in the presence of the catalyst, Fe, HCl, and methanol with H_2 gas. The ratio is 1:5 for the coupling product **(7b)** reacting with the catalyst, iron powder. Higher equivalents of the iron powder are required to complete reduction. The reaction mechanism of aromatic nitro-compounds is illustrated in Scheme 12.[52]

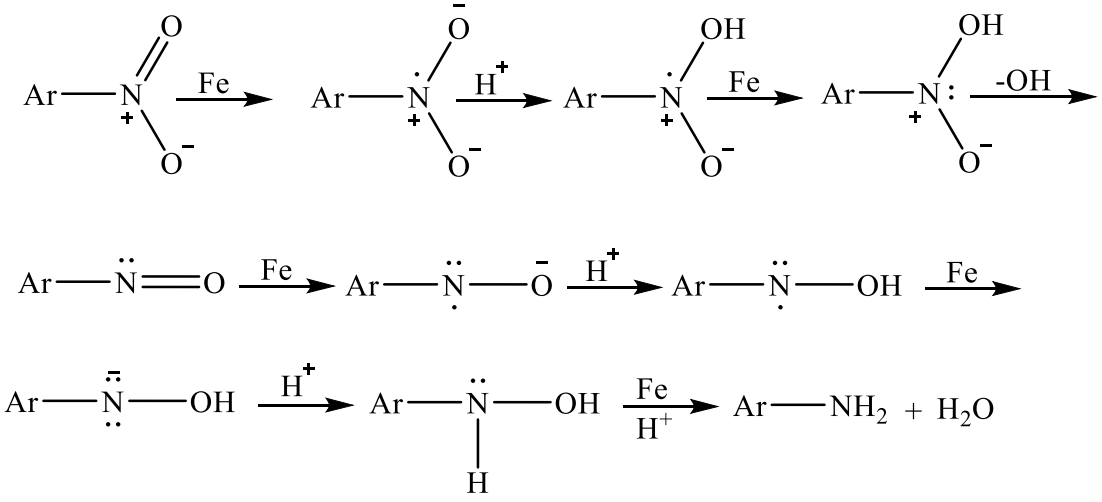

Scheme 12: The mechanism of reduction reaction.[52]

According to previous work in Dr. Mei's research group,[53] the procedure of Fe/HCl/H_2 in ultra-sound sonicator was effective for reducing the aromatic nitro compound to aromatic amine compound. The ^{1}H-NMR spectrum indicated that the reduction reaction was completed; however, the purification process failed to separate the final purified product from the extra inorganic catalyst and by products. The possible reason is that the reduction product **(8b)** was adherent to the surface of the inorganic catalyst/byproduct. The procedure of Fe/HCl/H_2 in ultra-sound sonicator was effective for reducing the aromatic nitro compound to aromatic amine compound but the purification process was not feasible.

N-deacetylation Reaction

N-deacetylation can be referred to as amide hydrolysis or nucleophilic acyl substitution reaction.[4,59] The reaction was achieved by the use of high temperatures, strong acids or bases catalyst since the low reactivity of aromatic sulfonamide.[58] It went through the nucleophilic addition- elimination mechanism. The N-deacetylation reaction of the coupling product, **(7a)**, is shown in Scheme 13.

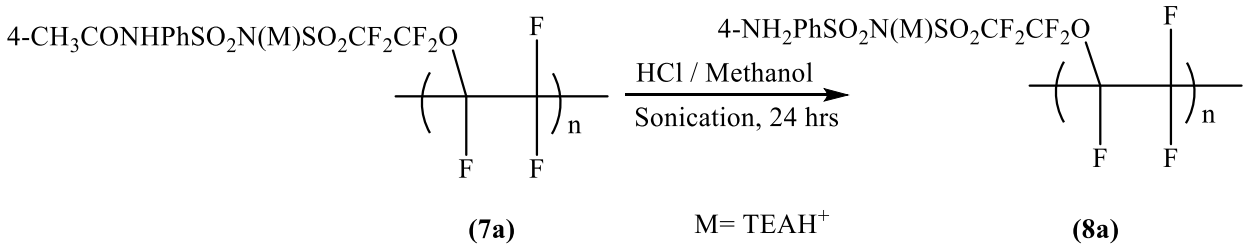

Scheme 13: The N-deacetylation reaction of the coupled product

The N-deacetylation reaction was carried out successfully after sonication with concentrated hydrochloric acid for 24 hours. The percent yield of the purified product for this reaction was 53.3 %. The purification process involves neutralization, filtration, solid-liquid

extraction, and vacuum sublimation. The filtration was used to get rid of the inorganic part (NaCl). The hydrolyzed side product from coupling reaction was removed after solid-liquid extraction. Neutralization and vacuum sublimation process were used to remove excess of starting material, **(4a)** in the coupling reaction as well. The final N-deacetylation product **(8a)** was contaminated with TEAH cation according to proton NMR. The reason is that TEAH cation and the final product (8a) has poor solubility in water and solid-liquid extraction was helpful only to remove the hydrolysis by-product.

After the N-deacetylation reaction was successfully carried out by converting the amide group to the primary amine, the chemical shift of amide group at 9.02 ppm disappear in compared to the appearance of the chemical shift of primary amine at 5.43 ppm the proton NMR spectra. Also, two new chemical shifts for the benzene ring appeared at 7.56 ppm and 6.67 ppm. Moreover, the FT-IR Spectrum showed the absorption for the primary amine around 3400 cm^{-1}.

The N-deacetylation reactions occur readily in acidic conditions such as HCl (pKa = -6.0), H_2SO_4 (pKa = -9.0) and $ClSO_3H$ (pKa = -6.6) under sonication or refluxing according to literature.[54] The mechanism in acidic condition is as shown in Scheme 14.[36]

The protonation of the carbonyl group (C=O) in amide **(A)** makes the carbon more electrophilic and susceptible to the weak nucleophilic attack first in step ii. And then the acid can protonate the secondary amine to ammonia salt, which is a better leaving group in step v.

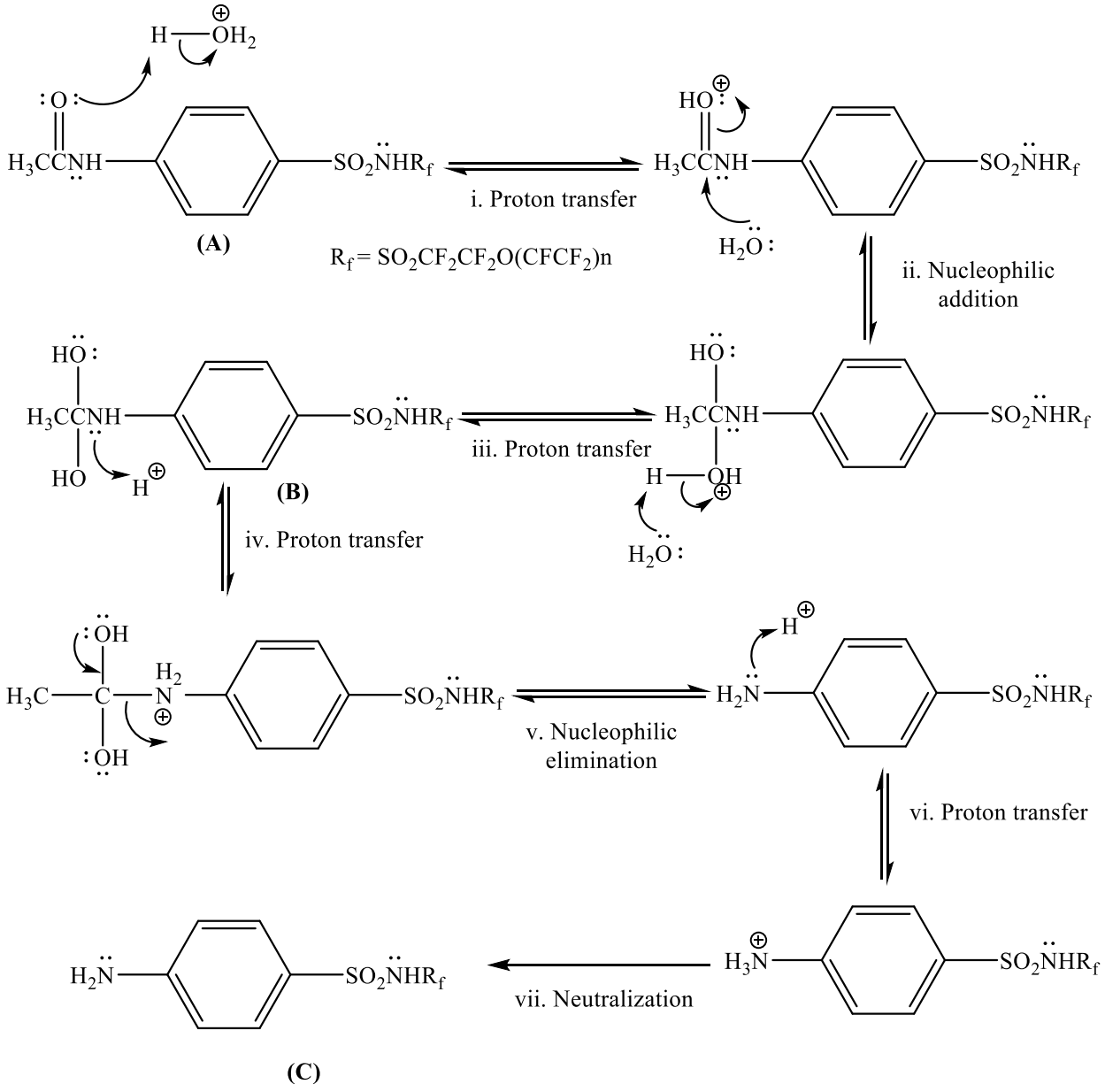

Scheme 14: The mechanism of the N-deacetylation catalyzed by a strong acid.[36]

The N-deacetylation of the PFSI aromatic acetamide in Scheme 13 is very effective to synthesize the PFSI aromatic amine compared to the reduction of the nitro substituted aromatic amide in Scheme 11. This strong electron withdrawing perfluoroalkyl backbone can destabilize the acetamide, which will be more reactive toward the nucleophile in the N-deacetylation.

Diazotization Reaction

The diazotization reactions are utilized in the synthesis of diazonium salts from primary or aromatic amines by using nitrous acid. The mechanism for the diazotization reaction is as shown in Scheme 15.[55] The reactions are usually conducted in organic solvents or aqueous media.[56] Excess amount of acid is normally used to avoid partial diazotization.

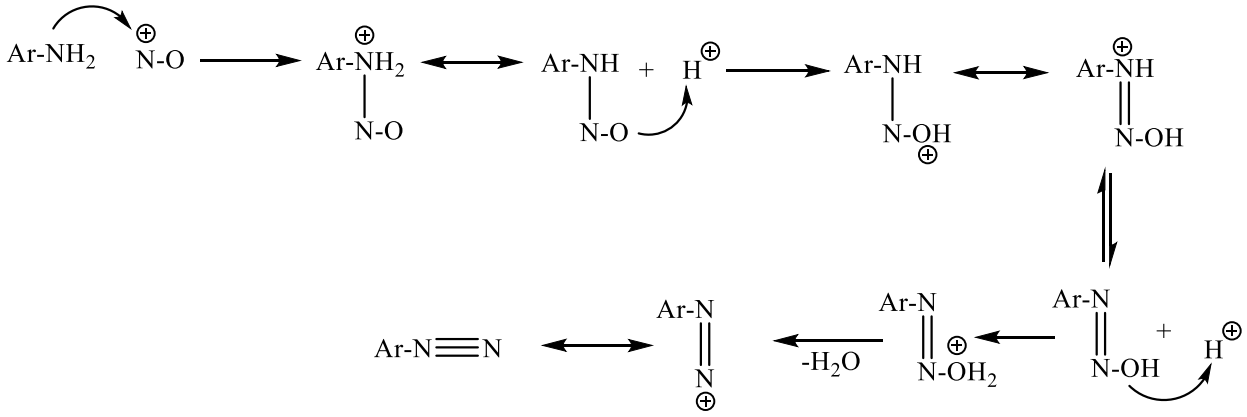

Scheme 15: Diazotization of Primary Aromatic Amines mechanism. [55]

Two diazotization reagents were tried to obtain diazonium salts **(9a)** as shown in Scheme 16.

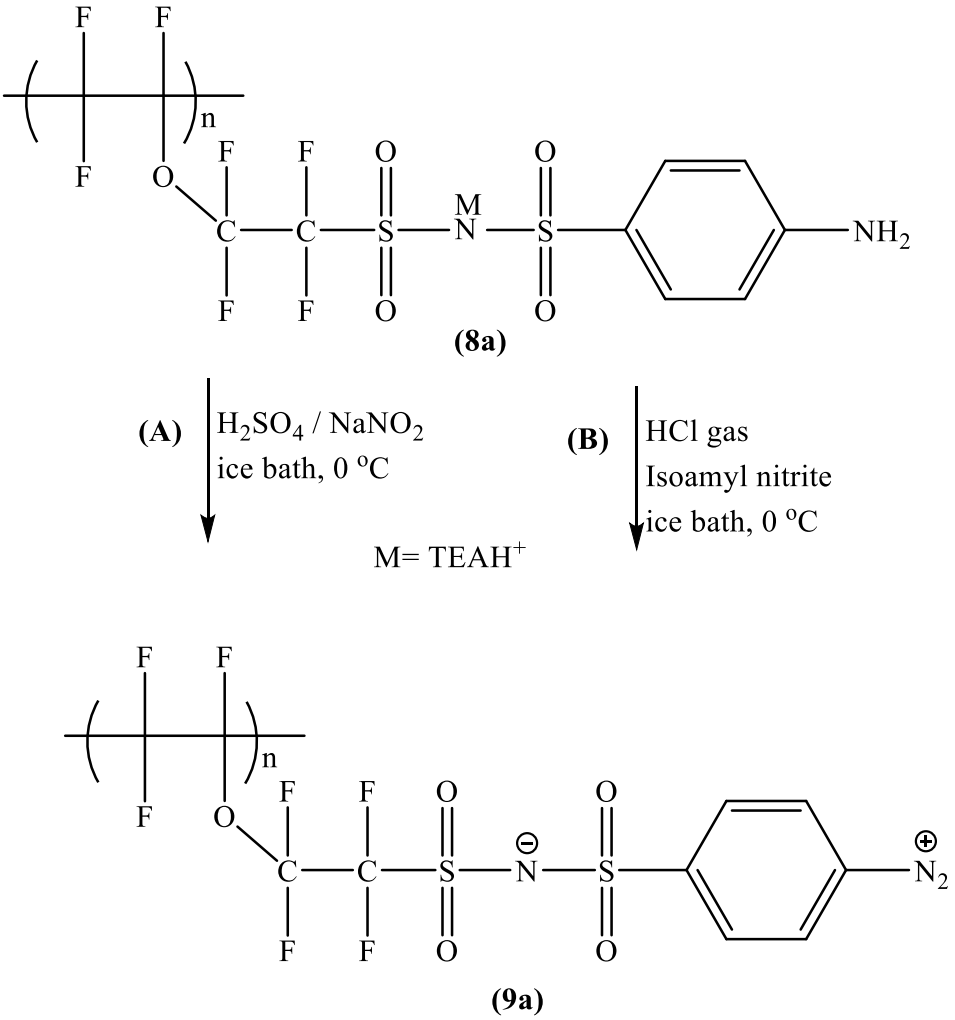

Scheme 16: The summary of two diazotization reactions

For the reaction **(A)**, conc. HCl was first attempted but failed due to the low solubility of starting material **(8a)**. Thus, conc. H_2SO_4 was utilized to complete the reaction. With dielectric constant around 100, H_2SO_4 is considered a very polar liquid.[33] The reaction **(A)** was successfully carried out according to ^{19}F-NMR and ^{1}H-NMR spectrums. The purification process includes vacuum filtration after poured into ice and drying under vacuum line. However, removing the excess of H_2SO_4 is troublesome. Other further purification methods, such as extraction from water and drying, were also tried but failed. The reaction **(A)** was repeated but

with smaller amount of H_2SO_4 (3mL rather than 10mL) and stirring for longer time (5 hrs rather than 2 hrs).

After purification, the ^{1}H-NMR, ^{19}F-NMR, and IR spectra showed the possibility that the final purified product **(9a)** was obtained and contaminated with TEAH cation. However, according to the GPC, the diazonium salt **(9a)** has a very low molecular weight (Mw: 2331). The possible reason for unreasonable molecular weight is that the majority of polymer may be lost during purification. According to the proton NMR, the possible product after the diazotization is shown in figure 9. The polymer is not a zwitterion as we designed.

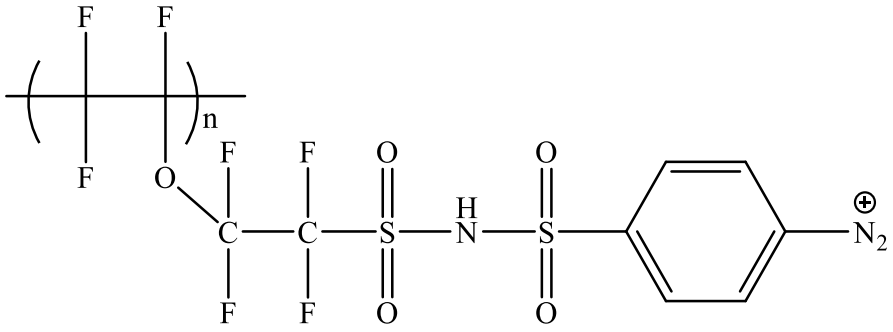

Figure 12: The possible protonation of diazonium salts **(9a)**

Another procedure, reaction **(B)**, was proposed to prepare the diazonium salt **(9a)** by the treatment of N-deacetylation product **(8a)** with isoamyl nitrite in the presence of HCl gas. In reaction **(B)**, organic diazotization agent, isoamyl nitrite, is used rather than inorganic $NaNO_2$. Generally, the procedure of reaction **(B)** is very simple because both isoamyl nitrite and HCl gas are easily removed after reaction. [46] According to ^{1}H-NMR and GPC results, the stable polymer zwitterionic product is not obtained. Therefore, the procedure **(B)** will be attempted again with different conditions and amount of organic reagents in order to obtain the diazonium salt **(9a)** with resorbable data, especially the GPC data.

CHAPTER 3

EXPERIMENTAL

General Consideration

NMR Spectroscopy

^{1}H and ^{19}F, nuclear magnetic resonance (NMR) spectra, were measured by using a Joel JNM-ECP-ECP 400-MHz FT NMR spectrometer. The chemical shifts were observed regarding parts per million (ppm) using high-frequency position conversion; the coupling constants are stated as J value in Hertz (Hz). The standardized reference material used for the ^{1}H NMR spectra was the tetramethylsilane (TMS) while for the ^{19}F NMR was trichlorofluoromethane ($CFCl_3$) external standards. The residue H in CD3CN, was found to be 1.97 ppm concerning TMS.

The splitting patterns of resonance were arranged as singlet (s), doublet (d), triplet (t), the quartet (q), and multiplet (m). A solution is having a concentration of 1–2 mmol/L was used to measure the NMR spectra. Similarly, a small volume of $CFCl_3$ gas was used only in ^{19}F NMR.

Gas Chromatography-Mass Spectrometer

The Shimadzu GCMS-QP2010 Plus GC was used to record the gas chromatography-mass (GC-MS) spectroscopy. The samples was prepared by dissolving around 1 mg of sample in 1 mL of acetone.

Infrared Spectroscopy

The infrared spectra were recorded with Shimadzu IR Prestige-21FIR. Then the fine powder sample was put on the lens of the attenuated total internal reflectance accessory. The infrared (IR) spectra was scanned from 4000 cm-1 to 450 cm-1, and the quotation of wavenumbers (cm^{-1}) to intensity abbreviations was strong (s), very strong (vs), and medium (m). Others include weak (w) and very weak (vw).

Glass Vacuum System

Several purification processes such as reduced pressure distillation, sublimation, and drying were carried out using a glass vacuum line as shown in Figure 13. The vacuum line was equipped with Teflon® glass-Teflon valves and it consisted of two manifolds. Among them, one manifold for vacuum line and another one is for purging the nitrogen/argon gas. It contains a built-in separation system, a liquid nitrogen trap, a diffusion pump and a mechanical Welch vacuum pump. In essence, an excellent dynamic vacuum is believed to be between 10^{-4} - 10^{-7} torr.

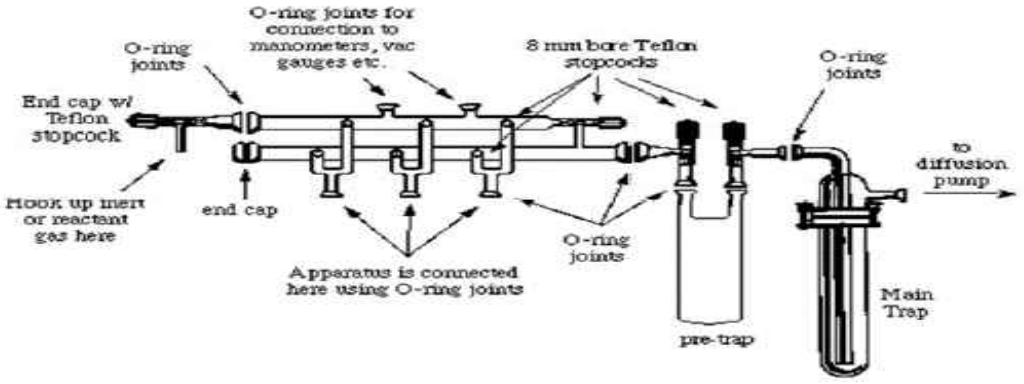

Figure 13: The diagram of a dual-manifolds glass vacuum line. Used with permission.[60]

Purification of Solvents and Experimental Practice

The starting materials: perfluorobenzoyl chloride, N-acetyl sulfanilyl chloride, and perfluoro(3-oxapent-4-ene) sulfonyl fluoride monomer (C_4F_8 S O_3) were all bought from commercial sources and were used as stated by the manufacturer unless advised otherwise. All the reactions were carried out in glassware unless specified otherwise. The compounds that readily react with the air or moisture were kept in a special dry box under nitrogen gas protection. Activated molecule sieve was used to dry the solvents.

Synthesis of the Initiator, Perfluorobenzoyl Peroxide

In a typical procedure, the mixture of hydrogen peroxide (1.50 mL, 63.94 mmol) and 4 M of sodium hydroxide (0.31 mL, 1.24 mmol) was added into a 25-mL round-bottom flask with a stir bar first. In an ice bath, perfluorobenzoyl chloride (0.50 g, 2.17 mmol) was then added dropwise over approximately 10 minutes by using a dropping funnel. While the solution was allowed to stir at 0°C, another 1 mL of 4 M of sodium hydroxide was added until the pH reached eleven. After that, the solution was allowed to stir another one hour at 0 °C. The crude product was got as a white precipitate, and then the white precipitate was filtered. Next, the crude product was recrystallized from chloroform/methanol mixture (1:2 by volume). In an ice bath, the crude product was dissolved in 1.5 mL of chloroform, and 3 mL of methanol was then added. The 0.385 grams of purified perfluorobenzoyl peroxide was obtained after filtration. The percentage yield is 77.4 %.

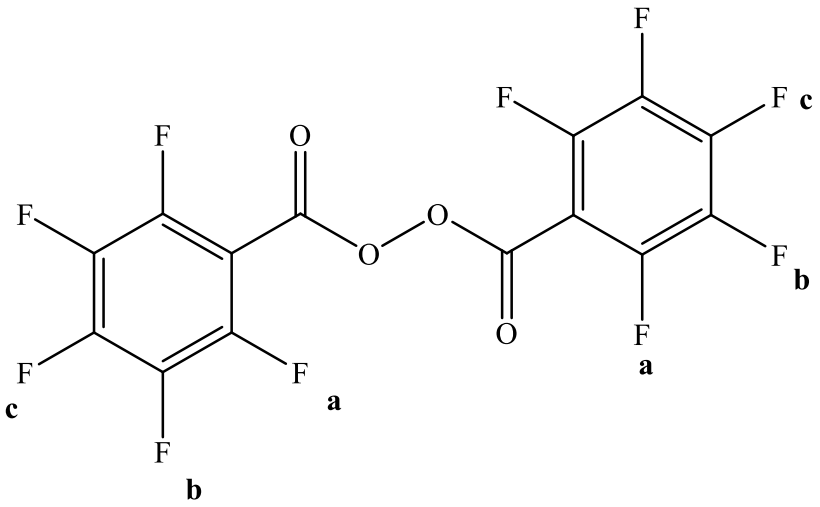

^{19}F NMR (400 MHz; CDCl3; ppm): δa -134.26 (2F, d), δb -143.73 (1F, t), δc -158.62 (2F, d).

Melting Point: 76-78 °C

IR (νmax/cm-1): 1786.08 m (C=O), 1056.99 m (C-O), 1651.07m (Ar), 1157.29 m, (Ar-F), and 991.41 vs, 906.54 m, and 802.39 vs (C-F).

Synthesis of 4-sulfamonylacetanilide

In a typical procedure, N-acetyl sulfanilyl chloride (5.0 g, 21.4 mmol) was dissolved in 30 mL of ammonia hydroxide (28-30%) and 20 mL of acetonitrile in a 100 mL round bottom flask. The solution was refluxed for 24 hours at 100 ^{o}C and the solvent was removed by the rotary evaporator. The solid crude product was washed by water and then vacuum filtered. The pure product was obtained with a yield of 72.3 %.

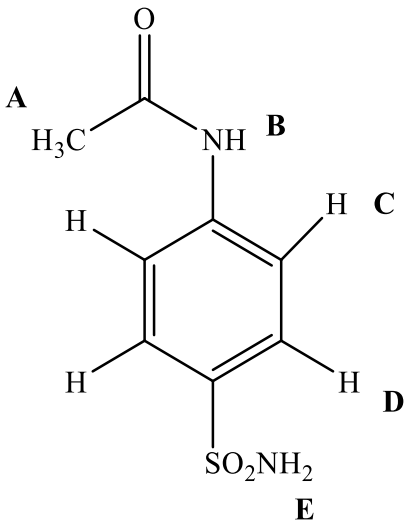

^{1}H NMR (400 MHz; CD_3CN; ppm): δ_A 2.10 (3H, s), δ_B 8.71 (1H, s), δ_C 7.78 (2H, d), δ_D 7.74 (2H, d), J_{CD} = 8 Hz, and δ_E 5.64 (2H, s).

IR (vmax/cm-1): 3367.71 m (NH), 3290.56 m, 3205.69, and 1593.20 m (NH_2), 1654.92 m (C=O), and 1315.45 s and 1153.43 vs (S=O).

MS (M^+, 100%), 214, 172, 156, 108, 92, and 65

Synthesis of 4-nitrobenzenesulfonyl amide

In a typical procedure, 4-nitrobenzenesulfonyl chloride (5.0 g, 22.6 mmol) was dissolved in 30 mL of ammonia hydroxide (28-30%) and 20 mL of acetonitrile in a 100 mL round bottom flask. The solution was refluxed for 24 hours at 100 ^{o}C and the solvent was removed by the

rotary evaporator. The solid crude product was washed by water and then vacuum filtered. The pure product was obtained with a yield of 78.4 %.

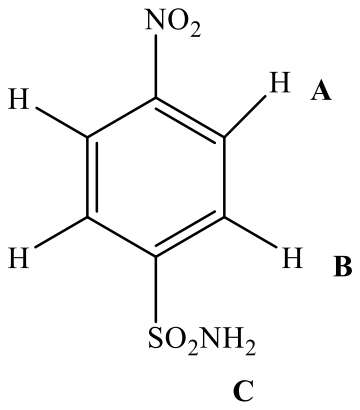

^{1}H NMR (400 MHz; CD_3CN; ppm): δ_A 8.37 (2H, d), δ_B 8.11 (2H, d), J_{AB} = 8 Hz, and δ_C 5.97 (1H, s).

IR (vmax/cm-1): 3332.99 w and 1612.49 w (NH), 1566.20 (C=C), 1516.05 m and 1346.31 s (NO), and 1311.59 m and 1161.15 s (S=O).

MS (M^+, 100%), 202, 156, 138, 122, 92, and 75

Synthesis of $FSO_2CF_2CF_2O(CFCF_2)n$

In a typical procedure, perfluoro (3-oxapent-4-ene) sulfonyl fluoride (5.0 g, 17.9 mmol) was placed in a Parr stainless steel reactor equipped with a stir bar. Perfluorobenzoyl peroxide (0.1 g, 0.44 mmol, 2% weight of the monomer) was then added, and the reactor was pressurized to 150–160 psi (1000– 1100 kPa) with argon gas and heated to 100°C for 5 days. Excess monomer was then removed by distillation in a Kugelrohr apparatus under vacuum at 145 °C. 2.0 grams product was obtained, and the percentage yield of polymer is about 40.6 %.

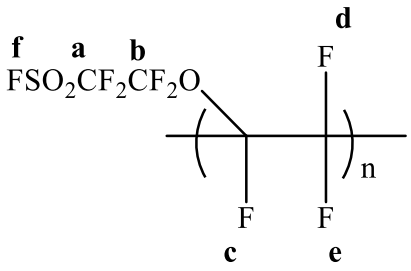

^{19}F NMR (400 MHz; CD_3CN; ppm): δa -112.32 (2F, m), δb -77.52 (2F, m), δc -138.19 (1F, m), δd and δe -115.82 and -118.43 (2F, d), and δf 45.82 (1F, s).

IR (νmax/cm-1): 1188.15 vs (S=O), 1138.00 vs (CF_2), and 987.55 m (C-F).

GPC (logM / RT): Mw: 45,564, and Polydispersity index (Mw/Mn): 2.024

Synthesis of 4-NO_2PhSO_2NHS$O_2$$CF_2CF_2O(CFCF_2)n$

In a typical procedure, in the glove box, 1.40 g (around 5.35 mmol) of poly fluorosulphonyl-tetrafluoroethyl trifluorovinyl ether and 1.10 g (5.44 mmol) of 4-nitrobenzene sulfonyl amide were added to in a 100-ml round bottom flask equipped with a rubber septum. And then, 15 mL of dry acetonitrile and 1 ml of trimethylamine were added to the flask. With the argon gas protection, the solution was refluxed at 100 ºC for five days. After that, rotary evaporator was used to remove solvents. The sticky product was dissolved in 50 mL of acetone, and then the solution was acidified with 5 mL of 1M HCl until the pH reached two. The rotary evaporator was used to remove acetone after acidification. Then the sticky product was then extracted with dichloromethane (3 X 25 mL) and washed with water (3 X 25 mL). The product was obtained after removing the solvent and drying over the night. And then the product was sublimated at 145 ºC overnight. The percent yield of 67.6 % was obtained.

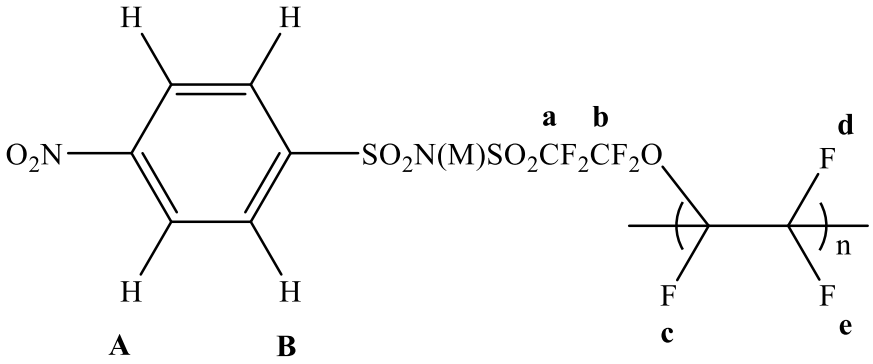

M= $TEAH^+$

^{1}H NMR (400 MHz; CD_3CN; ppm): δ_A 8.28 (2H, d), δ_B 8.06 (2H, d),), and J_{AB} = 8 Hz.

^{19}F NMR (400 MHz; CD_3CN; ppm): δa -113.67 (2F, m), δb -77.39 (2F, m), δc -137.56 (1F, m), δd and δe -116.67 and -118.68 (2F, d).

IR (νmax/cm-1): 1527.62 m and 1350.17 m (NO), 1284.59 m, 1157.29 vs and 1091.17 s (S=O), and 1049.28 s and 1141.86 vs (CF_2).

Synthesis of $CH_3CONHPhSO_2NHSO_2CF_2CF_2O(CFCF_2)_n$

In a typical procedure, in the glove box, 2.81 g (around 10.0 mmol) of poly perfluorosulfonyl-tetrafluoroethyl trifluorovinyl ether and 2.14 g (10.03 mmol) of benzenesulfonyl amide were added to in a 100-ml round bottom flask equipped with a rubber septum. And then, 42 mL of dry acetonitrile and 3 ml of trimethylamine were added to the flask. With the argon gas protection, the solution was refluxed at 100 ^oC for five days. The rotary evaporator was then used to remove solvents. The sticky product was dissolved in 20 mL of acetone, and then the solution was acidified with 3 mL of 6M HCl until the pH reached two. After removing the solvent, the crude product was washed by concentrated HCl. Next, the product was run through a chromatography column by using a 1:1 ratio of tert-butyl methyl ether to acetone to remove the excess starting material **(4a)**, R_f value of 0.82 on the TLC plate. The

purified product was obtained after removing the solvent and drying over the night. The percent yield of 70.6 % was obtained.

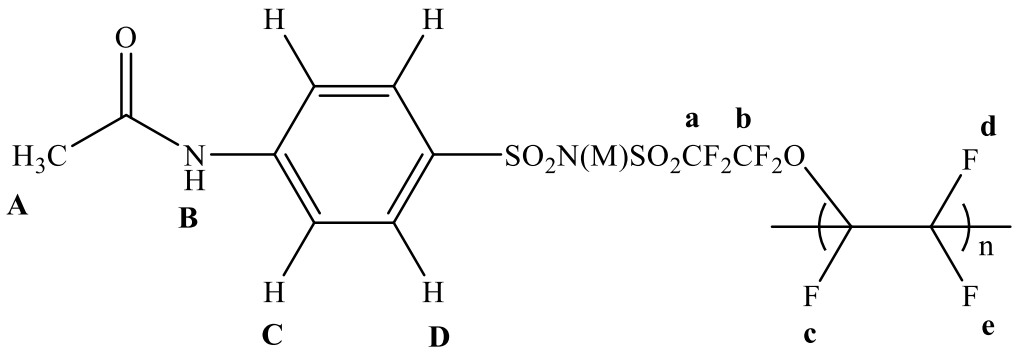

M= $TEAH^+$

^{1}H NMR (400 MHz; CD_3CN; ppm): δ_A 2.09 (3H, s), δ_B 9.02 (1H, s), δ_C 7.78 (2H, d), δ_D 7.73 (2H, d), and J_{CD} = 8 Hz.

^{19}F NMR (400 MHz; CD_3CN; ppm): δa -111.13 (2F, m), δb -76.61 (2F, m), δc -138.67 (1F, m), δd and δe -116 and -119 (2F, d).

IR (νmax/cm-1): 3283.84 (NH), 1654.92 m (C=O), 1593.20 m (C=C), 1315.45 m, 1242.16 m, and 1153.43 vs (S=O), and 1045.42 s (CF_2).

GPC (logM / RT): Mw: 47,076, and Polydispersity index (Mw/Mn): 1.881

Synthesis of 4-$NH_2PhSO_2NHSO_2CF_2CF_2O(CFCF_2)_n$

In a typical procedure, the coupled product (1.2 g, 1.30 mmol) was added into a 100 mL round bottom. Then 25 mL of methanol and 14 mL of concentrated acid were added to it till it is acidic. The solution was allowed to react under the sonication overnight. The solution was then neutralized with 6.0M of NaOH solution. Next, the solid liquid extraction was then carried out by using acetone as a solvent. The impurities were removed by vacuum sublimation at 125 ^oC overnight. The purified product (53.3 %) was obtained.

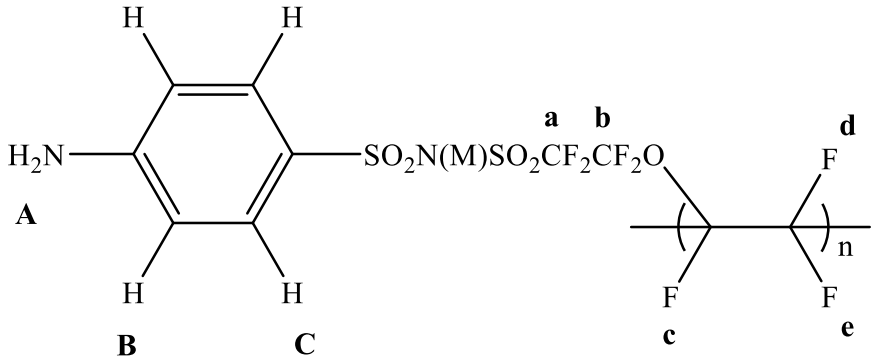

M= $TEAH^+$

^1H NMR (400 MHz; CD_3CN; ppm): δ_A 5.43 (2H, s), δ_B 7.56 (2H, d), δ_C 6.70 (2H, d), and J_{BC} = 8 Hz.

^{19}F NMR (400 MHz; CD_3CN; ppm): δa -113.67 (2F, m), δb -77.31 (2F, m), δc -137.78 (1F, m), δd and δe -116.67 and -118.68 (2F, m).

IR (νmax/cm-1): 3475.73 w, and 1627.92 m(NH), 3379.29 w and 3244.27 w (NH_2), 1597.06 (C=C), 1365.60 w, 1257.59 s, and 1149.57 vs (S=O), and 1056.42 s (CF_2). GPC (logM / RT): Mw: 56,920, and Polydispersity index (Mw/Mn): 1.97

Synthesis of 4-N_2^+ $PhSO_2N^-SO_2CF_2CF_2O(CFCF_2)n$

In a typical procedure, 0.240 g (1.40 mmol) of N-deacetylation product, 0.250 g (3.63 mmol) of $NaNO_2$, and 3 mL of concentrated H_2SO_4 were added to a 25 mL round bottom flask equipped with a stir bar. The solution was stirred for 5 hours in an ice bath and then poured onto ice. The purified product was obtained after vacuum filtration and drying over the night. The percent yield of 60.7 % was obtained.

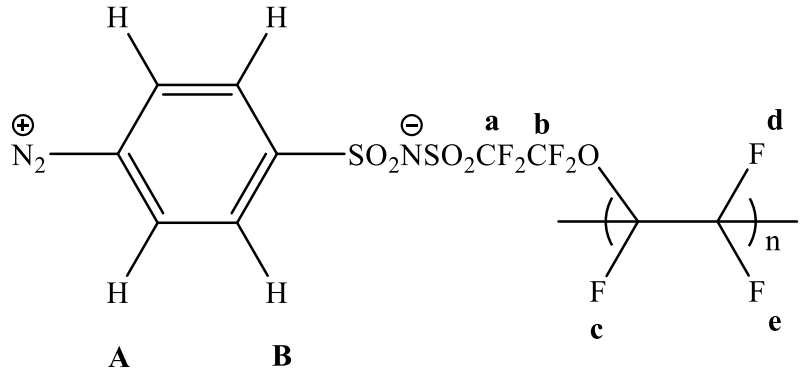

^{1}H NMR (400 MHz; CD_3CN; ppm): δ_A 8.62 (2H, d), and δ_B 8.25 (2H, d), and J_{AB} = 8 Hz.

^{19}F NMR (400 MHz; CD_3CN; ppm): δa -111.49 (2F, m), δb -77.24 (2F, m), δc -136.36 (1F, m), δd and δe -116.69 and -118.34 (2F, m).

IR (νmax/cm-1): 2357.01 w (N≡N), 1292.31 m, and 1176.58 s (S=O), 1415.75 m and 1134.14 vs, and 1037.70 s (CF_2). GPC (logM / RT): Mw: 2331, and Polydispersity index (Mw/Mn): 1.13

CHAPTER 4

CONCLUSION

One new diazonium N-(perfluoroalkyl) benzenesulfonimide (PFSI) polymer, from perfluoro (3-oxapent-4-ene) sulfonyl fluoride monomer, is first prepared with overall 60.7 % yield. Spectroscopic techniques, including GC-MS, IR, NMR, and GPC are used for characterization of all the intermediates and the final product. Two synthetic routes were tried to and one of them succeeded in preparing the target polymer.

The perfluorobenzoyl peroxide initiator was easily prepared. The homopolymerization of $FSO_2CF_2CF_2OCF=CF_2$ was successful with relatively low yield because of the low conversion rate of free radical polymerization.

For the para substituted benzenesulfonychlorides, the ammonolysis reactions are also very easy to carry out with reasonable good yield. The next coupling reactions were completed successfully in extreme dry condition to reduce the hydrolysis byproduct. The excess starting material para substituted benzenesulfonyl amide, **(4b)**, was removed by vacuum sublimation. For another coupling reaction **(A**) from 4-sulfamonylacetanilide, **(4a),** the excess **4a** was removed through column chromatography. The yield of coupling products was around 70%. Due to the difficulty to remove the $TEAH^+$, DIEA is proposed to replace the TEA as the organic base catalyst.

The purification of the next reduction product was unsuccessful due to the big amount iron powder used. N-deacetylation reaction is comparable facile to carry out and obtain the purified PFSI aromatic amine product. The percent yield of the N-deacetylation product was around 50 %.

Two groups of diazotization reagents, include inorganic sodium nitrate with HCl or concentrated sulfuric acid and isoamyl nitrate with HCl gas, were attempted to conducted diazotization reaction. Till now, the concentrated H_2SO_4 with $NaNO_2$ was effective to obtain diazonium salts. The yield of the final purified product was around 60. Another diazotization with organic diazotization regents was not completed and will be tried again in the near future.

REFERENCES

[1] Spiegel, C. Designing and building fuel cells; McGraw-Hill, Two Penn Plaza, New York, **2007**; pp 3.

[2] Papageorgopoulos D. DOE fuel cell technology program overview and introduction to the 2010 fuel cell pre-solicitation workshop in DOE fuel cell pre-solicitation workshop. Department of Energy, Lakewood, Colorado; **2010**.

[3] [Barbir F. PEM Fuel Cells: Theory and Practice. 1 st ed.; Elsevier Academic Press: New York, **2005**

[4] Devanathan R. Recent developments in proton exchange membranes for fuel cells. Energy Environ Sci **2008**; 1:101–19.

[5] Hickner, M.; Ghassemi, H.; Kim, Y.S.; Einsla, B.; McGrath, J.E. Alternative Polymer Systems for Proton Exchange Membranes (PEMs). Chem. Rev. **2004**, 104, 4587- 4612.

[6] Wand, G. Fuel cell history, Part One. www.ogniwa-paliwowe.info, **2006**.

[7] Wang, Y.; Chen, K.S.; Mishler, J.: Cho, S.C.; Adroher, X.C. A review of polymer electrolyte membrane fuel cells: Technology, applications, and needs on fundamental research (2011). US DOE Publications. Paper 132.

[8] Hua, Mei, Perfluoroalkyl (Aryl) Sulfonimide Zwitterions. Ph.D. Dissertation, Clemson University, Clemson, SC, **2006**.

[9] Walter, Katie. The unitized regenerative fuel cell: Science and technology review, May 1**997**, p. 13, http: //www.llnl.gov/str/Mitlit.html.

[10] Ryan Baker and Jiujun Zhang Institute for fuel cell innovation. National Research of Canada, 4250 Wesbrook Mall, Vancouver, British Columbia V6T 1W5, Canada, **2011**.

[11] Steele, B.C.H., and Heinzel, Angelika. Materials for fuel-cell technologies: Nature, **2001** v. 414, p. 345–352.

[12] Cheng, X.; Shi, Z.; Glass, N.; Zhang, L.; Song, D.; Liu, Z. S.; Wu, S.; Merida, W. A. A Review of PEM Hydrogen Fuel Cell. Journal of Power Sources. **2007**, 165, 739-756.

[13] Schmittinger, W.; Vahidi, A.; A Review of the Main Parameters Influencing Longterm Performance and Durability of PEM Fuel Cells. Journal of Power Sources. **2008** v 180[1], p.1-14.

[14] Thampan, T.; Malhotra, S.; Zhang, J.; Datta R. PEM Fuel Cell as a Membrane Reactor. Catal. Today**, 2001**, 67[1-3], 15-32.

[15] Litster, S.; Mclean, G. PEM Fuel Cell Electrodes. J. Power Source. **2004**, 130, 61.

[16] Panchenko, A.; Dilger, H.; Moller, E.; Sixt, T.; Roduner, E. Insitu EPR investigation of Polymer Electrolyte Membrane Degradation in Fuel Cell Application. J. Power Sources 2004, 127, 325-330, doi:10.1016/j.jpowsour.**2003**.09.047

[17] Hogarth, W.H.J; da Costa, J.C.D; Lu, G.Q. J. Power Sources. **2005**, 142 223.

[18] Thompson, S.D.; Jordan, L.R.; Forsyth, M. Platinum electrodeposition for polymer electrolyte membrane fuel cells. Electrochim. Acta, **2001**, 46, 1657-1663.

[19] Yu, T.L.; Lin, H.; Su1, P.; and Wang, G. Structures of Membrane Electrode Assembly Catalyst Layers, The Open Fuels & Energy Science Journal, **2012**, Volume 5

[20] Creager, S. E. Proposal for DOE project, **2006**

[21] Smitha, B.; Sridhar, S.; Khan. A. A. Solid Polymer Electrolyte Membrane for Fuel Cell. J. Mebran. Sci. **2005**, 259, 10-26.

[22] Moilanen, D. E., Spry, D. B., Fayer, M. D.Water Dyanmics and Proton Transfer I Nafion Fuel Cell Membranes. Langmuir **2008**, 24 [8], 3690-3698

[23] Fuel Cells, Types of Fuel Cells. http;//www. Fuelcells.Org/fuel/fctypes.html, **2000**.

[24] Mauritz, K.A.; Moore, R.B. State of Understanding Nafion. Chem. Rev. **2004**, 104 4535-4585.

[25] Hongxiang Teng. Review Overview of the Development of the Fluoropolymer Industry. Appl. Sci. **2012**, 2, 496-512; doi:10.3390/app2020496. http;//www.mdpi.com/journal/applsci

[26] Olah, G. A.; Iyer, P. S.; Prakash, G. K. S.Perfluorinated Resinsulfonic Acid (Nafion- Hw) Catalysis on Synthesis. Synthesis **1986**, 7, 513

[27] Honma, I.; Nakajima, H.; Nishikawa, O.; Sugimoto, T.; Nomura, S. Family of High-Temperature Polymer-Electrolyte Membranes Synthesized From Amphiphilic Nanostructured Macromolecules, J. Electrochem. Soc., **2003**, 150, A616.

[28] Arcella, V.; Ghielmi, A.; Polastri, F.; Vaccarono, P. Fluorinated membranes, EP 1589062 A2, **2005**

[29] Shen Wu, H.; Martin, C. W.; Chen, X. K. Low equivalent weight ionomer, US 7094851 B2, **2006**

[30] Y.G. Chun, C.S. Kim, D.H. Peck, D.R. Shin, J. Power Sources 71 (**1998**) 174.

[31] Gould, Elizabeth-Ann. The Photochemistry of "Super" Photoacid N-Methyl- 6-Hydroxyquinolinium and Other Novel Photoacids. Ph.D. Dissertation, Georgia Institute of Technology, Atlanta, GA, **2012**.

[32] Yang, T.F.; Hourng L.W.; Yu, T.L.; Chi, P.H.; Su, A. High performance proton exchange membrane fuel cell electrode assemblies. J. Power Sources, **2010**, 195, 7350-7369.

[33] Lee, D.; Hwang, S. Effect of loading and distributions of Nafion ionomer in the catalyst layer for PEMFCs. Int. J. Hydrog. Energy **2008**, 33, 2790–2794.

[34] Gadallah, F. F.; Elofson, R. M. J. Org. Chem. **1969**, 34, 3335-3339.

[35] Koppel, I. A.; Taft, R. W.; Anivia, F.; Zhu, S. Z.; Hu, L. Q.; Sun, K. S.; DesMarteau, D. D.; Yagupolskii, L. M.; Yagupolskii, Y. L.; Vlasoz, V. M.; Notario, R.; Maria, P. C. The

Gas-Phase Acidities of Very Strong Neutral Bronsted Acids. J. Am. Chem. Soc. **1994**, 116, 3047

[36] Zhang, M.; Sonoda, T.; Mishima, M.; Honda, T.; Leito, I.; Koppel, I. A.; Bonrath, W.; and Netscher, T. Gas-Phase Acidities of bis[(perfluoralkyl)]imides. Effects of the perfluoroalkyl group on acidity. J.Phys.Org Chem. **2014**, 27 676-679

[37] Delamar, M.; De´sarmot, G.; Fagebaume, O.; Hitmi, R.; Pinsonc, J.; Save´ ant, J.-M.Carbon 35 (6) (**1997**) 801–807; Brooksby, P.A.; Downard, A.J. Langmuir 20 (12) **2004** 5038 5045.

[38] Foropoulos, J. Jr.; DesMarteau, D. D., J. Am. Chem. Soc., 104, **1982**, 4260 and Foropoulos, J. Jr.; DesMarteau, D. D., Inorg. Chem., 23, **1984**, 3720

[39] Allongue, P.; Delamar, M.; Desbat, B.; Fagebaume, O.; Hitmi, R.; Pinson, J.; Save´ant, J.- M. J. Am Chem. Soc. **1997**, 119, 201-207.

[40] Ortiz, B.; Saby, C.; Champagne, G. Y.; Be´langer, D. J. Electroanal. Chem. **1998**, 455, 75 81.

[41] Saby, C.; Ortiz, B.; Champagne, G. Y.; Be´langer, D. Langmuir **1997**, 13, 6805-6813.

[42] Delamar, M.; Hitmi, R.; Pinson, J.; Save´ant, J. M. J. Am. Chem. Soc. **1992**, 114, 5883-5884

[43] a) Mei, H.; Ibrahim, F. *Journal of Fluorine Chemistry,* 199, 46–51, **2017**. b) Mei, H.; D'Andrea, D.; Nguyen, T.-T.; Nworie,C. *J. Power Sources*. 248, 1177-1180, **2014**. C) Mei, H.; Nworie, C.; Abban, G.; Alayyaf, A.; MacCloud, R. *Int. J. of Hydrogen Energy,* 41 (5), 3628-3637, **2016**. d) Mei, H.; D'Andrea, D.; Nguyen, T.-Tr.; Nworie, C. *Journal of Power Sources*, 248, 1177-1180, **2014**.

[44] Polym. Chem., **2013**, 4, 3370-3383.

[45] Schank, K., Methodicum Chimicum, Kowski, F.Z., Eds.; Academic Press: New York, **1975**; Vol. 6, pp 159.

[46] Cai, K.J., He, H.Q., Chang, Y.W. and Xu, W.M. (**2014**) An Efficient and Green Route to Synthesize Azo Compounds through Methyl Nitrite. *Green and Sustainable Chemistry*, **4**, 111-119.

[47] Venzo, A.; Antonello, S.; Gascón, J. A.; Guryanov, I.; Leapman, R. D.; Perera, N. V.; Sousa, A.; Zamuner, M.; Zanella, A.; Maran, F. *Analytical Chemistry* **2011**, *83*(16), 6355–6362.

[48] Karty J.; Organic Chemistry, Principles and Mechanism, 1st ed., W. W. Norton and Company, New York –London, **2014**, pp 1011-1027

[49] Atkins J R, Sides C R, Creager S E, Harris J L, Pennington W T, Thomas B H and DesMarteau DD. J. New Mater. Electrochem. Syst. **2003** 6.

[50] Huyser, E. S. *Free-radical chain reactions*; Wiley-Interscience: New York, **1970.**

[51] Sir Derek Barton, F. R. S.; Davidollis, W. F. R. S.,Comprehensive Organic Chemistry,**1979**.

[52] Kumar, P. S.; Lokanatha Rai, K. M. Chemical Papers 66 (8) 772–778 (**2012**)

[53] Nworie, C. Synthesis of a 4-(Trifluoromethyl)-2-Diazonium Perfluoroalkyl Benzenesuflonylimide (PFSI) Zwitterionic Monomer for Proton Exchange Membrane Fuel Cell. MS. Thesis, East Tennessee State University, Johnson City, TN, **2014**.

[54] Abban, G. Methodology Study of N-deacetylation of 4-acetamido perfluoroalkylbenzenesulfonimide. MS. Thesis, East Tennessee State University, Johnson City, TN, **2015**.

[55] Shaw, R. The Chemistry of Diazonium and Diazo Groups, Patai, S., Eds.; John Wiley & Sons: New York; **1978**; pp 199-164.

[56] Patai, S. The Chemistry of Diazonium and Diazo Groups (II), John Wiley & Sons, Chichester, New York, Brisbane, Toronto, An Interscience Publication, **1978**, 647

[57] Mei, H.; Ibrahim, F. *Journal of Fluorine Chemistry* **2017**, 199, 46–51.

[58] Ibrahim, F. Synthesis of Diazonium (Perfluoroalkyl) Arylsulfonimide Monomers from Perfluoro (3-Oxapent-4-ene) Sulfonyl Fluoride for Proton Exchange Membrane Fuel Cell Thesis, East Tennessee State University, Johnson City, TN, **2016**.

[59] Chalkova E.; Fedkin, M. V.; Wesolowski., D. J.; Lvov, S. N. Effect of TiO_2 Surface Properties on Perfromance of Nafion-Based Composite Membranes in High Temperature and Low Relative Humidity PEM Fuel Cell. J. Electrochem. Soc. **2005**, 152, A1742.

[60] Toreki, R. The Glassware Gallery: Schlenk Lines and Vacuum Lines. http://www.ilpi.com/inorganic/glassware/vacline.html (accessed Mar 15, 2016).

[61] Lepore, S. D.; Khoram, A.; Bromfield, D. C.; Cohn, P.; Jairaj, V.; Silvestri, M. A. The Journal of Organic Chemistry **2005**, 70 (18), 7443–7446.

[62] McKeen, L. W. Fluoropolymers. In *Film Properties of Plastics and Elastomers*; Elsevier, 2012; pp 255–313. https://doi.org/10.1016/B978-1-4557-2551-9.00011-6.

[63] Sayler, T. S.; Thrasher, J. S.; Fernandez, R. E.; Arduengo, A. J.; Bakker, M. G.; Shaughnessy, K. H.; Desmarteau, D. D. 80–124.

[64] Teng, H. Overview of the Development of the Fluoropolymer Industry. *Appl. Sci.* **2012**, *2* (2), 496–512. https://doi.org/10.3390/app2020496.

APPENDICES

APPENDIX A1: GC-MS Chromatogram of 4-sulfamonylacetanilide, **(4a)**

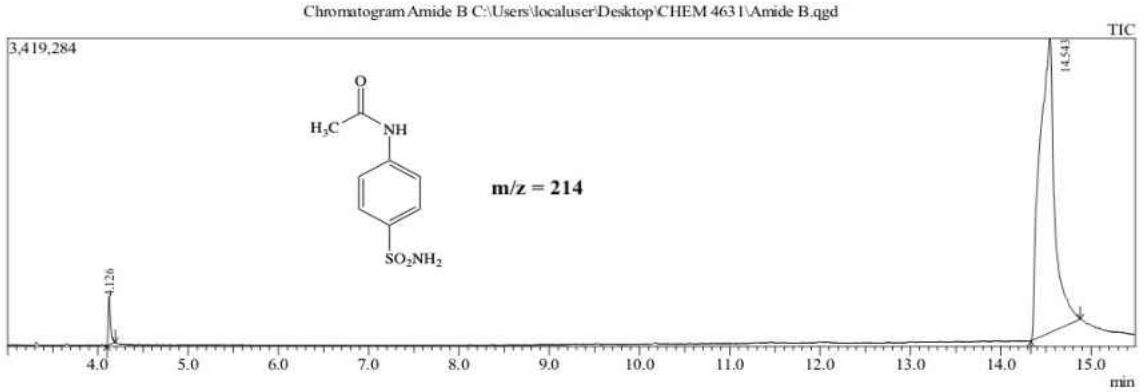

Peak Report TIC

Peak#	R.Time	I.Time	F.Time	Area	Area%	Height	Height%	A/H	Mark	Name
1	4.126	4.099	4.190	914843	2.36	537200	14.14	1.70		
2	14.543	14.333	14.879	37847511	97.64	3261464	85.86	11.60		
				38762354	100.00	3798664	100.00			

Spectrum

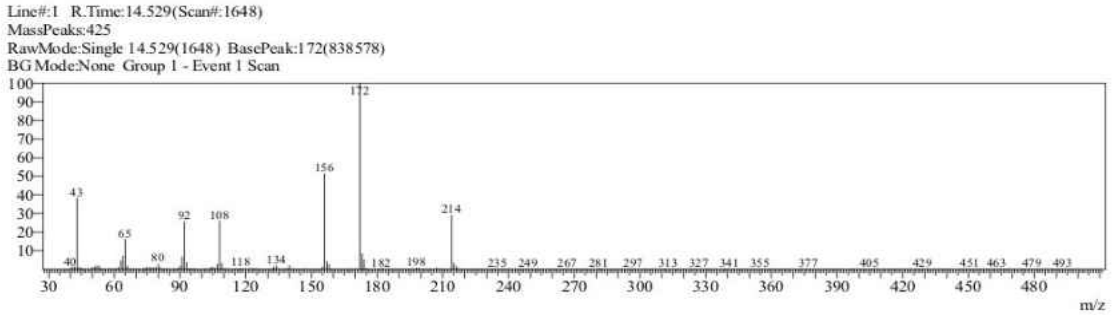

APPENDIX A2: GC-MS Chromatogram of 4-nitrobenzenesulfonyl amide, **(4b)**

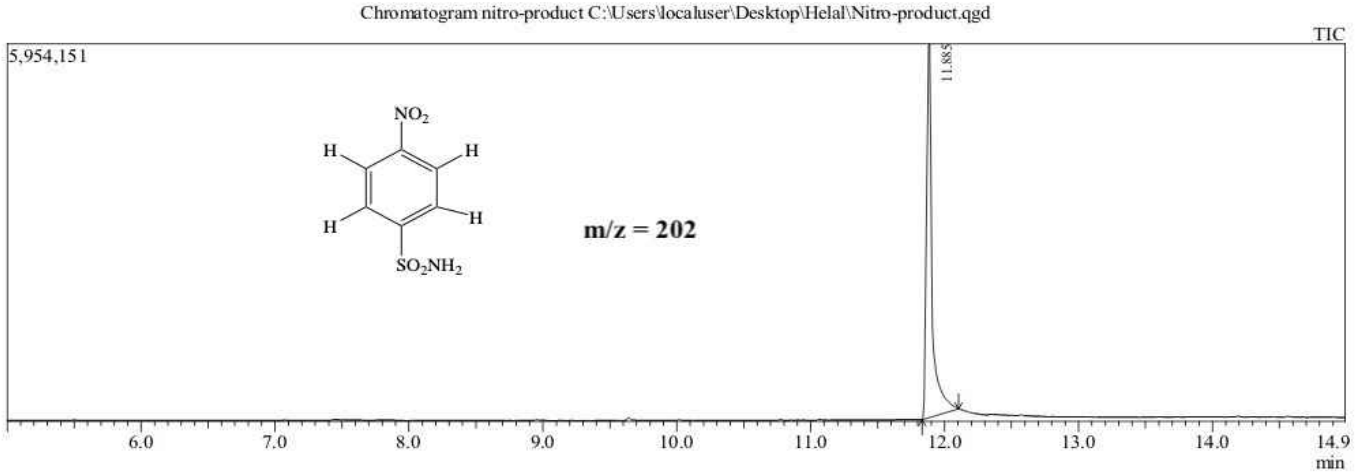

Peak Report TIC

Peak#	R.Time	I.Time	F.Time	Area	Area%	Height	Height%	A/H	Mark	Name
1	11.885	11.832	12.105	17364868	100.00	5893028	100.00	2.95		
				17364868	100.00	5893028	100.00			

Spectrum

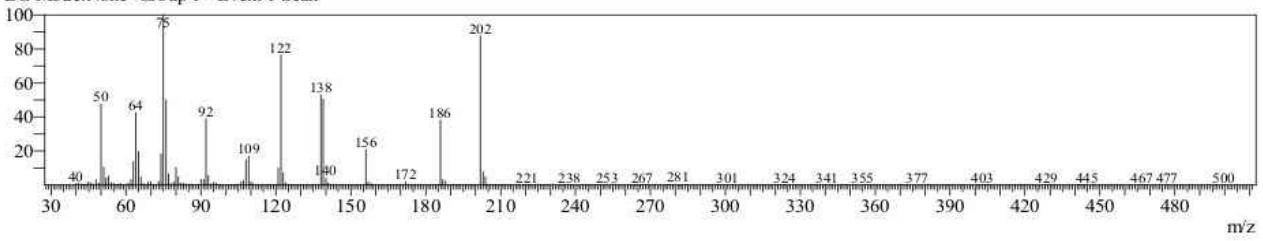

APPENDIX A3: The Gel permeation chromatography (GPC) data for $FSO_2CF_2CF_2O(CFCF_2)n$, **(6)**

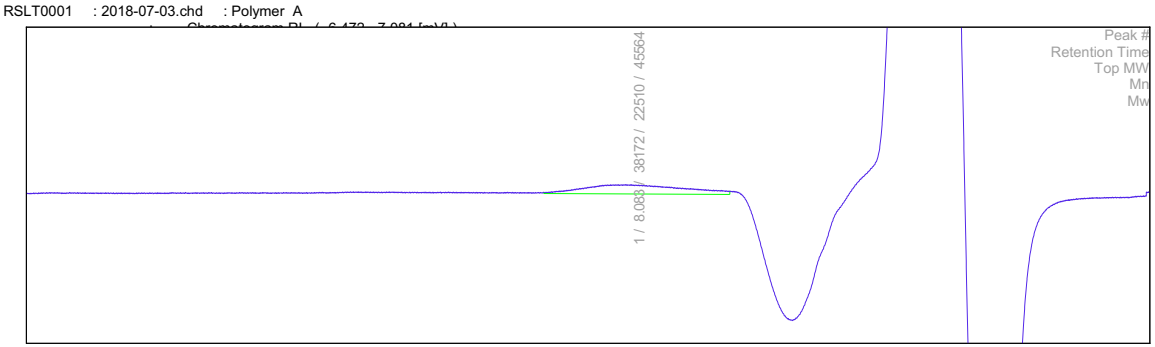

RSLT0001 : 2018-07-03.chd : Polymer A
: Chromatogram RI (-6.472 - 7.081 [mV])

- RI - Mn: 22510 Mw: 45564 Mz: 77397 Mw/Mn: 2.024

APPENDIX A4: The Gel permeation chromatography (GPC) data for $CH_3CONHPhSO_2N(M)SO_2CF_2CF_2O(CFCF_2)n$, **(7a)**

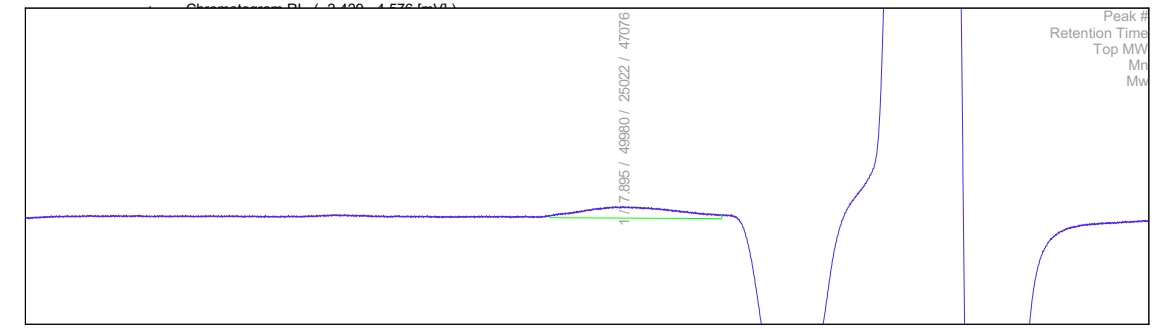

RSLT0002 : 2018-07-03.chd : Polymer B
: Chromatogram RI (-2.429 - 4.576 [mV])

- RI - Mn: 25022 Mw: 47076 Mz: 76612 Mw/Mn: 1.881

APPENDIX A5: The Gel permeation chromatography (GPC) data for 4-$NH_2PhSO_2N(M)SO_2CF_2CF_2O(CFCF_2)n$, **(8a)**

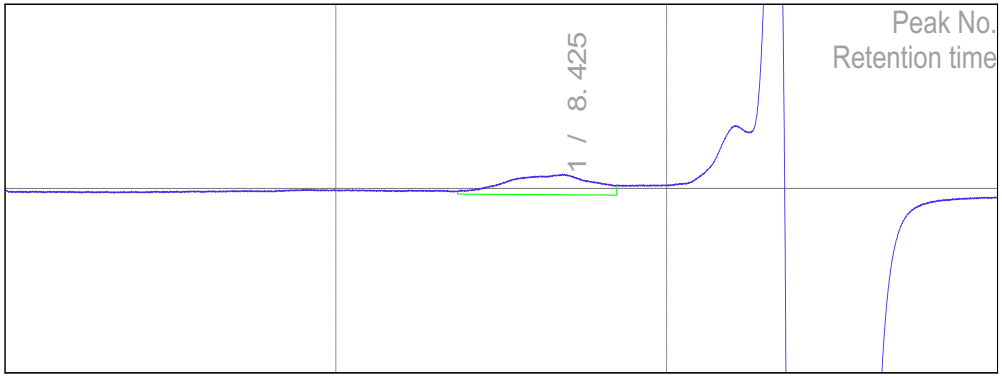

Result of molecular weight calculation (RI)

Peak 1 Valley Peak

	[min]	[mV]	[mol]		
Peak start	6.838	-0.092	315,350	Mn	28,890
Peak top	8.425	0.394	28,995	Mw	56,920
Peak end	9.243	0.082	7,806	Mz	106,974
				Mz+1	162,516
				Mv	56,920
Height [mV]			0.564	Mp	28,996
Area [mV*sec]			50.263	Mz/Mw	1.879
Area% [%]			100.000	Mw/Mn	1.970
[eta]			56920.01147	Mz+1/Mw	2.855

APPENDIX A6: The Gel permeation chromatography (GPC) data for 4-$N2^{+}PhSO2N^{-}SO2CF_2CF_2O(CFCF_2)n$, **(9a)**

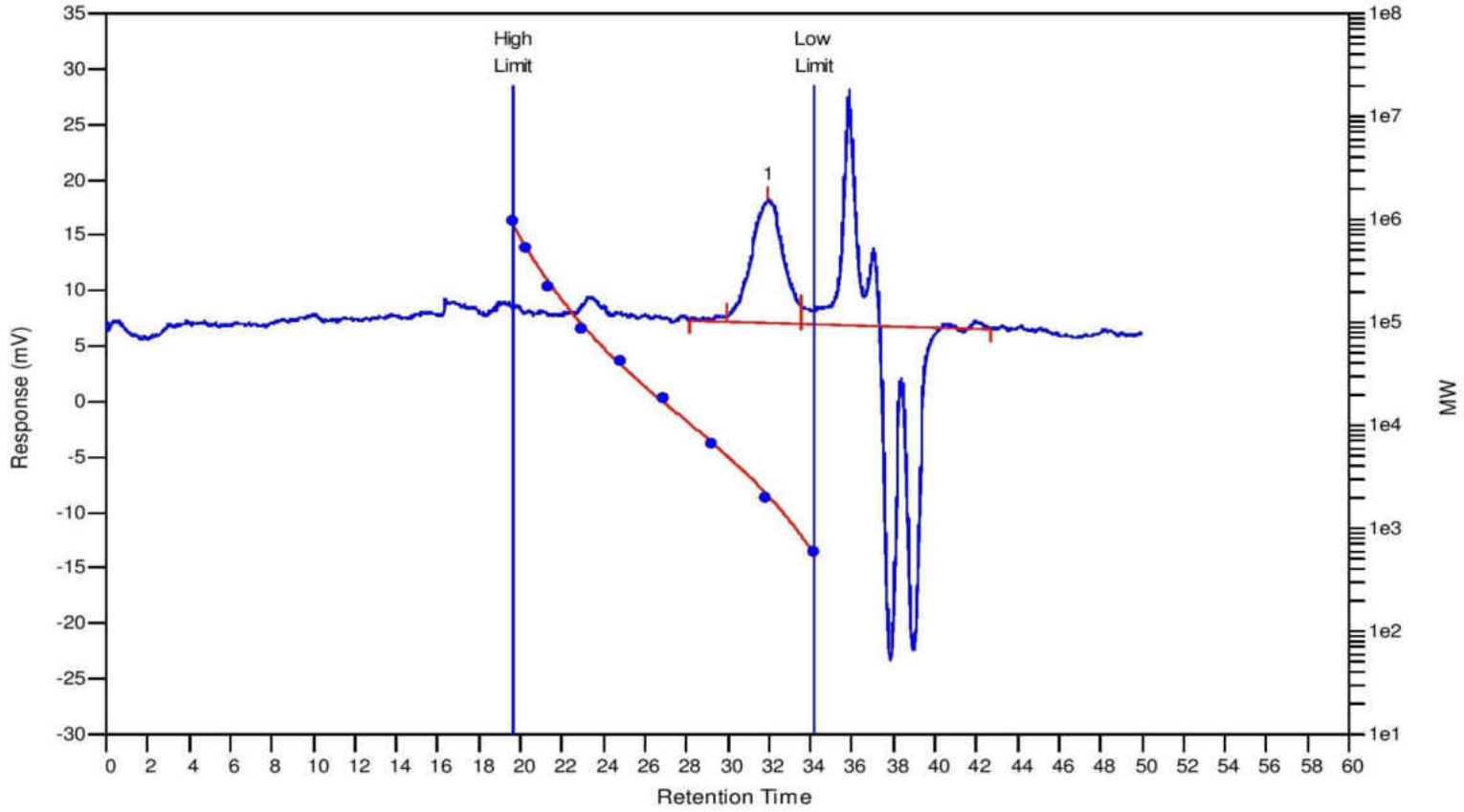

MW Averages

Peak No	Mp	Mn	Mw	Mz	Mz+1	Mv	PD
1	2084	2050	2331	2626	2923	2288	1.13707

APPENDIX A7: ^{19}FNMR spectrum of perfluorobenzoyl peroxide, **(2)**, 400MHZ, CDCl3

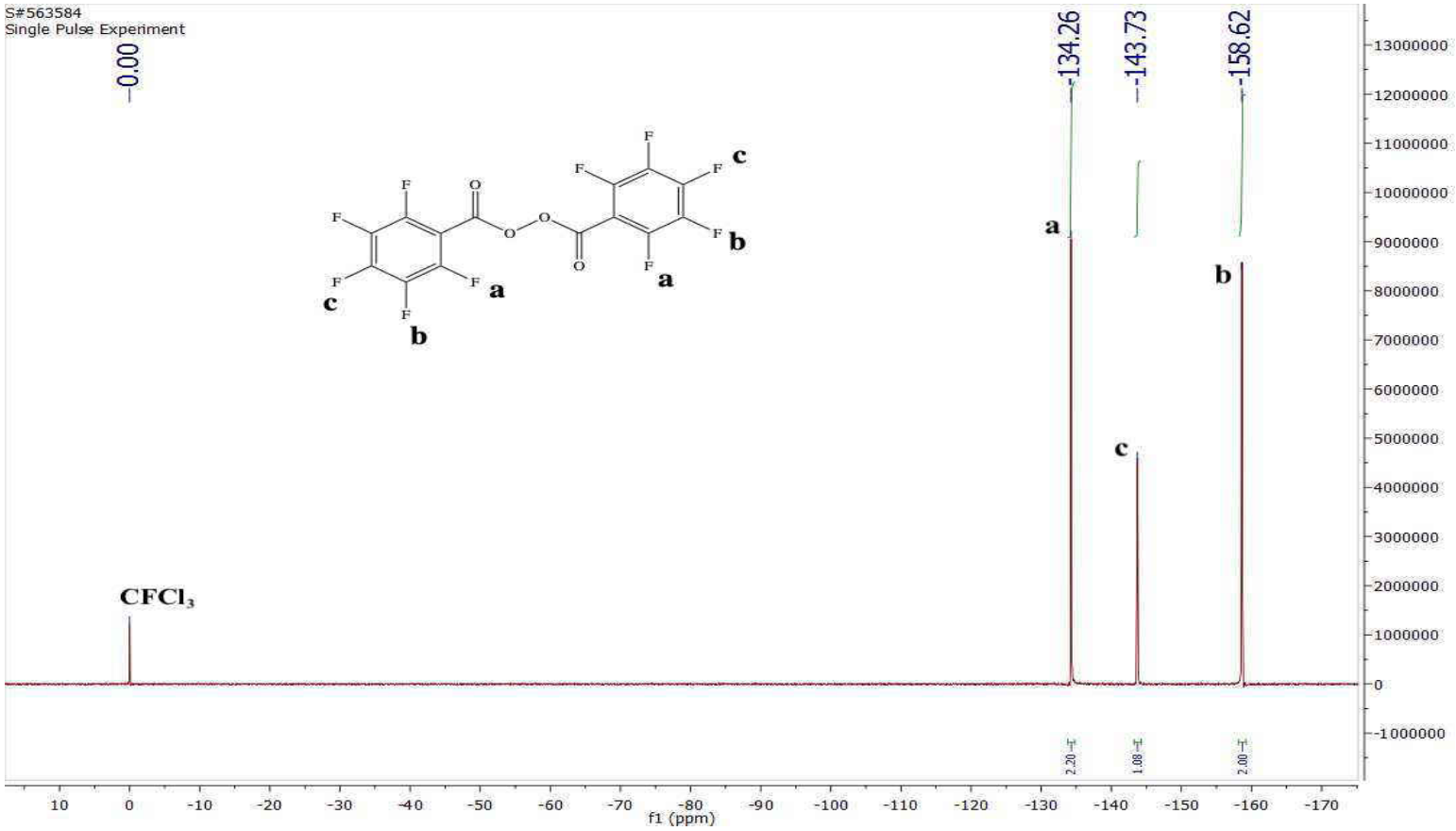

APPENDIX B1: ^{19}FNMR spectrum of $FSO_2CF_2CF_2O(CFCF_2)n$, **(6)**, 400$MH_{Z,}$ CD_3CN

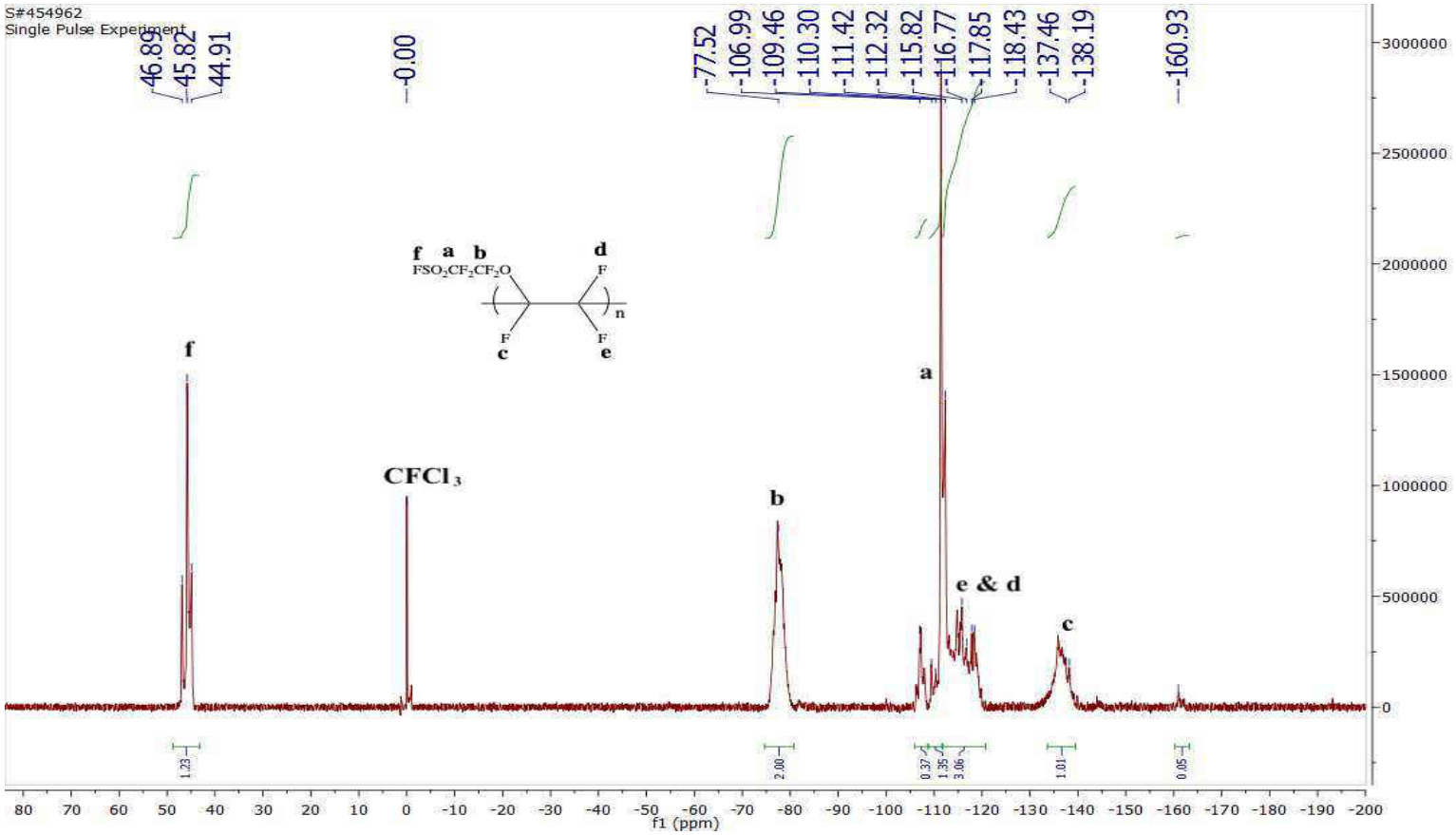

APPENDIX B2: ^{19}FNMR spectrum of 4-$NO_2PhSO_2N(M)SO_2CF_2CF_2O(CFCF_2)n$, **(7b)**, 400MHZ, CD_3CN

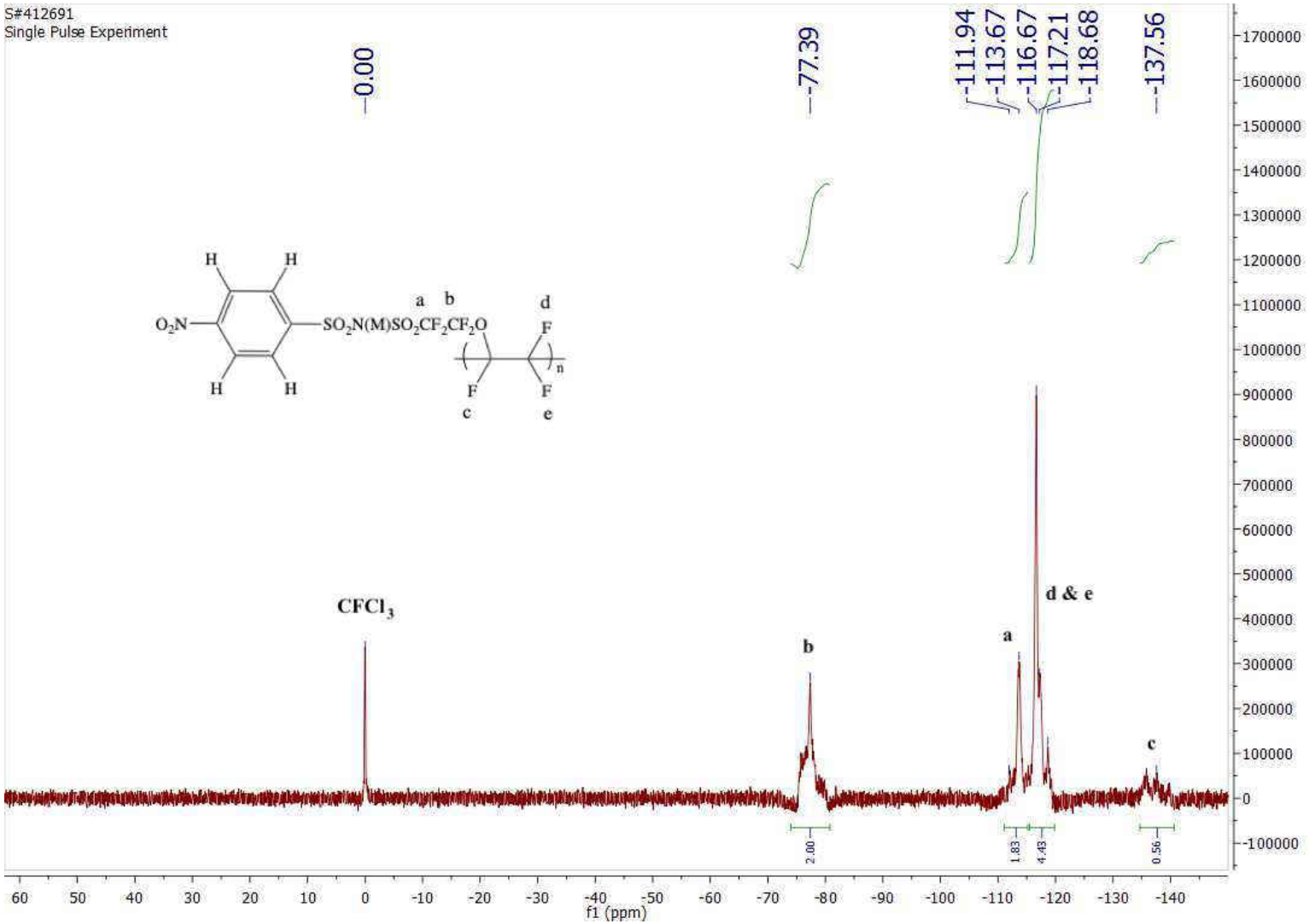

APPENDIX B3: ^{19}F NMR spectrum of $CH_3CON(M)PhSO_2NHSO_2CF_2CF_2O(CFCF_2)n$, **(7a)**, $400MH_{Z,}$ CD_3CN

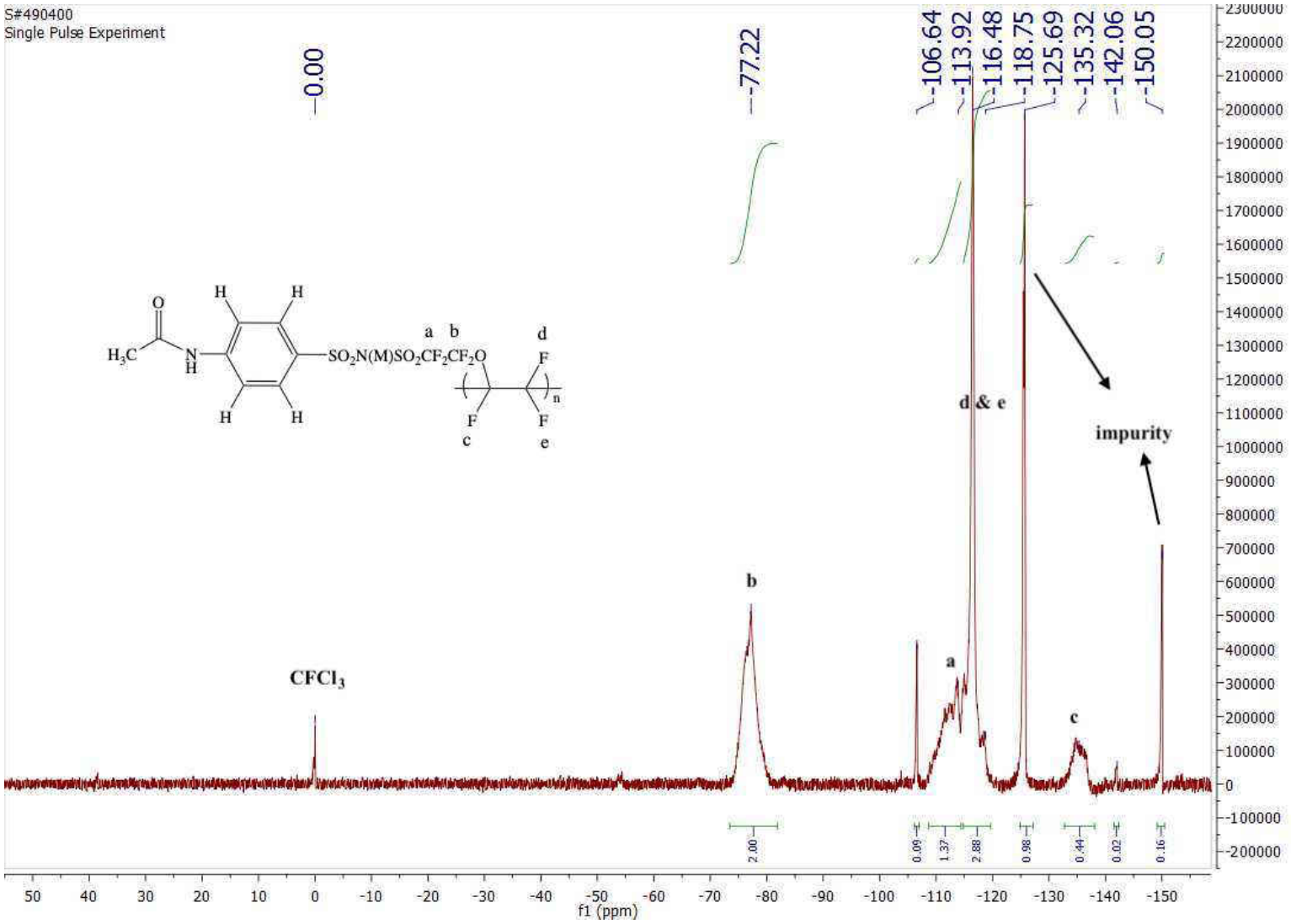

APPENDIX B4: ^{19}F NMR spectrum of 4-$NH_2PhSO_2N(M)SO_2CF_2CF_2O(CFCF_2)n$, **(8a)**, 400$MH_{Z,}$ CD_3CN

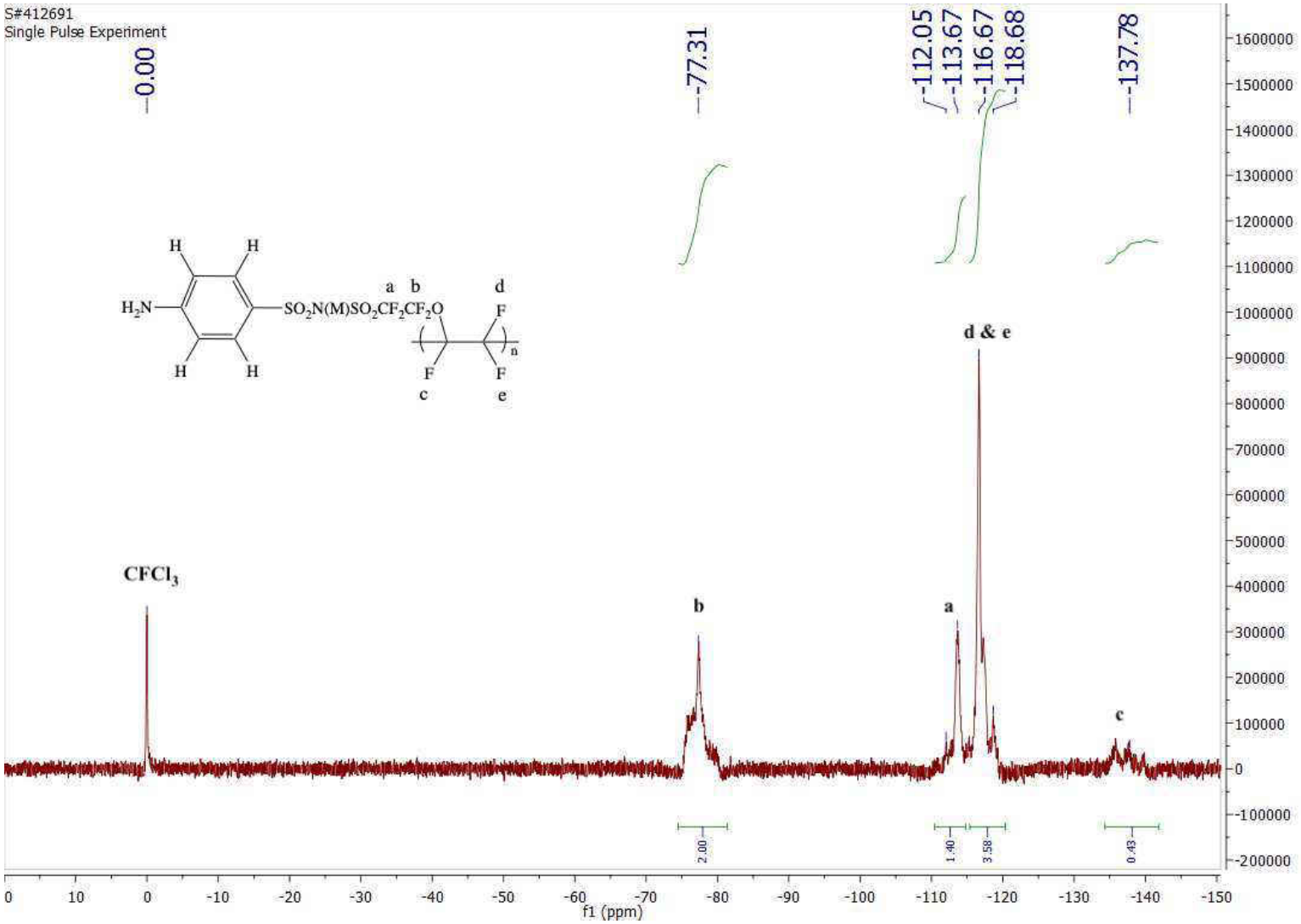

APPENDIX B5: ^{19}FNMR spectrum of 4- N_2^+ $PhSO_2N^-SO_2CF_2CF_2O(CFCF_2)n$, **(9a)**, 400MHZ, CD_3CN

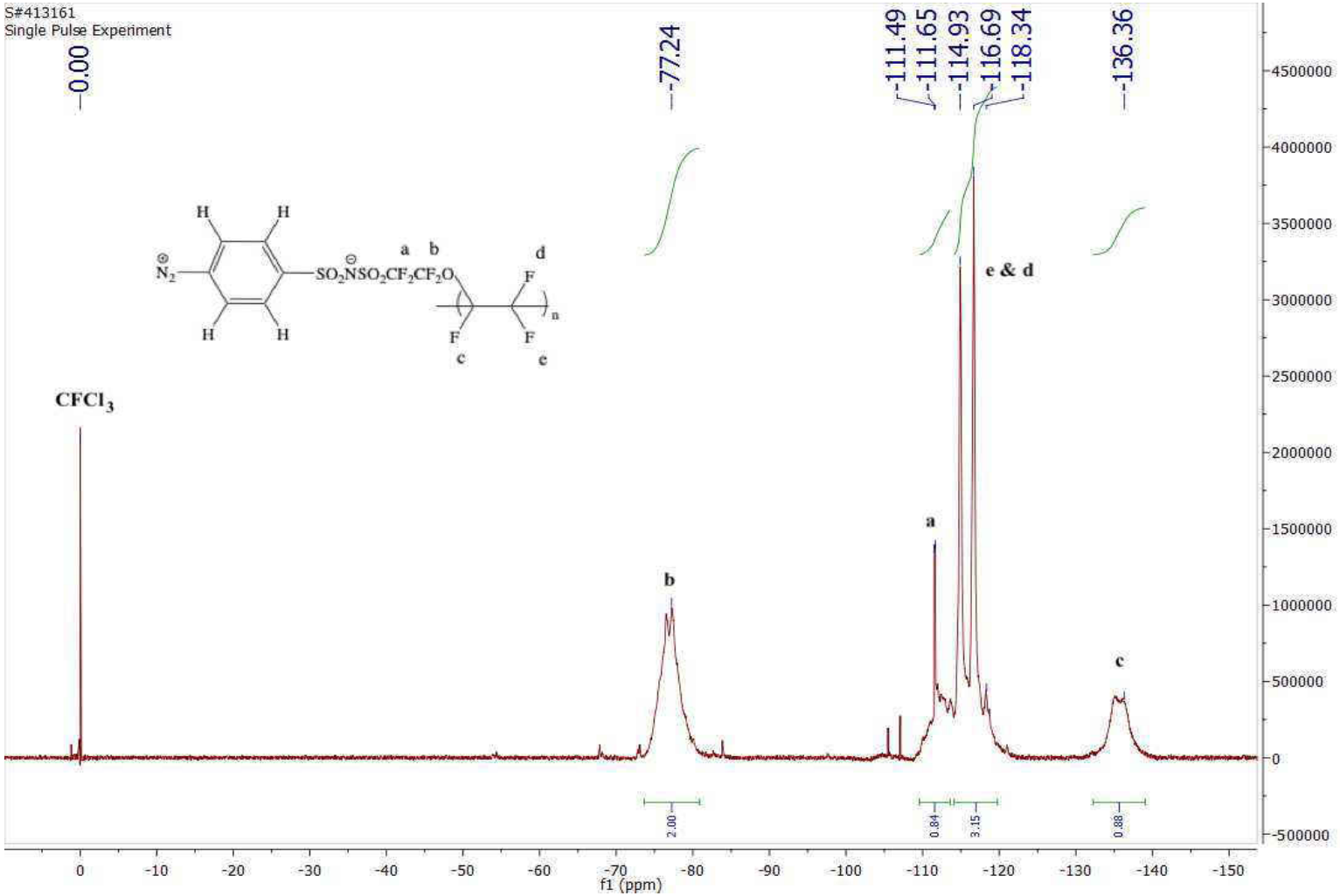

Appendix C1: ^{1}H NMR spectrum of 4-sulfamonylacetanilide, **(4a)**, 400$MH_{Z,}$ CD_3CN

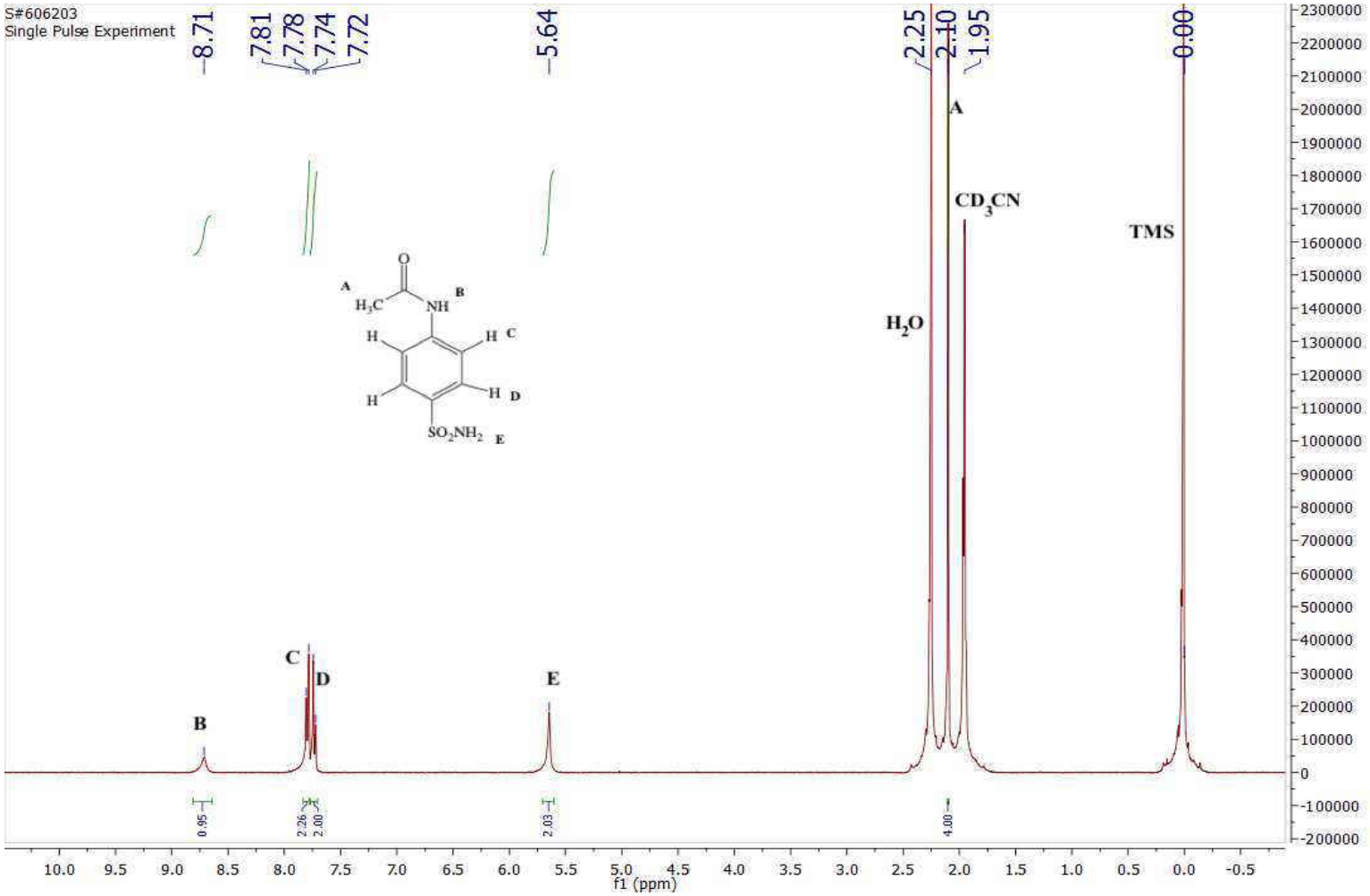

Appendix C2: ^{1}H NMR spectrum of 4-nitrobenzenesulfonyl amide, **(4b)**, 400MHZ, CD_3CN

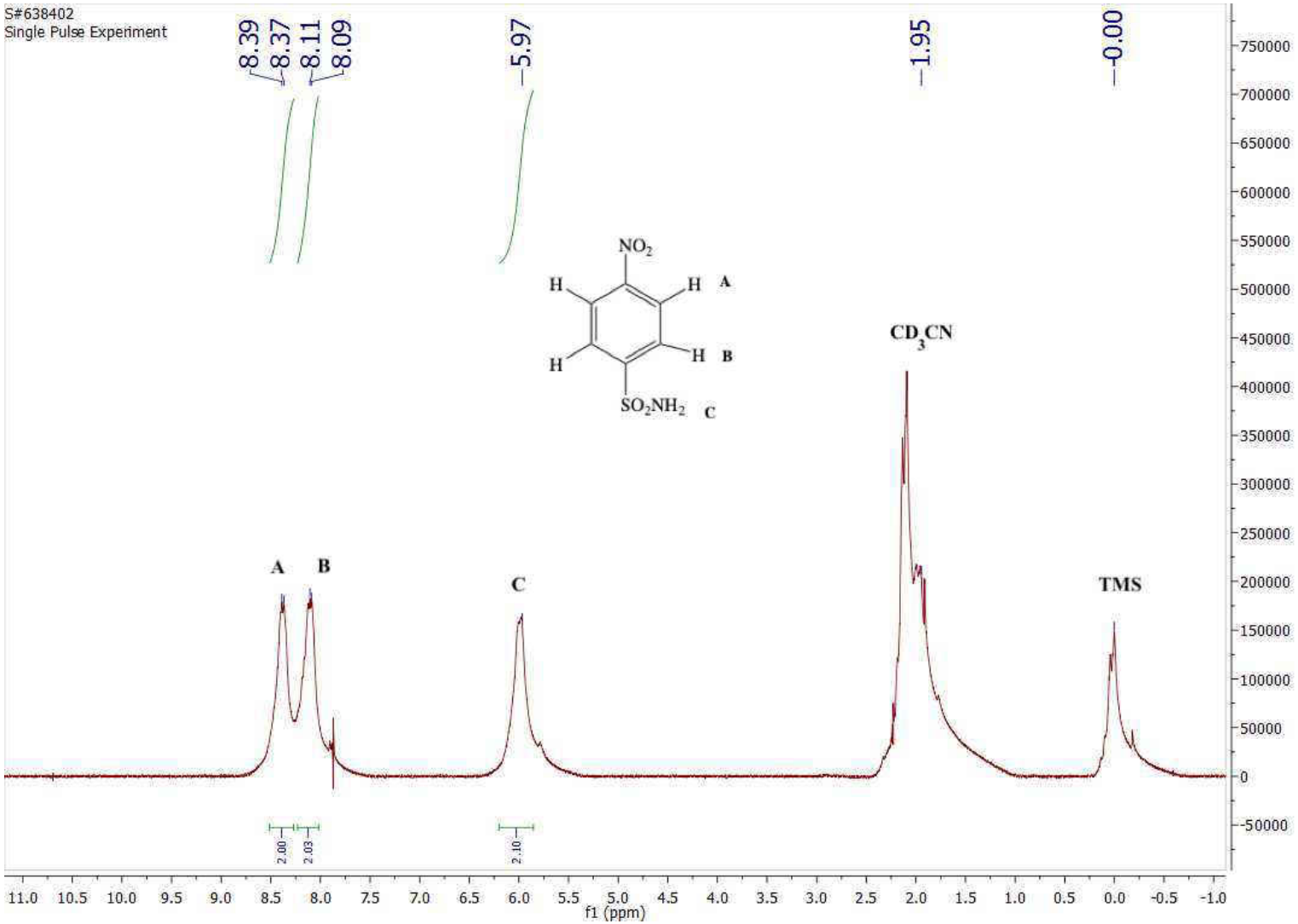

Appendix C3: ^{1}H NMR spectrum of 4-$NO_2PhSO_2N(M)SO_2CF_2CF_2O(CFCF_2)n$, **(7b)**,400$MH_Z$, CD_3CN

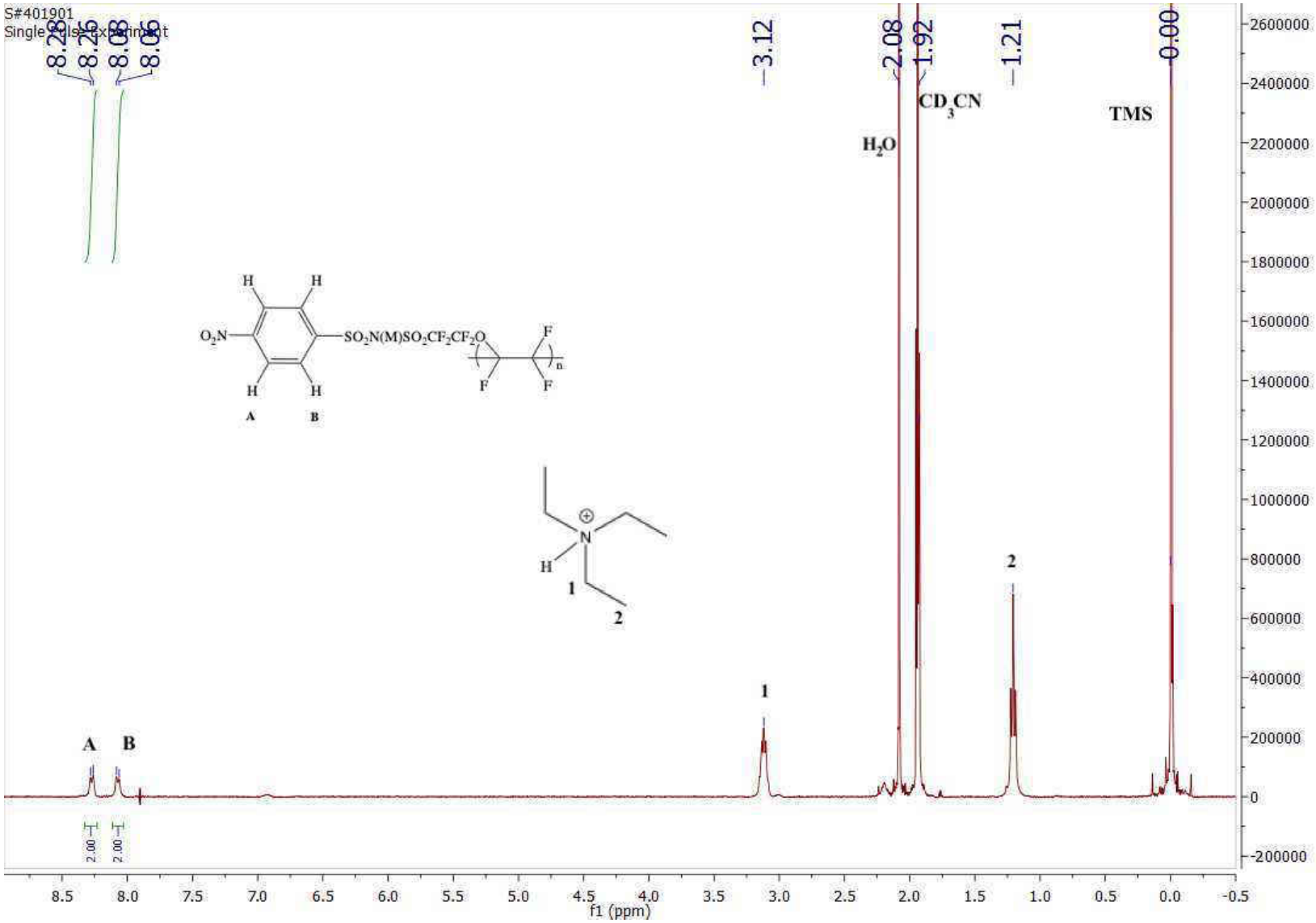

Appendix C4: Expanded ^{1}H NMR spectrum of 4-$NO_2PhSO_2N(M)SO_2CF_2CF_2O(CFCF_2)n$, **(7b)**,400$MH_{Z,}$ CD_3CN

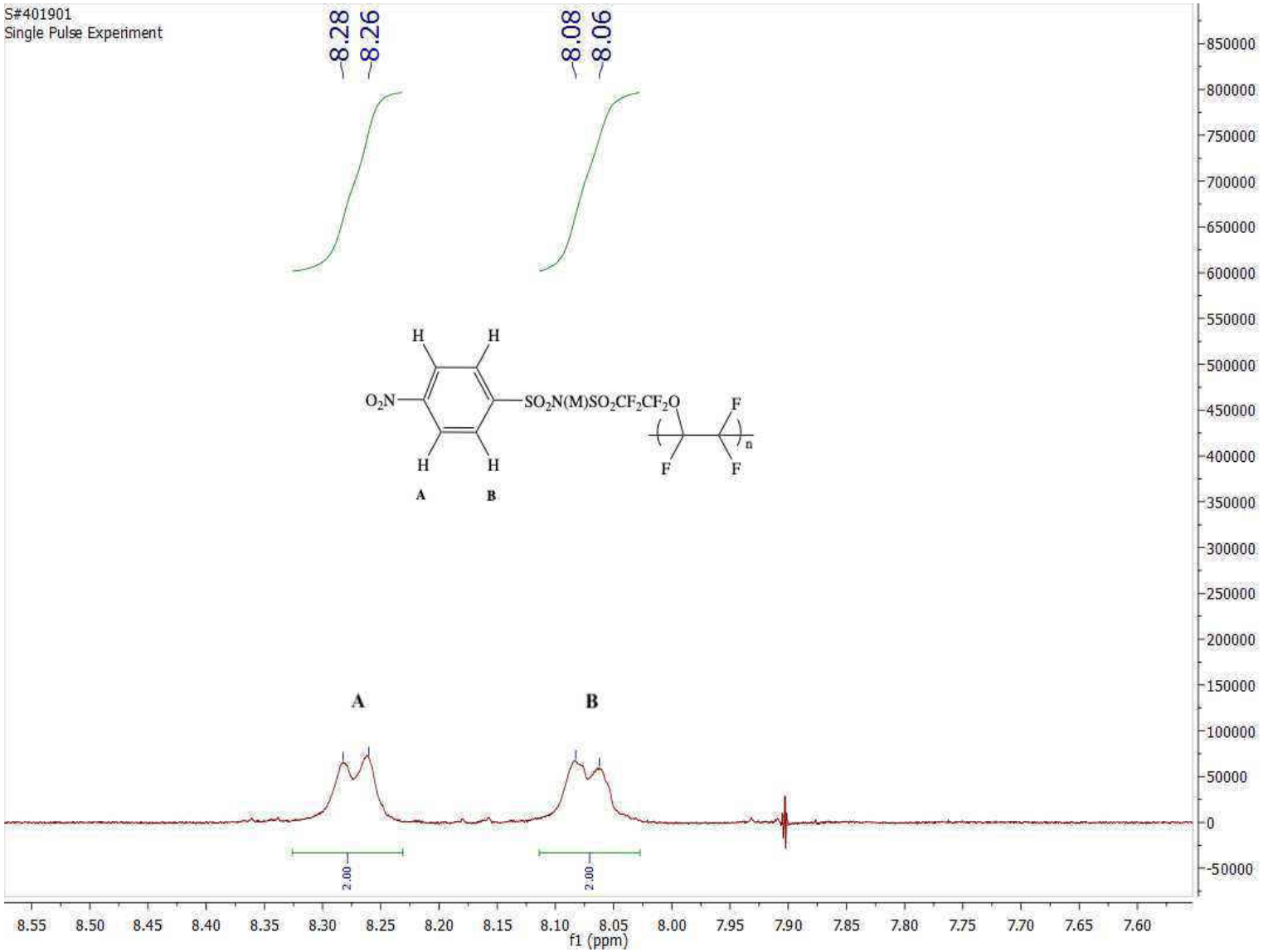

Appendix C5: ^{1}H NMR spectrum of $CH_3CONHPhSO_2N(M)SO_2CF_2CF_2O(CFCF_2)n$, **(7a)**, $400MH_{Z,}$ CD_3CN

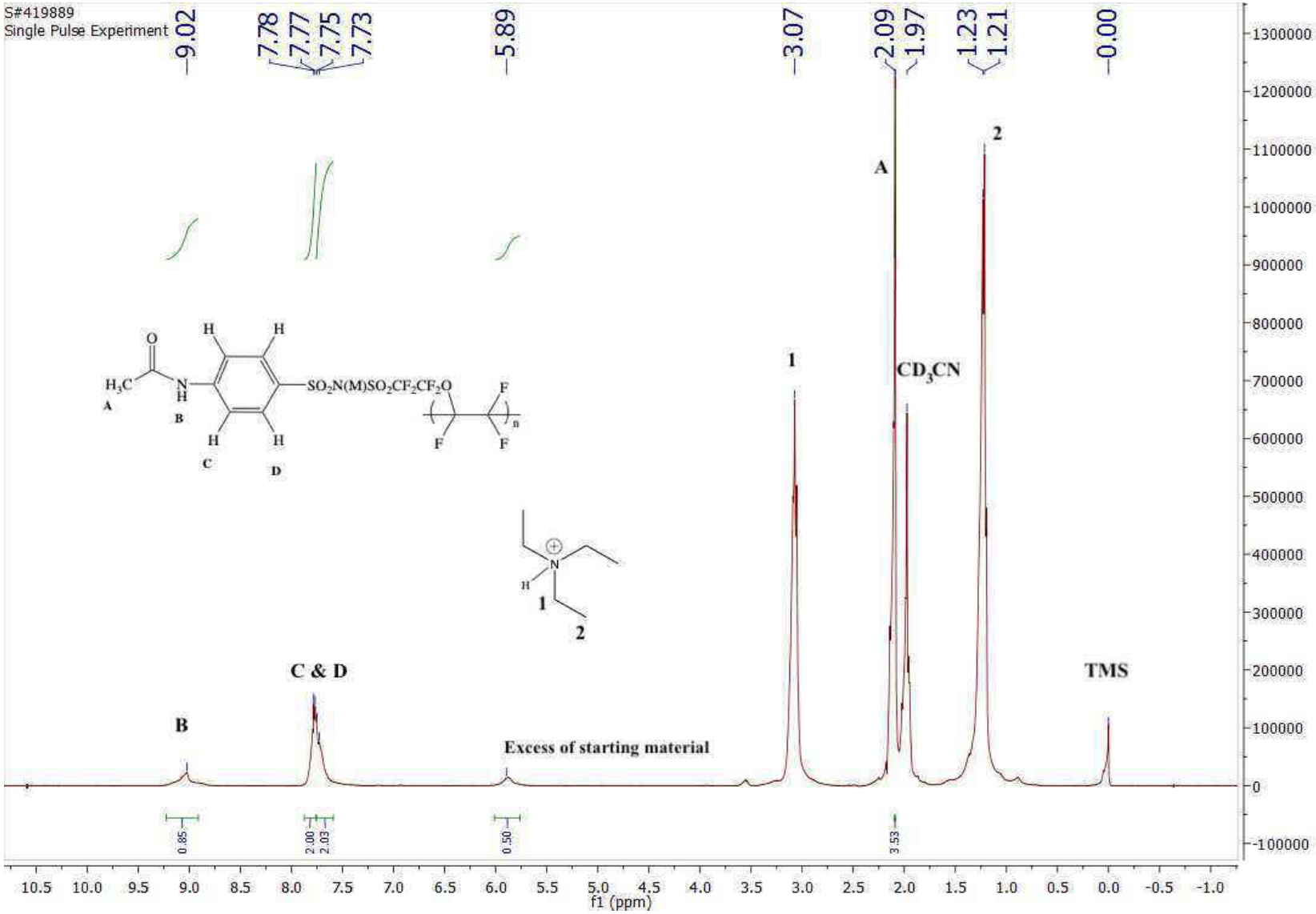

Appendix C6: ^{1}H NMR spectrum of 4-$NH_2PhSO_2N(M)SO_2CF_2CF_2O(CFCF_2)n$, **(8a)**, 400$MH_{Z,}$ CD_3CN

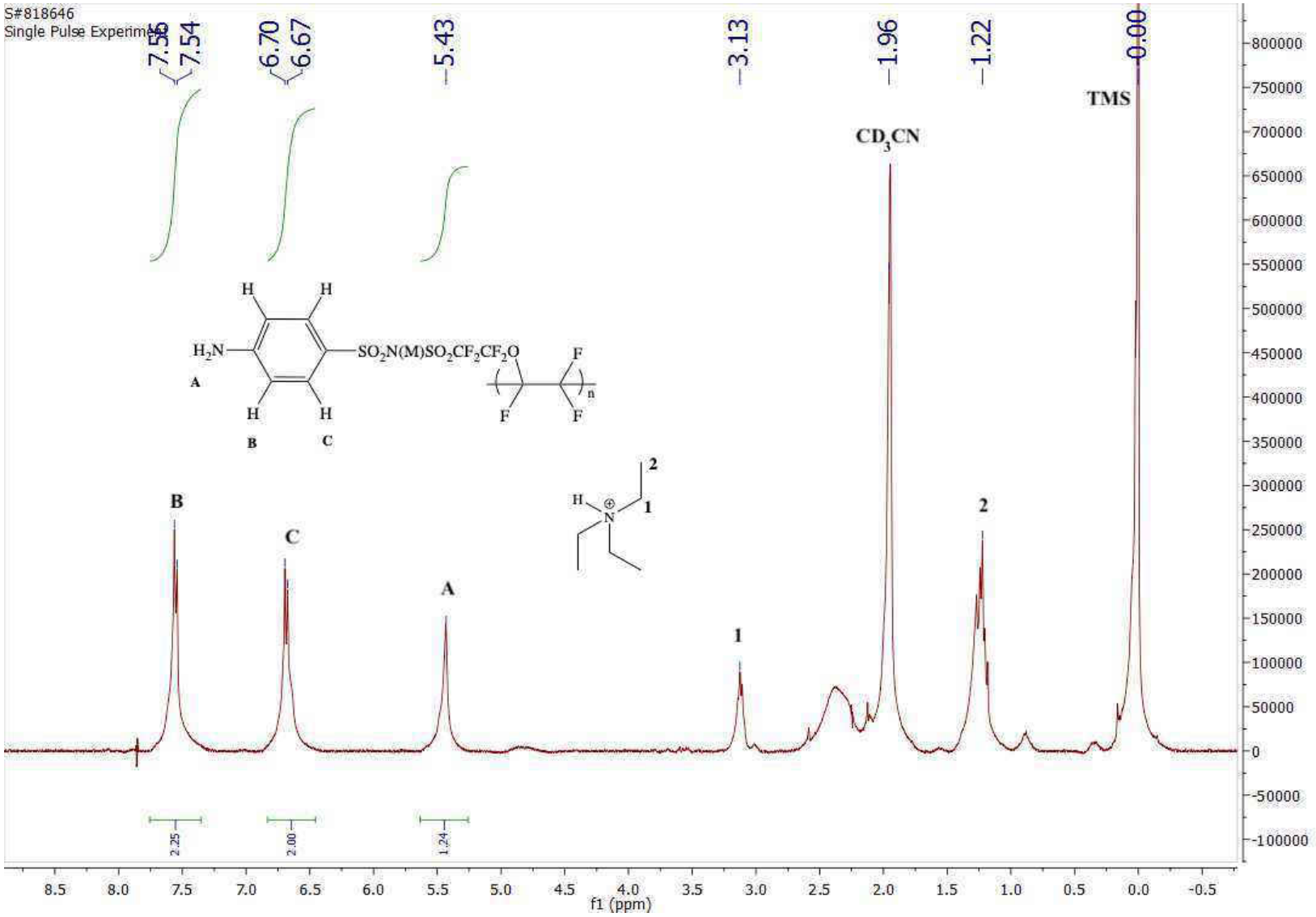

Appendix C7: Expanded ^{1}H NMR spectrum of 4-$NH_2PhSO_2N(M)SO_2CF_2CF_2O(CFCF_2)n$, **(8a)**, 400$MH_{Z,}$ CD_3CN

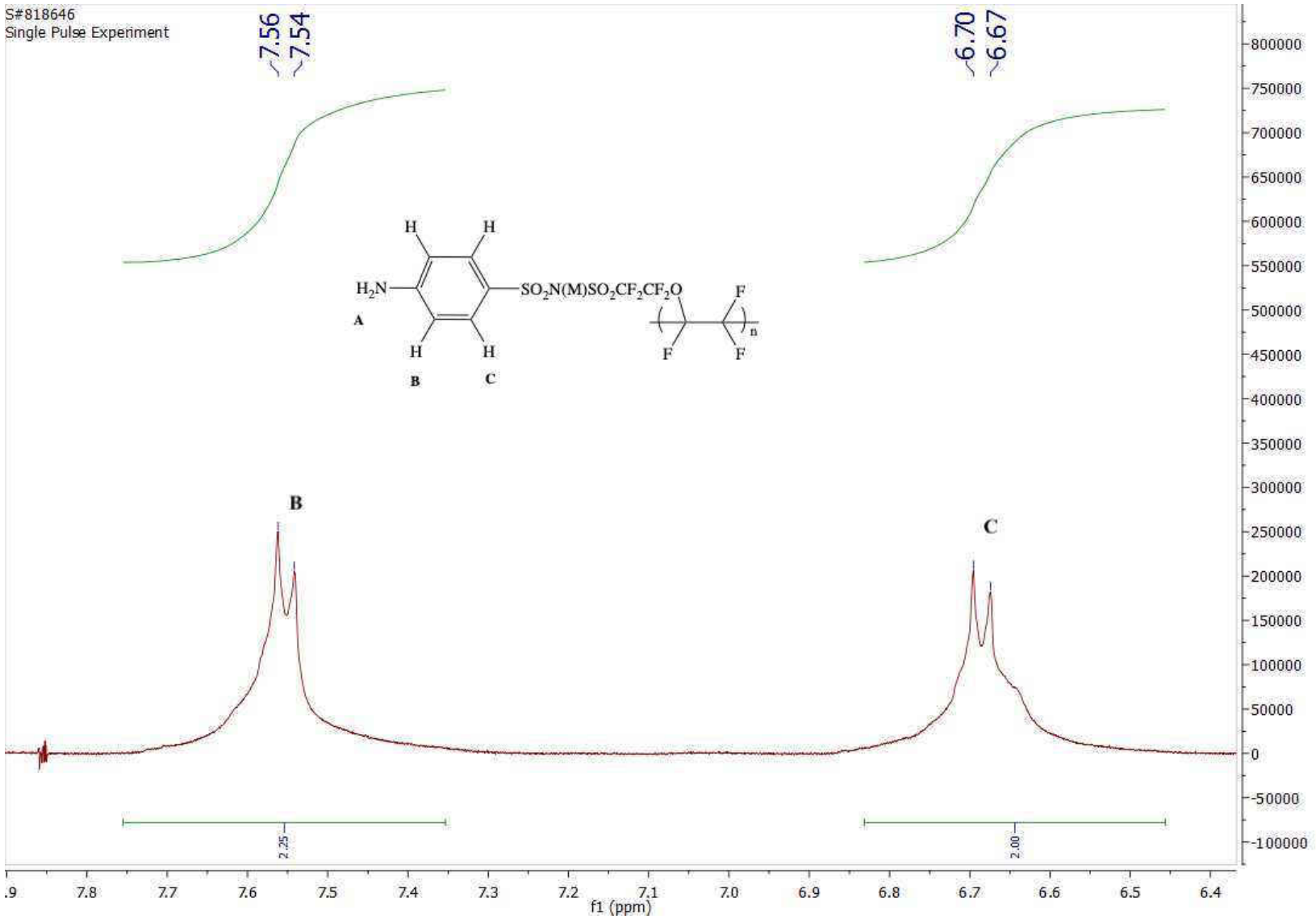

Appendix C8: ^{1}H NMR spectrum of 4-$N_2^{+}PhSO_2N^{-}SO_2CF_2CF_2O(CFCF_2)n$, **(9a)**, 400$MH_{Z,}$ CD_3CN

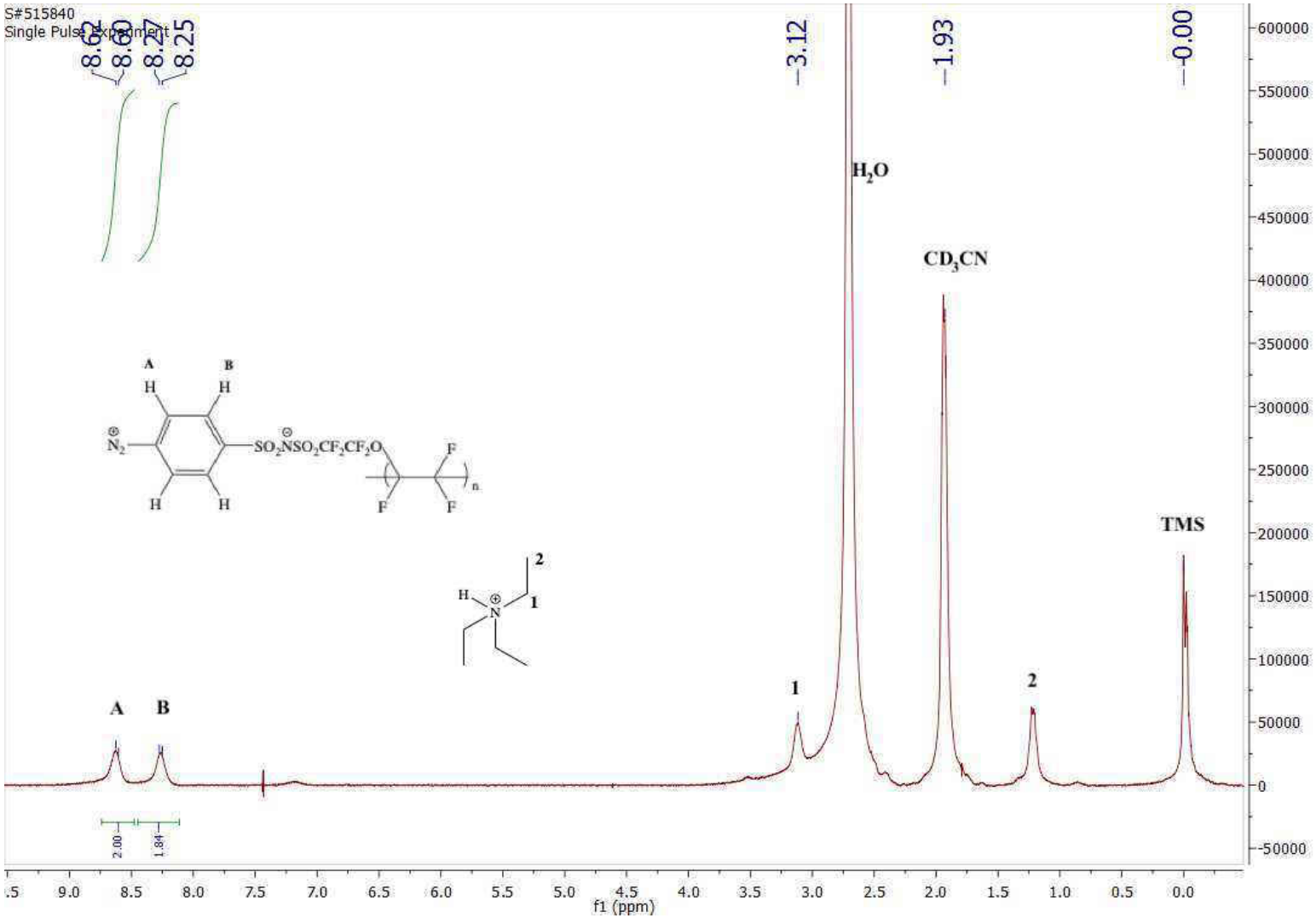

APPENDIX D1: FT-IR Spectrum of perfluorobenzoyl peroxide, **(2)**

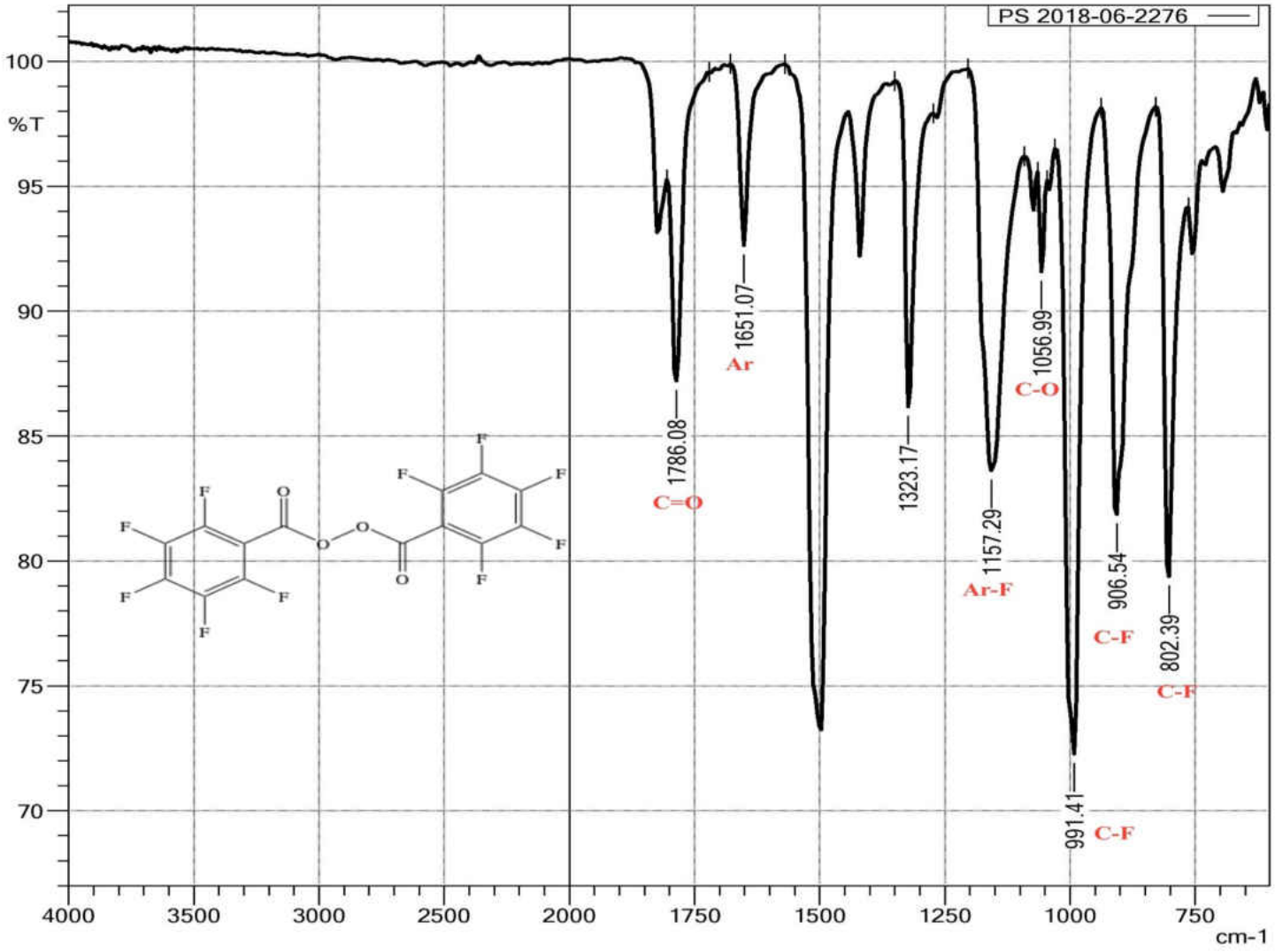

APPENDIX D2: FT-IR Spectrum of 4-sulfamonylacetanilide, **(4a)**

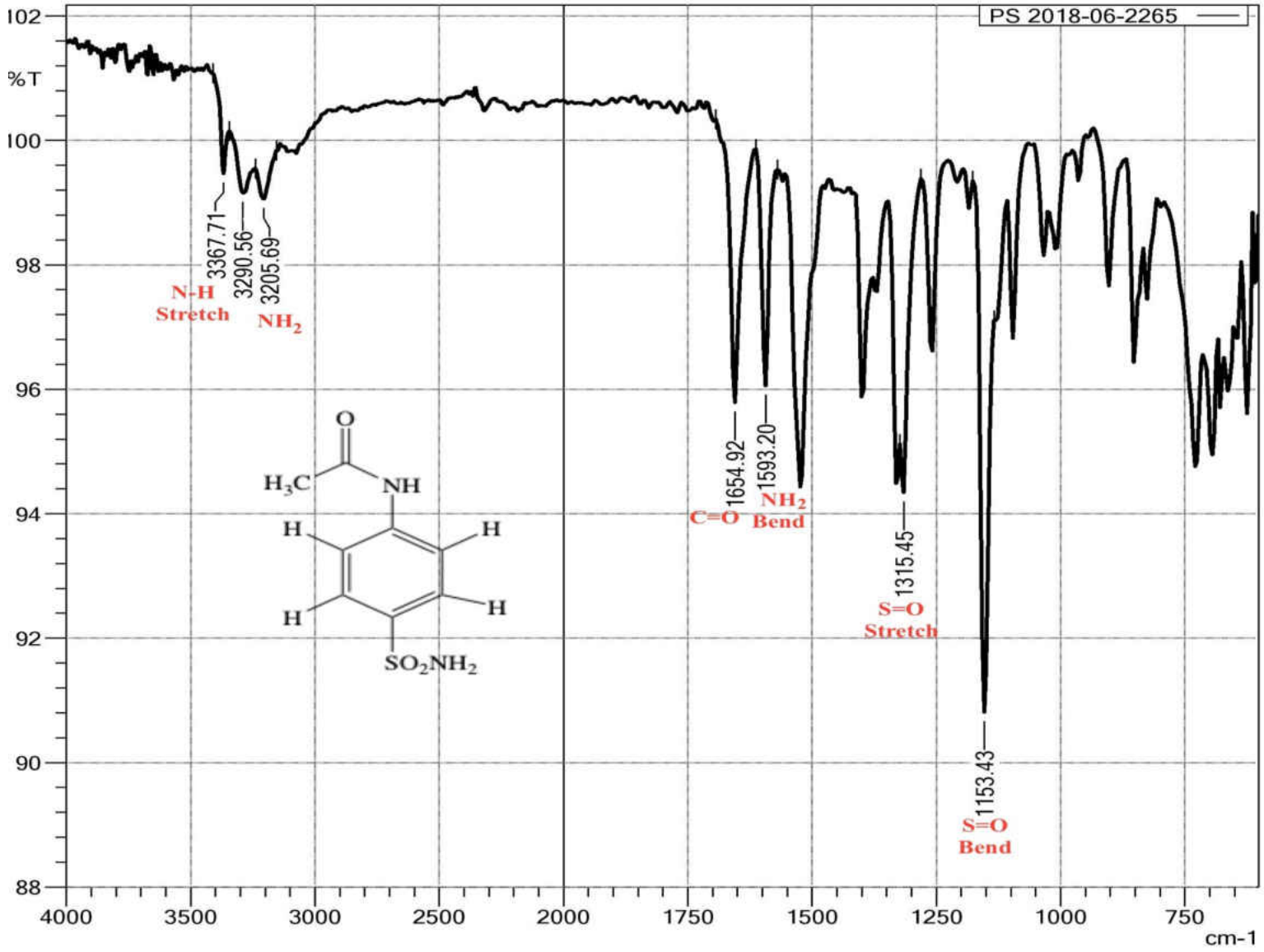

APPENDIX D3: FT-IR Spectrum of 4-nitrobenzenesulfonyl amide, **(4b)**

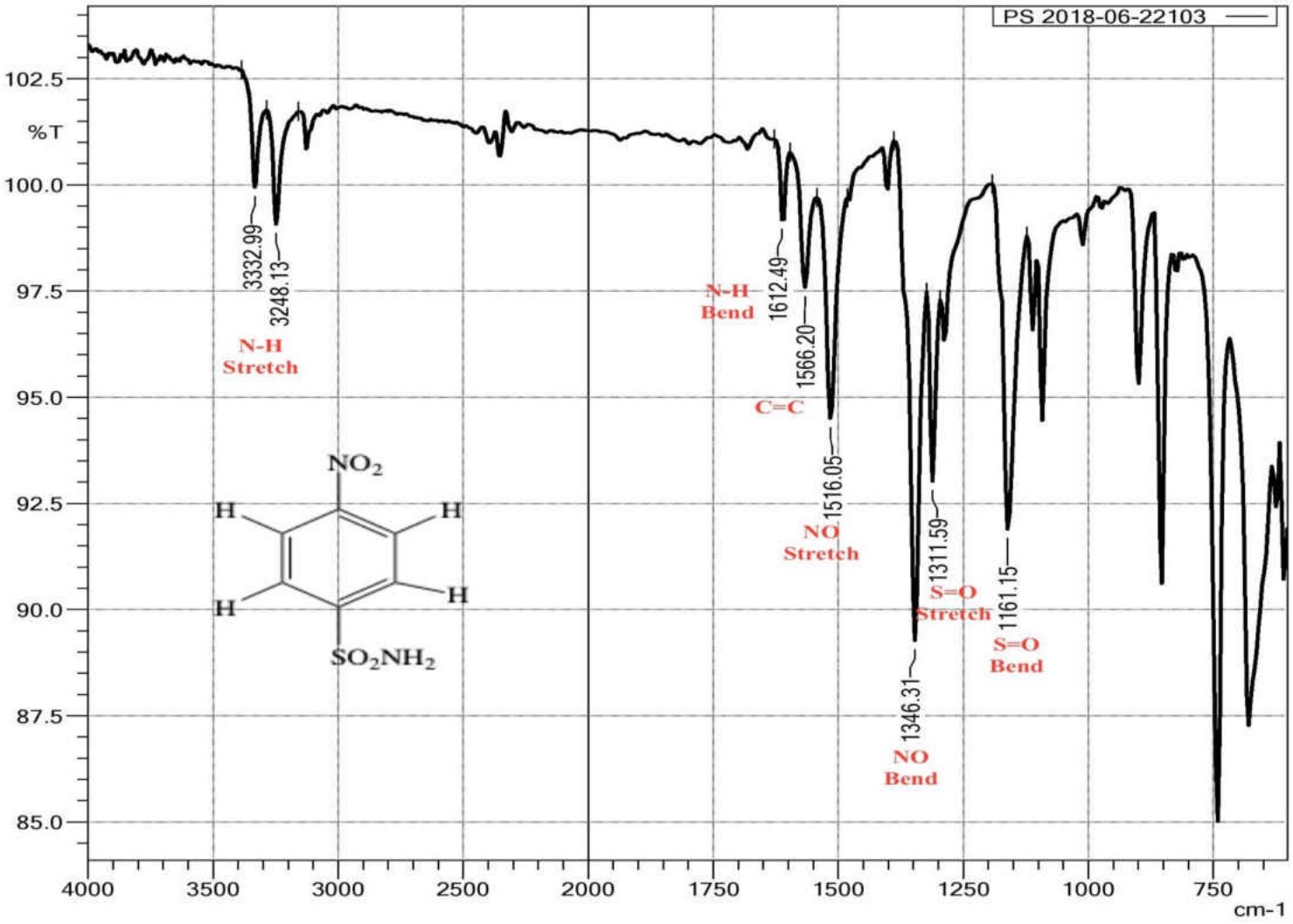

APPENDIX D4: FT-IR Spectrum of $FSO_2CF_2CF_2O(CFCF_2)n$, **(6)**

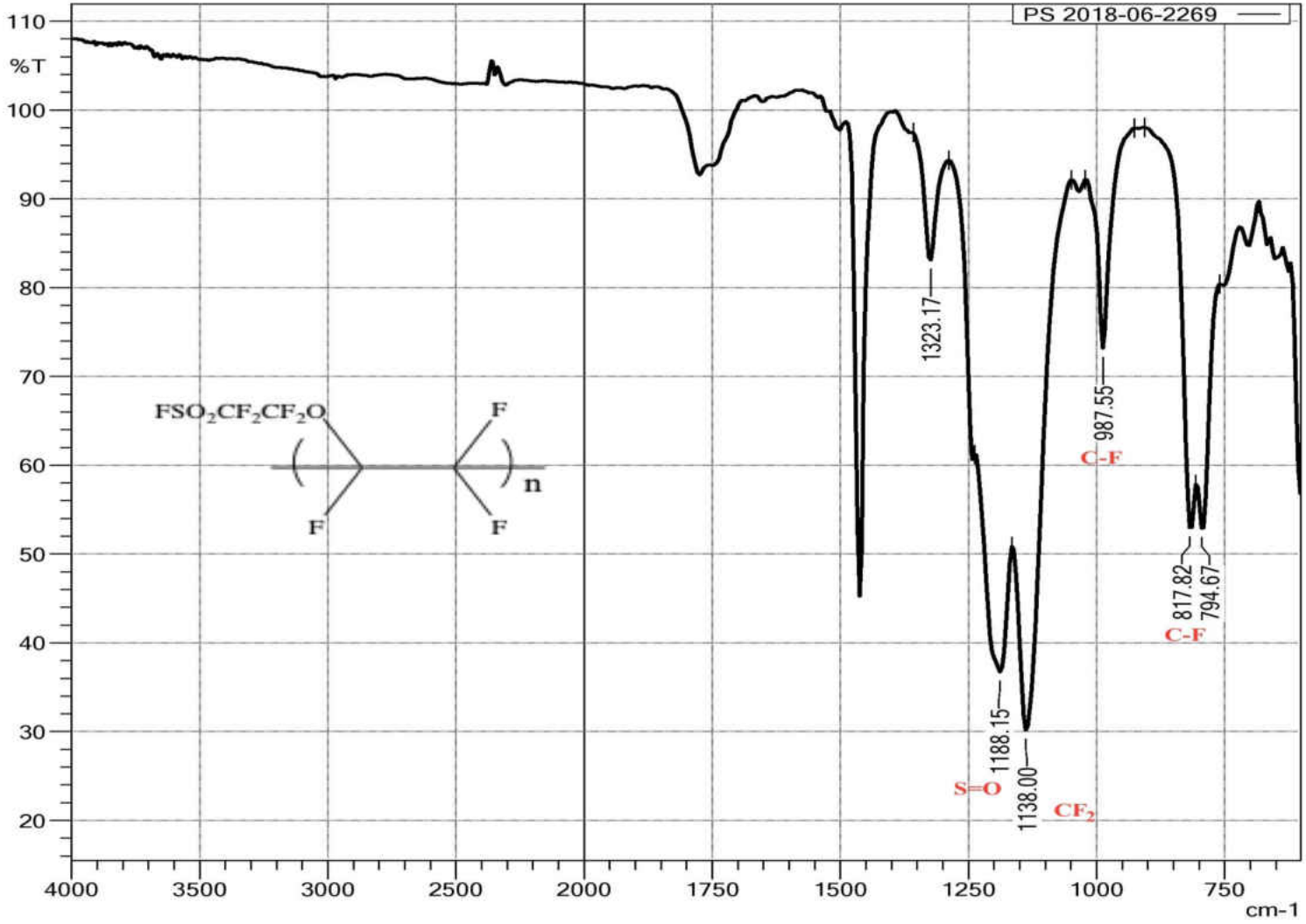

APPENDIX D5: FT-IR Spectrum of 4-$NO_2PhSO_2N(M)SO_2CF_2CF_2O(CFCF_2)n$, **(7b)**

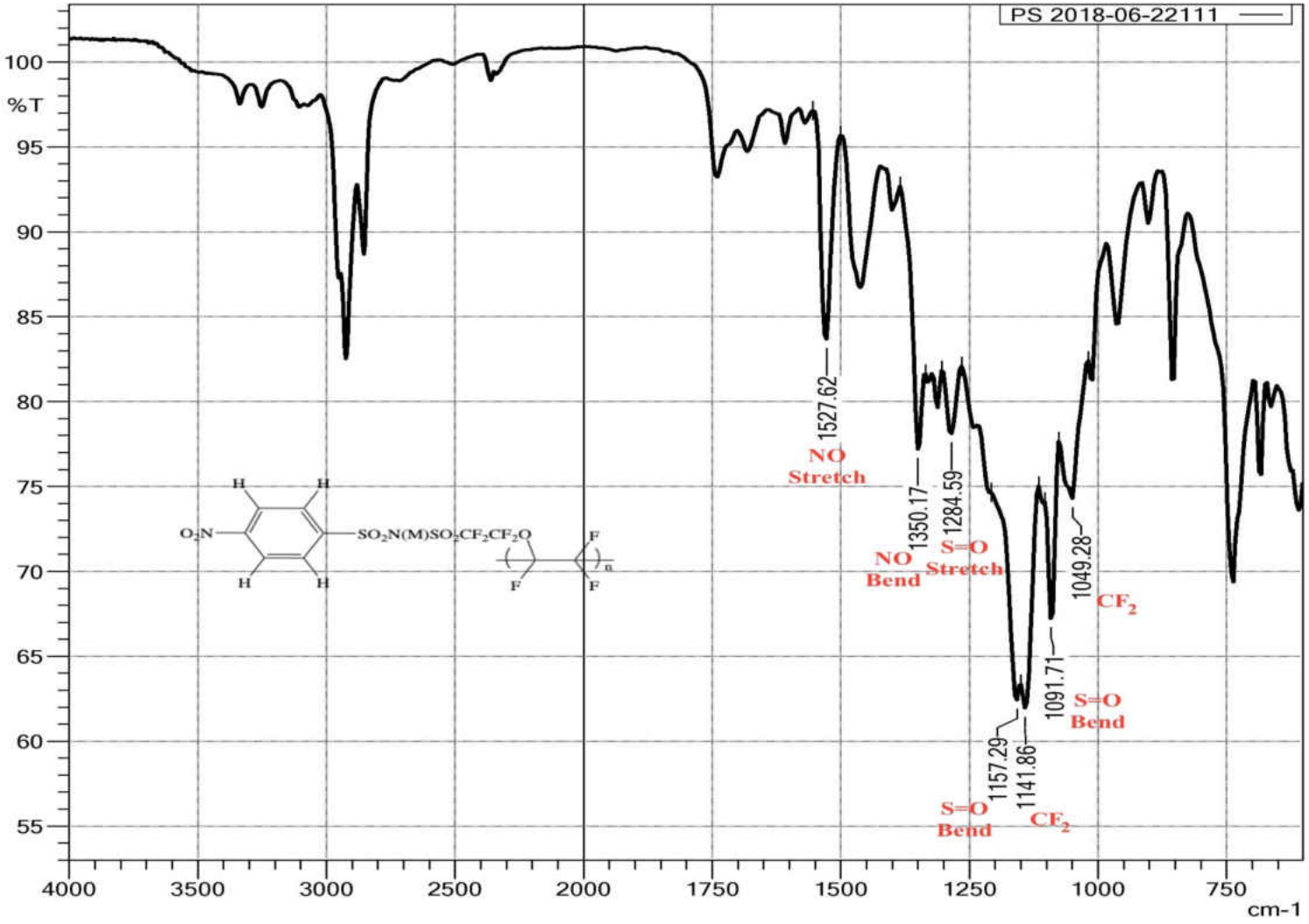

APPENDIX D6: FT-IR Spectrum of $CH_3CONHPhSO_2N(M)SO_2CF_2CF_2O(CFCF_2)n$, **(7a)**

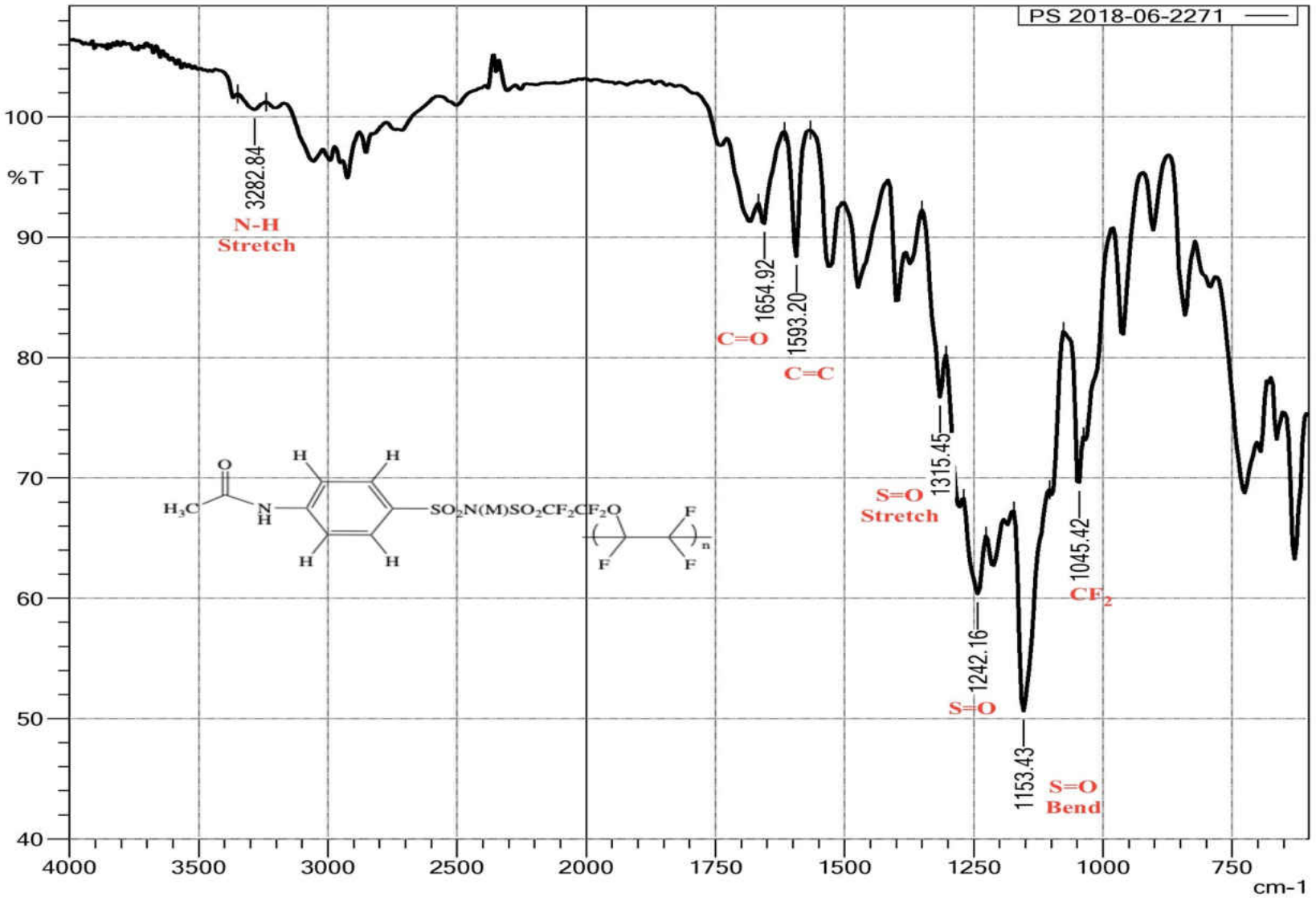

APPENDIX D7: FT-IR Spectrum of 4-$NH_2PhSO_2N(M)SO_2CF_2CF_2O(CFCF_2)n$, **(8a)**

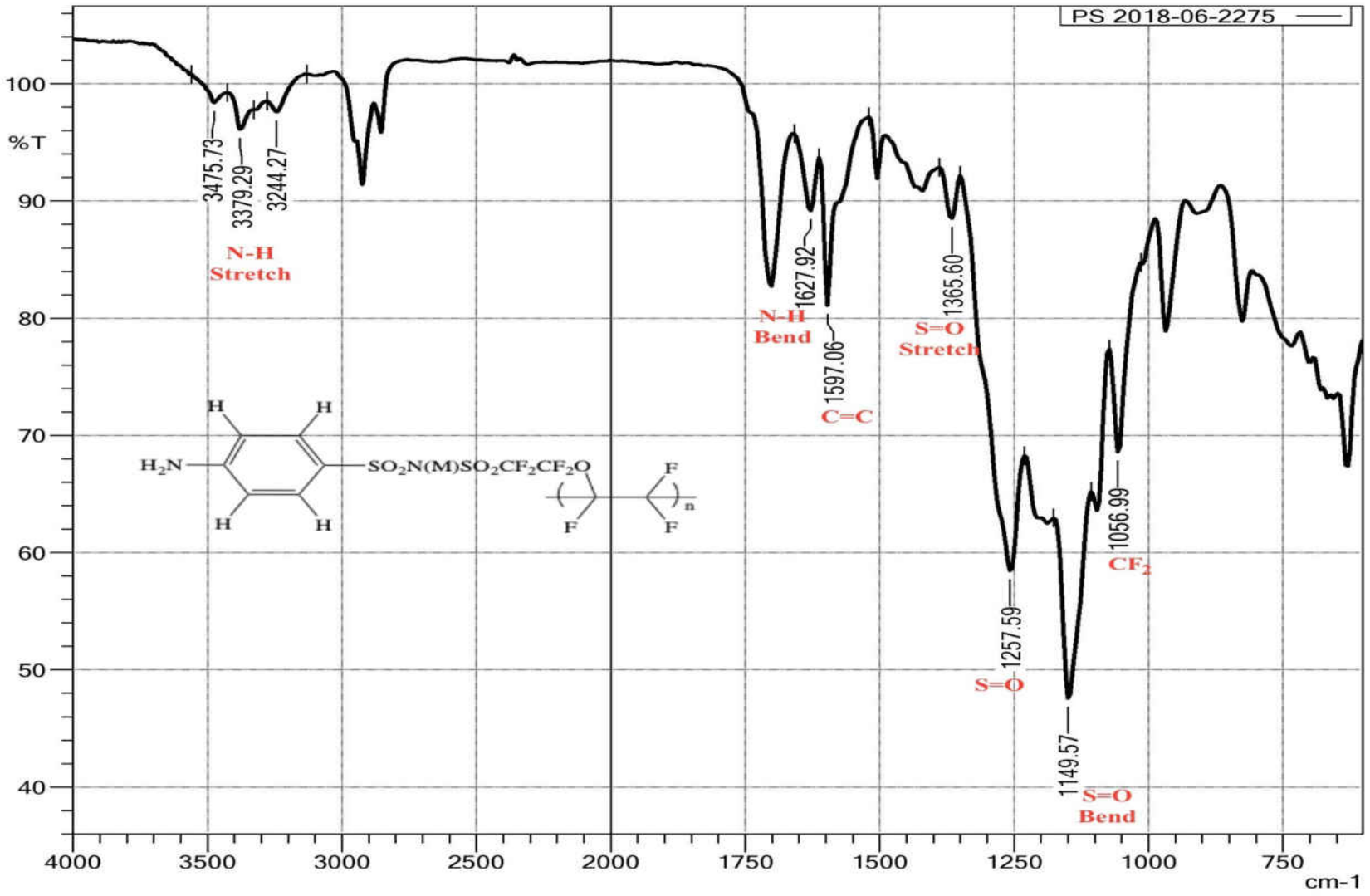

APPENDIX D8: FT-IR Spectrum of 4-$N_2^+PhSO_2N^-SO_2CF_2CF_2O(CFCF_2)n$, **(9a)**

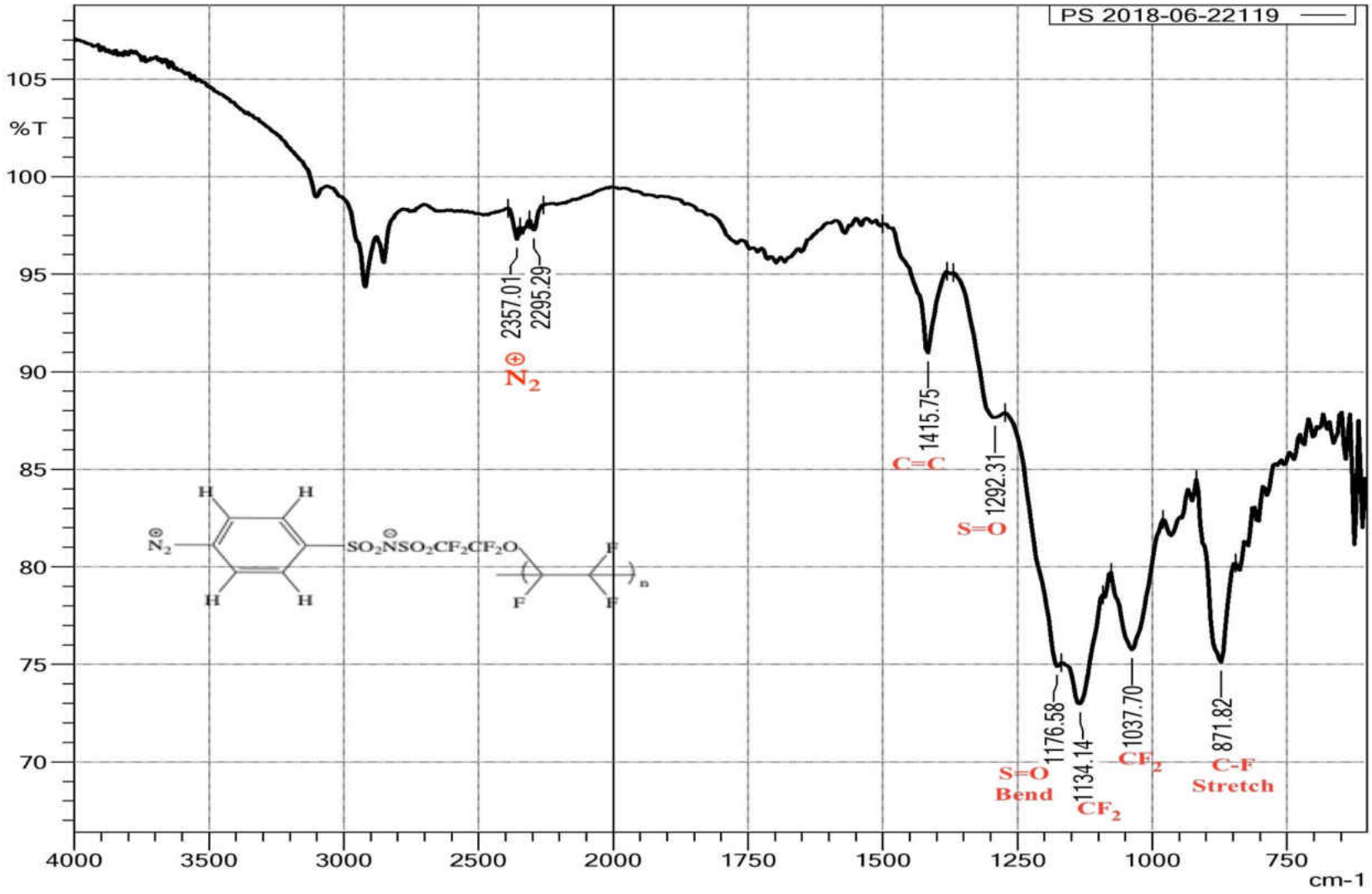

VITA

HELAL ALHARBI

Education:	M.S. Chemistry, East Tennessee State University, Johnson City, Tennessee 2019
	B.S. Chemistry, Qassim University, Qassim, Kingdom of Saudi Arabia, 2013
Professional Experience:	Teaching Assistant, Qassim University, Qassim, Kingdom of Saudi Arabia, 2013-2014
Award:	First Place, Natural Science Poster Presentation (Group A) at the 2018 Appalachian Student Research Forum, Johnson City, TN, USA, April 2018.